A transmon-based quantum switch for a quantum random access memory

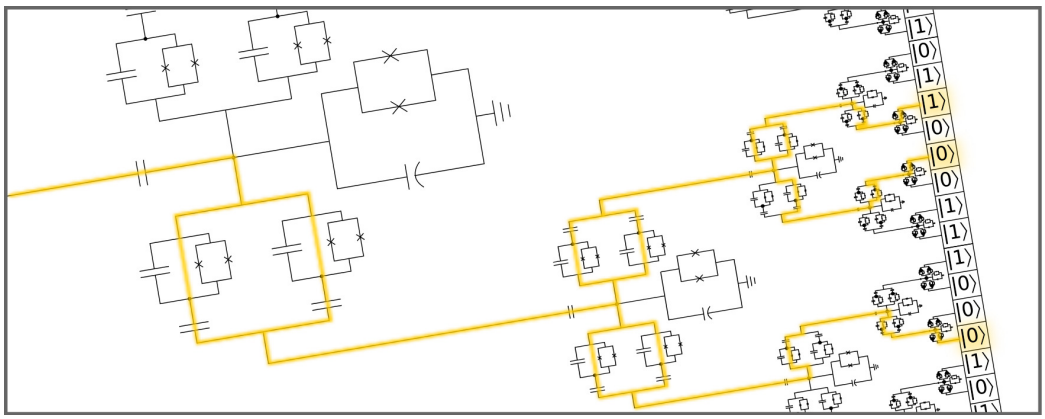

THESIS

submitted in partial fulfillment of the
requirements for the degree of

MASTER OF SCIENCE
in
PHYSICS

Author :	Arnau Sala Cadellans
Student ID :	S-1441426
Supervisor :	C. W. J. Beenakker
2nd corrector :	Miriam Blaauboer

Leiden, The Netherlands, June 29, 2015

A transmon-based quantum switch for a quantum random access memory

Arnau Sala Cadellans

Instituut-Lorentz, Leiden University, P.O. Box 9500, 2300 RA Leiden, The Netherlands
Kavli Institute of Nanoscience, Delft University of Technology, Lorentzweg 1, 2628 CJ Delft, The Netherlands

June 29, 2015

Abstract

In this thesis, the necessary elements to build up a quantum switch, the central element in a quantum random access memory, are proposed and analyzed. A network with quantum switches at its nodes forms the bifurcation path that leads an address register from a root node to an array of memory cells, activating, quantum coherently, only the quantum switches that the register encounters in its path to the memory cells. Transmon qubits and SQUIDs are used to design a superconducting device capable of routing a register of microwave photons through a bifurcation network, allowing for superposition of paths. In order to give rise to all the required interactions between the device and the address register, a non-linear capacitor, composed of two plates with carbon nanotubes in between, is introduced into the transmon. The dynamic operation of the quantum switch is analyzed using Langevin equations and a scattering approach, and probabilities of reflection and transmission of photons by (or through) the switch are computed, both for single- and two-photon processes. Computations show that, with parameters taken from up-to-date similar devices, probabilities of success are above 94%. Applications of quantum random access memories are discussed, as well as other applications of quantum switches. Also, solutions are proposed to the challenges that emerge during the study of the dynamics of the quantum switch.

Contents

Version of June 29, 2015– Created June 29, 2015 - 21:15

Chapter 1

Introduction

1.1 Quantum information processing

With the latest advances in experimental quantum computation [1–10], the forthcoming development of a quantum computer seems just a matter of time. Improvements have been made in the field of superconducting qubits, where some authors [1] have realized a two-qubit superconducting processor with which they have implemented, with great success, the Grover search and the Deutsch-Jozsa quantum algorithms [11]. Another group [2] has implemented a three-qubit version of the Shor's algorithm [11] –within a circuit quantum electrodynamics architecture– to factorize the number 15. Also with trapped ions [3], quantum algorithms involving very few qubits have been realized. New advances in this field admit to scale the quantum processor from 10 to 100 qubits, allowing the implementation of quantum simulations in a regime where its classical counterpart fails [4]. Within quantum optics implementation of quantum algorithms to factorize (small) numbers [5] and to solve systems of linear equations [6] using a two-qubit quantum processor have been demonstrated. One of the benefits of working with optical quantum systems is that they can naturally integrate quantum computations with quantum communication[12]. A lot of research, with promising outcomes due to the atom-like properties of the elements in a solid-state device [7], is being conducted in the field of condensed matter, where some authors are working with high-fidelity two-qubit gates [8]. They have also been able to create a multi-qubit register, an indispensable element for implementing a quantum-error-correction protocol [8]. The Grover's quantum search algorithm has also been proven in these systems [9]. A solid-state device fabricated using NV (Nitrogen-vacancy) centers in diamonds has relatively long coherence times –even at room temperature– and can be optically coupled to other systems [7].

It is even possible to combine these disciplines to create a hybrid device [10]. Though in all these cases only few qubits were considered, there is no reason to believe that a larger device, capable of handling more inputs, cannot be constructed [4, 7, 13].

In any case, to perform quantum computations, a universal quantum computer must be capable of storing information within quantum states to use it later in a further stage of an algorithm and it must also have access to classical (or quantum) data as a superposition of the entries. Examples of algorithms with these requirement are the Grover search [11] and the Deutsch-Jozsa [11] algorithms. For these reasons, just like a classical computer needs a processor capable of doing classical operations and a memory to keep and extract the data, a quantum computer also needs some sort of RAM memory able to handle quantum information.

1.2 Why a quantum RAM? Quantum memory theory

Any computer needs some memory device for storing or extracting information. Given that current computers work with may bits, this device has to be composed of multiple instances of "memory cells" where single bits can be stored. Nowadays, the device used for these purposes is a random access memory (RAM), which is a device whose memory cells can be addressed at will (randomly) instead of sequentially (like in a CD or a hard drive). This instrument [14] consists of an array of memory cells, where the information (bits) is kept, and an electronic circuit in a tree-like structure that routes an "address register" from a root node –connected to the processor– to each of the memory cells, as shown in FIG. 1.1. When the address register –which contains the instructions to reach the desired memory cell– is sent to the memory device, a path through the tree-like circuit that leads to the target cell is opened. Common RAM memories composed of $N = 2^n$ memory cells require the manipulation of $N - 1$ nodes of the bifurcation path.

In the quantum world, a memory cell can be a qubit with a long enough coherence time [4, 7, 13], but when working with a multiple-qubits algorithm, a single memory cell may not be enough. In these cases, a collection of memory cells with a proper addressing scheme is needed. For algorithms such as the Grover search, a memory –which may only contain a classical database– with a quantum addressing scheme is required. This memory is a device that returns a superposition of the data hosted by some of its cells [11].

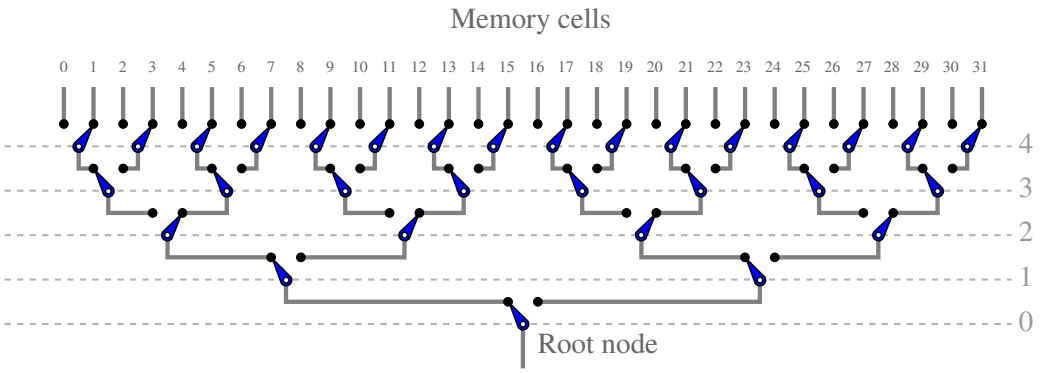

Figure 1.1: *A common random access memory can be schematically represented with this diagram [14]. This diagram contains a root node in the 0th level that bifurcates into two transmission lines (solid gray). A switch at every node (black) decides which path leads to the chosen memory cell and which paths remain unconnected.*

An interesting architecture (the bucket brigade architecture) for a quantum random access memory (QRAM) was proposed by Giovannetti, Lloyd and Maccone [15]. It consists of a device similar to FIG. 1.1 but with quantum switches at the nodes. These quantum switches are elements that can be in three states, one of them being a ground state and the other two being excited states. The ground state is the *wait* state: the path is closed. The other two excited states are either *left* or *right* (open the path that goes to the left/right). Given the quantum nature of the switch, it is also possible to prepare it in the state *left and right*.

Within this scheme, to evaluate a memory cell, an initial register is needed. This register contains the instructions to reach the target cell: if the path from the root node to the cell is *root-left-left-right-left-right*, then the first element of the register contains *left*, the second contains *left*, etc. One more element in the register is needed to interact with the content of the memory cells and bring back the information it stores. When the register reaches the root node, the quantum switch reads (and keeps) its first element and evolves from *wait* to *left*. The register continues (without its first element) to the second node and so on. After the register has gone through all the nodes, a single element is left. This element reads the content of the memory cell and is emitted back through the path that is still open. If instead of a classically-defined register a quantum register with a superposition of states is sent in, the output would be a superposition of the content of the memory cells evaluated.

A quantum generalization of a conventional RAM would require the manip-

ulation and entanglement of $O(N)$ quantum switches whereas, with the bucket brigade architecture only $O(\log(N))$ switches must be thrown, thus reducing the number of elements that have to be coherently entangled.

The benefits of working with a QRAM include the possibility of realizing algorithms that require the manipulation of data in a superposition state and the possibility of sending a query and receiving an answer with total anonymity: if instead of a definite question (evaluation of a memory cell) a superposition of questions is sent, an output with a superposition of answers will be sent back, and only who has a complete knowledge of the original question can extract the right answer out of the output [16].

1.2.1 Quantum memory implementation

The most important element of a QRAM, that makes it different from any other device capable of storing information, is the quantum switch that routes the incoming register through the right path to the memory array. This element can in principle be realized with many different elements, but only a solid-state implementation, using superconducting qubits, will be discussed. This choice has been made based on the simplicity of its structure –it is analytically tractable and easy to fabricate– and the apparently small probability of errors, as various authors show in their single-photon transistors based on circuit quantum electrodynamics (cQED) [17, 18] or nanoscale surface plasmons [19]. A superconducting-based device can be combined with other systems, such as diamonds [10], etc.

The other basic element of a memory, the array of memory cells, can be realized in multiple ways –it can be a quantum device or a classical memory with only classical information– without affecting the dynamics of operation described previously and it is not in the focus of this project.

Thus, the device to be developed must absorb the first element of a register composed of photons –microwave photons, since these are the kinetic elements in cQED systems– and route the rest of the photons, independently of their state, according of the state of the absorbed photon.

1.3 Other attempts

Different approaches have been proposed by [20] for building a QRAM such as an optical implementation, using polarized photons and trapped atoms. Also a phase

gate implementation, using phase shifters (e.g. superconducting qubits) and microwave photons is discussed in the same paper [20]. Alternatively, the authors propose to use multilevel atoms controlled by lasers to induce Raman transitions so they absorb and emit photonic registers. Other alternatives have been proposed, such as using a beam splitter based on Superconducting Quantum Interference Devices (SQUID) to route some photons carrying the information through the desired path [21]. Others propose to use toroidal resonators as quantum switches [22].

Regarding the beam splitters (BS), there has been some research too. In references [23–25] the authors use cQED devices to act as BS in a way such that there are two incoming photons through two different transmission lines and the BS sends the input photons to one of the outgoing transmission lines, or both, creating an entangled state or just separating even modes from odd modes. This option is in disagreement with the structure of a QRAM (or a RAM) because there is a single incoming transmission line that bifurcates several times, whereas the authors consider multiple incoming transmission lines. The authors in [26] have designed a beam splitter that separates an incoming photon into even and odd modes. This design is not useful either because once the modes have been separated the beam cannot be split again, thus it is not possible to create a tree-like structure with more than one node. Finally, other authors [27] have designed a device that can send a photon to one transmission line or another depending on its frequency. With this device, a photon that goes to the left in one node will go to the left in all the successive nodes as well, so it may not be a good option because the only two memory cells accessible from the root node would be the rightmost node and the leftmost node.

1.4 Thesis outline

During this project I have proposed and analyzed the necessary elements to build up a quantum random access memory with the architecture proposed by Giovannetti *et al.* in [15]. Transmon qubits and SQUIDs are used to design a multilevel system, mimicking artificial atoms with non-linear energy levels, capable of routing a register from the root node to the target cell minimizing the quantum decoherence processes. The register is sent via microwave photons through superconducting waveguides (transmission lines).

In the second chapter I introduce all the necessary elements to construct a quantum switch that satisfies the requirements needed to route a register of photons through the desired path. A lightweight analysis of the proposed device is

conducted to check that no more elements are needed and that the switch can, in principle, work as expected. A Lagrangian of the system is derived in this section. In the third chapter, an in-depth analysis of the device is conducted. A Hamiltonian, derived from the Lagrangian, is quantized and the equations of motion, containing relaxation and dephasing elements, are obtained. The fourth chapter contains the calculation of scattering amplitudes and probabilities of reflection and transmission processes involving one and two photons. Numerical calculations, with realistic parameters, are carried out to check the performance of the quantum switch. The dynamics of operation of this device is derived in this chapter. The possibility of implementing this element into a quantum random access memory is treated in the chapter 5. The sixth chapter contains an interesting discussion of the possibilities of the quantum switch beyond a QRAM.

In the appendices, the reader will find the derivation of some of the formulas and also a review of some (failed) attempts to study the dynamics of operation of the quantum switch.

Chapter 2

The Quantum Switch as a central element

2.1 A first guess

In order to find the right elements that compose a quantum switch it is convenient to write down a basic Hamiltonian containing all the necessary terms to generate the desired interaction. Once the Hamiltonian has been set, we can proceed to find the physical elements –capacitors, inductors, Josephson junctions or other elements of cQED systems– corresponding to each term of the Hamiltonian. To make this process simpler, let us first consider the case where only one incoming transmission line and only one outgoing transmission line are present. This simplified quantum switch has to decide whether the incoming photons (the address register) can be transmitted or not.

As explained before, the address register consists of an array of photons. Each of the photons can be in two states (or a superposition) that tells the quantum switch in which directions the other photons of the register have to be forwarded. These states are defined by the energy of the photons.

The system has to be composed of two artificial "atoms" T and S. The first atom, the control element, absorbs a photon from the incoming transmission line and, depending on the state of the photon, decides whether the other photons will be transmitted through S to the outgoing transmission line or be reflected. The reason for using exactly two elements T and S is simple: the first photon has to be always absorbed by a control element (T), while the other photons are absorbed by S and emitted back into the incoming transmission line or transmitted through S, depending on the state of T. To achieve this goal, the Hamiltonian must contain

kinetic terms describing the energy of the levels of T and S

$$H_0 = \omega_{T1} a_{T1}^\dagger a_{T1} + \omega_{T2} a_{T2}^\dagger a_{T2} + \omega_{S1} a_{S1}^\dagger a_{S1} + \omega_{S2} a_{S2}^\dagger a_{S2}. \tag{2.1}$$

In this equation, $a_{T1}^\dagger$ and $a_{T2}^\dagger$ are the ladder operators that excite the levels of T. $a_{S1}^\dagger$ and $a_{S2}^\dagger$ are the ladder operators that excite the levels of S. Since the photons can only be in two states, with energies ω_{T1} and ω_{T2}, I have only considered the two lowest energy levels of T and S. The energies of the levels satisfy $\omega_{T1} < \omega_{T2}$ and $\omega_{S1} < \omega_{S2}$. I have also chosen $\omega_{T2} - \omega_{T1} \neq \omega_{T1}$ to make sure that it is not possible to excite the second level of T (ω_{T2}) by sending two photons with energy ω_{T1} each. If that were the case, the control element would absorb also the second photon of the register instead of forwarding it. Moreover, there has to be an extra term that, in case that the levels of T are occupied, enforces a shift in the energies of S, so they can be excited by incoming photons with energies ω_{T1} and ω_{T2}.

$$\begin{aligned} H_J = &- J_{11} a_{T1}^\dagger a_{T1} a_{S1}^\dagger a_{S1} - J_{12} a_{T1}^\dagger a_{T1} a_{S2}^\dagger a_{S2} \\ &- J_{21} a_{T2}^\dagger a_{T2} a_{S1}^\dagger a_{S1} - J_{22} a_{T2}^\dagger a_{T2} a_{S2}^\dagger a_{S2}. \end{aligned} \tag{2.2}$$

The elements with J_{ij} decrease the energy of the j-th level in the S atom when the i-th level in the T atom is occupied. I have also included a term that couples T and S to the transmission lines. Actually this term has to couple T and S to the incoming transmission line and only S to the outgoing transmission line, because the photon absorbed by T must not be transmitted.

$$H_c = \frac{a_{T1}^\dagger b_\omega}{\sqrt{\pi\tau}} + \frac{a_{T2}^\dagger b_\omega}{\sqrt{\pi\tau}} + \frac{a_{S1}^\dagger b_\omega}{\sqrt{\pi\tau}} + \frac{a_{S2}^\dagger b_\omega}{\sqrt{\pi\tau}} + \frac{a_{S1}^\dagger c_\omega}{\sqrt{\pi\tau}} + \frac{a_{S2}^\dagger c_\omega}{\sqrt{\pi\tau}} + h.c. \tag{2.3}$$

Here b and c are the frequency-dependent ladder operators for the incoming and outgoing transmission lines, respectively. A momentum integral should be included in this expression to account for all the possible momenta an incoming (or outgoing) photon can have. The coupling constant, which in this simple case I make the same for all the possible processes, has this form to show its explicit dependence on the lifetime τ of the atomic excitations. This equation shows how a photon (b or c) is absorbed (and emitted) by the T or S atom-like elements.

This Hamiltonian can be realized by using a transmon qubit coupled to an incoming transmission line for T; and a SQUID coupled to the same incoming transmission line together with the transmon and also coupled to an outgoing transmission line for S [28, 29]. This device is shown in FIG. 2.1. The Hamiltonian that describes this system is found by performing a Legendre transformation of its Lagrangian (for a derivation of the Lagrangian and also the Hamiltonian see Appendix A).

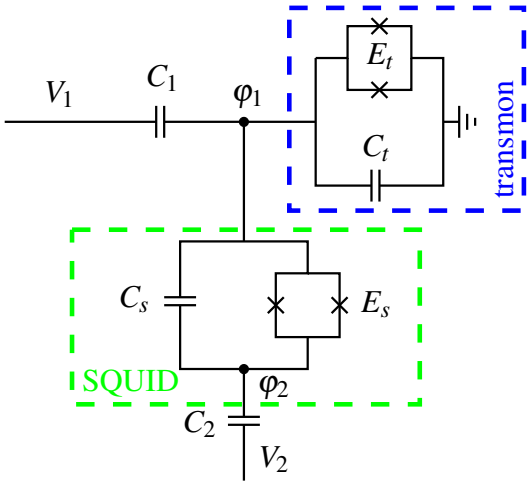

Figure 2.1: *A candidate for a device whose Hamiltonian contains all the desired interactions could be this system composed of a transmon qubit (blue box) with Josephson energy E_t and a SQUID (green box) with Josephson energy E_s. They are capacitively coupled to an incoming transmission line with potential V_1 and an outgoing transmission line with potential V_2. At each node of the circuit a flux can be defined. These are the dynamical variables of the system.*

$$\begin{aligned} L = &\frac{C_1}{2}(\dot{\varphi}_1 - V_1)^2 + \frac{C_2}{2}(\dot{\varphi}_2 - V_2)^2 + \frac{C_s}{2}(\dot{\varphi}_1 - \dot{\varphi}_2)^2 + \frac{C_t}{2}\dot{\varphi}_1^2 \\ &+ E_t \cos\left(\frac{\varphi_1}{\varphi_0}\right) + E_s \cos\left(\frac{\varphi_1 - \varphi_2}{\varphi_0}\right), \end{aligned} \tag{2.4}$$

$$\begin{aligned} H = &\frac{1}{2\gamma}\left(p_1^2 + \frac{C_1 + C_s + C_t}{C_2 + C_s} p_2^2 + \frac{2C_s}{C_2 + C_s} p_1 p_2 \right. \\ &+ 2C_1 V_1 p_1 + 2\frac{C_2 C_s}{C_2 + C_s} V_2 p_1 \\ &\left. + 2C_2 \frac{C_1 + C_s + C_t}{C_2 + C_s} V_2 p_2 + 2\frac{C_1 C_s}{C_2 + C_s} V_1 p_2 \right) \\ &- E_t \cos\left(\frac{\varphi_1}{\varphi_0}\right) - E_s \cos\left(\frac{\varphi_1 - \varphi_2}{\varphi_0}\right), \end{aligned} \tag{2.5}$$

where $\varphi_0 = \hbar/2e$ is the flux quantum divided by 2π, p_1 and p_2 are the conjugate momenta of φ_1 and φ_2 and $\gamma = C_1 + C_t + \frac{C_s C_2}{C_s + C_2}$. This Hamiltonian contains four terms (second and third lines) that describe the coupling between the transmon and the SQUID and the transmission lines. By choosing the right values of

the capacitances it is possible to weaken the interaction between the transmon and the outgoing transmission line (V_2), so the photons absorbed by the transmon are never transmitted forward. From the cosines it is possible obtain H_J after expanding them in a Taylor series and quantizing the fluxes*.

Let me now analyze with more detail the Eq. (2.1, 2.2, 2.3). $a^\dagger_{T1}$ excites the first level of a multilevel system, whereas $a^\dagger_{T2}$ excites a second –or higher– level. These are given by a ladder operator and some power of ladder operators, respectively. This means that, before quantizing the Hamiltonian, there should be different powers of the momenta or the fluxes φ_1 and φ_2 –such as p_1^4 or φ_1^4; these may come from the cosines– and also powers of the fluxes times the potential, such as $p_1^3 V_1$†, that describe how the highest energy level of the transmon (or the SQUID) is excited directly from the ground state with a single photon. These last elements are not in the Hamiltonian derived from (2.4).

2.2 The need for a non-linear element

A Hamiltonian that describes a transmission line coupled to the third level of a transmon –a transmon whose higher energy levels can be excited by the absorption of a single photon, without the need to go through all the lower levels– must contain either $p_1^3 V_1$ or $\varphi_1^3 V_1$. Alternatively, it can contain a function with e.g. $p_1 + V_1$ in its argument such that its Taylor expansion gives rise to the desired interaction.

In cQED circuits there are typically two kinds of elements: capacitive elements, whose energy depends on the derivative of fluxes and on potentials; and inductive elements, whose energy depends only on the fluxes, such as inductors or Josephson junctions [29]. An inductive element cannot depend on $\varphi - V$‡, the element to be introduced in the system has to be a capacitive element. If this is a capacitor whose capacitance is a non-linear function of the potential –and its energy is not a quadratic function of the potential–, the Hamiltonian may contain a function that depends on $\dot{\varphi}$ and V and whose Taylor expansion will give rise to the desired terms§.

*See Appendix A

†The Hamiltonian must contain even powers of operators to ensure that the energy is conserved (bounded from below). Thus, the coupling to the transmission lines is given by $p_1^3 V_1$. This means that the third –and not the second– level of the transmon (or the SQUID) is coupled to the transmission lines. This coupling is obtained in Chapter 3.

‡This follows from the Kirchhoff's circuit laws and the dependence of the current on the flux and momentum for the different inductive elements [30].

§If the energy of the capacitor is not a quadratic function of the potential, then the Legendre

Non-linear capacitors are not common in this kind of circuits, but they have been studied for decades. In the related literature capacitors with two different non-linear behaviors can be found. Some of them are made of ferroelectric thin films or ferroelectric ceramics and show a capacitance that decreases with the applied voltage [31–33]. Others show a capacitance that increase with the voltage, such as those made out of antiferroelectric materials [34] or semiconductor devices that, under some conditions, behave as non-linear capacitors due to the presence of a space charge near a junction [35].

There is another well studied semiconductor device that show both behaviors: the MOS capacitor. Depending on whether it is a p-type or a n-type MOS, it will exhibit a capacitance that increases or decreases with the voltage [36–38].

Some work has been done on the quantum level as well. The capacitance due to the presence of quantum wells in heterojunctions gives rise to a strong non-linear behavior of the capacitor, whose capacitance drops off very fast with small variations of the potential [39]. Another source of non-linear behavior is the finiteness of the density of states (DOS) in small devices. For a two-plate capacitor, this gives rise to a capacitance that decreases for increasing potential [40]. But, if carbon nanotubes are placed between the plates of the capacitor, due to the finiteness of the DOS of the nanotubes the capacitance will increase with small variations of the potential [41, 42].

In the model I propose I am using a non-linear capacitor with a behavior similar to the last one. For simplicity I have used a curve for $C(V)$ (capacitance as a function of the potential across the plates of the capacitor) only valid near $V \to 0$, given that only (small) quantum fluctuations of V have been considered. The capacitance as a function of the potential I have used is

$$C(V) = C_0 + C_1 V^2. \tag{2.6}$$

If the chosen capacitor had a capacitance given by $C(V) = C_0 - C_1 V^2$ or $C(V) = C_0 \pm C_1 V$, the obtained Hamiltonian would not conserve energy. The energy of a ferroelectric or a MOS capacitor, expanded in a Taylor series around small V, is a function that is not bounded from below. With these capacitors, the Hamiltonian drives the system to a region with large values of V. In this new domain, the Taylor expansion is no longer a valid approximation, so it does not make sense to consider only small potentials. The only way to obtain a Hamiltonian that

transformation may give rise to a non-quadratic function of the potential whose Taylor expansion gives terms with higher powers of the momentum.

does not contain terms such as $a^\dagger$ or $a^\dagger a^\dagger a$ (odd powers of the momentum or the flux) is to use Eq. (4.33) for the voltage dependence of the capacitor, leading to an energy function of the form

$$E(V) = \frac{C}{2}\left(V^2 + \alpha V^4\right). \tag{2.7}$$

As will be shown later on (Section 2.5), the odd energy levels of a transmon constructed with this capacitor are coupled to the transmission lines, whereas the even levels are not. It is only possible to excite an even level if an odd (inferior) level had been excited first.

2.3 A multilevel device using non-linear capacitors

Consider the system shown in FIG. 2.2. It contains the three required transmission lines. This device is composed of a transmon qubit with a non-linear capacitor and two SQUIDs with linear capacitors. I have not included non-linear capacitors on the SQUIDs because they would make impossible to perform the Legendre transformation of the Lagrangian analytically. Moreover, with one non-linear capacitor is enough to generate all the desired interactions. Using Eq. (2.7) for the energy of the nonlinear capacitor in the transmon, the Lagrangian of this system reads

$$\begin{aligned} L =& \frac{C_1}{2}(\dot{\varphi}_1 - V_1)^2 + \frac{C_2}{2}(\dot{\varphi}_2 - V_2)^2 + \frac{C_3}{2}(\dot{\varphi}_3 - V_3)^2 \\ &+ \frac{C_{s2}}{2}(\dot{\varphi}_1 - \dot{\varphi}_2)^2 + \frac{C_{s3}}{2}(\dot{\varphi}_1 - \dot{\varphi}_3)^2 + \frac{C_t}{2}\left(\dot{\varphi}_1^2 + \alpha_t \dot{\varphi}_1^4\right) \\ &+ E_{Jt}\cos\left(\frac{\varphi_1}{\varphi_0}\right) + E_{J2}\cos\left(\frac{\varphi_1 - \varphi_2}{\varphi_0}\right) + E_{J3}\cos\left(\frac{\varphi_1 - \varphi_3}{\varphi_0}\right). \end{aligned} \tag{2.8}$$

Despite the presence of the nonlinear equation, the Hamiltonian can be constructed analytically with the conjugate momenta p_1, p_2 and p_3 and the fluxes defined, as a function of the momenta, as

$$\dot{\varphi}_1 = \frac{2^{1/3}\gamma}{f(x)} - \frac{f(x)}{2^{1/3}\beta} \tag{2.9}$$

$$\dot{\varphi}_2 = \frac{p_2 + C_2 V_2 + C_{s2}\dot{\varphi}_1}{C_2 + C_{s2}} \tag{2.10}$$

$$\dot{\varphi}_3 = \frac{p_3 + C_3 V_3 + C_{s3}\dot{\varphi}_1}{C_3 + C_{s3}}, \tag{2.11}$$

Version of June 29, 2015– Created June 29, 2015 - 21:15

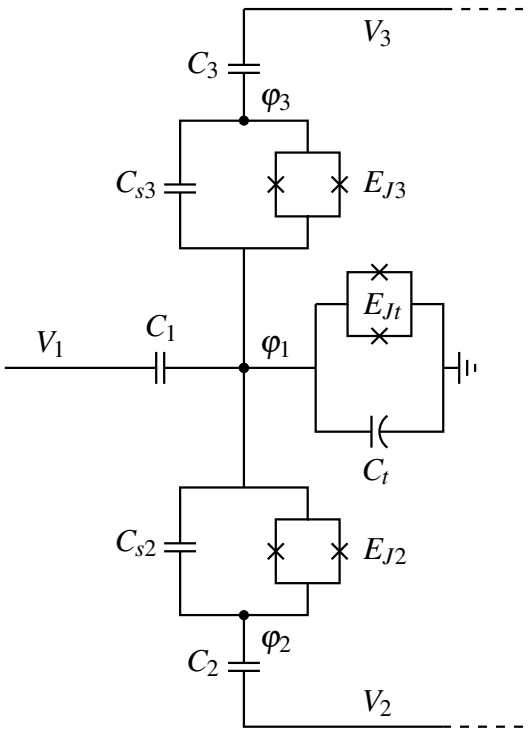

Figure 2.2: *This system contains one incoming (V_1) and two outgoing (V_2, V_3) transmission lines. It is composed of a transmon with a non-linear capacitor (C_t) and two SQUIDs with linear capacitors (the symbol used for the non-linear capacitor is also a commonly used symbol for capacitors, especially in the US, but is not the generic).*

with

$$f(x) = \left(-3\beta^2 x + \sqrt{4\beta^3\gamma^3 + (3\beta^2 x)^2} \right)^{1/3} \tag{2.12}$$

$$\beta = 6C_t\alpha_t \tag{2.13}$$

$$\gamma = C_1 + C_t + \frac{C_2 C_{s2}}{C_2 + C_{s2}} + \frac{C_3 C_{s3}}{C_3 + C_{s3}} \tag{2.14}$$

$$x = p_1 + C_1 V_1 + \frac{C_{s2}}{C_2 + C_{s2}} (p_2 + C_2 V_2) + \frac{C_{s3}}{C_3 + C_{s3}} (p_3 + C_3 V_3) . \tag{2.15}$$

The resulting Hamiltonian contains the function $f(x)$, which is not an easy function to work with. Instead I have expanded the Hamiltonian in a Taylor series in x. Since the Hamiltonian must contain interactions such as a coupling between the third level of the transmon and the third level of the SQUID, a term containing three times $a^\dagger a$ for the transmon and three times $a^\dagger a$ for the SQUID should appear

in the equation, i.e., a product of up to twelve momenta (each of them contains one ladder operator, and a total of 12 is needed). To obtain this term, the Taylor expansion of the Hamiltonian goes up to the twelfth order:

$$\begin{aligned} H =& \frac{p_2^2 + 2p_2C_2V_2 - C_{s2}C_2V_2^2}{2(C_2+C_{s2})} + \frac{p_3^2 + 2p_3C_3V_3 - C_{s3}C_3V_3^2}{2(C_3+C_{s3})} - \frac{C_1V_1^2}{2} \\ &+ \frac{x^2}{2\gamma} - \frac{\beta x^4}{12\gamma^4} + \frac{\beta^2 x^6}{18\gamma^7} - \frac{\beta^3 x^8}{18\gamma^{10}} + \frac{11\beta^4 x^{10}}{162\gamma^{13}} - \frac{91\beta^5 x^{12}}{927\gamma^{16}} \\ &- E_{Jt}\cos\left(\frac{\varphi_1}{\varphi_0}\right) - E_{J2}\cos\left(\frac{\varphi_1-\varphi_2}{\varphi_0}\right) - E_{J3}\cos\left(\frac{\varphi_1-\varphi_3}{\varphi_0}\right). \end{aligned} \tag{2.16}$$

After replacing x by the expression in Eq. (2.15), the Hamiltonian contains $V_1^2p_1^2$, $V_1^3p^2$, etc, which describe the process where one or several transmon states decay into more than one photon in the transmission lines or several photons are absorbed by the transmon at the same time. These processes must be eliminated. To do so I have expanded the Hamiltonian in a power series of V_1, V_2 and V_3 and I have checked under what conditions on the capacitances terms of order $O(V^2)$ can be omitted (C_1, C_{s2}, C_{s3} smaller that C_2, C_3).

Next I have also also expanded the Hamiltonian in Eq. (2.16) for p_1, p_2 and p_3, keeping only the largest terms, up to order $O(p^6)$ –that is, keeping p_1^6 and also $p_1^6p_2^6$. The final equation can be separated in six parts, each of them describing a different behavior. The first equation, H_1, contains even powers of the momenta and the fluxes without mixing them. From this expression, the Hamiltonian describing the energy of the levels can be derived.

$$\begin{aligned} H_1 =& \frac{1}{2\gamma}p_1^2 + \left(\frac{1}{2(C_2+C_{s2})} + \frac{C_{s2}^2}{2(C_2+C_{s2})^2\gamma}\right)p_2^2 \\ &+ \left(\frac{1}{2(C_3+C_{s3})} + \frac{C_{s3}^2}{2(C_3+C_{s3})^2\gamma}\right)p_3^2 \\ &- \frac{\beta}{12\gamma^4}p_1^4 - \frac{C_{s2}^4\beta}{12(C_2+C_{s2})^4\gamma^4}p_2^4 - \frac{C_{s3}^4\beta}{12(C_3+C_{s3})^4\gamma^4}p_3^4 \\ &+ \frac{\beta^2}{18\gamma^7}p_1^6 + \frac{C_{s2}^6\beta^2}{18(C_2+C_{s2})^6\gamma^7}p_2^6 + \frac{C_{s3}^6\beta^2}{18(C_3+C_{s3})^6\gamma^7}p_3^6 \\ &- (E_{Jt}+E_{J2}+E_{J3})\cos\left(\frac{\varphi_1}{\varphi_0}\right) - E_{J2}\cos\left(\frac{\varphi_2}{\varphi_0}\right) - E_{J3}\cos\left(\frac{\varphi_3}{\varphi_0}\right). \end{aligned} \tag{2.17}$$

The cosines have been conveniently separated using trigonometrical identities and placed inside the different expressions that conform the Hamiltonian, according to the physical processes they describe. The second part of the Hamiltonian

describes the coupling between the energy levels. It contains products of even powers of the momenta and also the fluxes:

$$\begin{aligned} H_2 = & \sum_{\substack{i=1 \\ j>i}}^{3} \sum_{m=1}^{3} \sum_{n=1}^{3} A_{ijmn} p_i^{2m} p_j^{2n} \\ & - E_{J2} \left(\cos\left(\frac{\varphi_1}{\varphi_0} \right) - 1 \right) \left(\cos\left(\frac{\varphi_2}{\varphi_0} \right) - 1 \right) \\ & - E_{J3} \left(\cos\left(\frac{\varphi_1}{\varphi_0} \right) - 1 \right) \left(\cos\left(\frac{\varphi_3}{\varphi_0} \right) - 1 \right). \end{aligned} \tag{2.18}$$

The coefficients A_{ijmn} can be found in the Appendix B. The interaction with the transmission lines, also obtained by expanding the Hamiltonian in Eq. (2.16), is described by

$$\begin{aligned} H_3 = & \left(C_1 V_1 + \frac{C_{s2} C_2 V_2}{C_{s2} + C_2} + \frac{C_{s3} C_3 V_3}{C_{s3} + C_3} \right) \frac{1}{\gamma} p_1 \\ & - \left(C_1 V_1 + \frac{C_{s2} C_2 V_2}{C_{s2} + C_2} + \frac{C_{s3} C_3 V_3}{C_{s3} + C_3} \right) \left(\frac{\beta}{3\gamma^4} \right) p_1^3 \\ & + \left(\left(C_1 V_1 + \frac{C_{s2} C_2 V_2}{C_{s2} + C_2} + \frac{C_{s3} C_3 V_3}{C_{s3} + C_3} \right) \left(\frac{C_{s2}}{(C_{s2} + C_2)\gamma} \right) + \frac{C_2 V_2}{(C_{s2} + C_2)} \right) p_2 \\ & - \left(C_1 V_1 + \frac{C_{s2} C_2 V_2}{C_{s2} + C_2} + \frac{C_{s3} C_3 V_3}{C_{s3} + C_3} \right) \left(\frac{\beta}{3\gamma^4} \right) \left(\frac{C_{s2}}{C_{s2} + C_2} \right)^3 p_2^3 \\ & + \left(\left(C_1 V_1 + \frac{C_{s2} C_2 V_2}{C_{s2} + C_2} + \frac{C_{s3} C_3 V_3}{C_{s3} + C_3} \right) \left(\frac{C_{s3}}{(C_{s3} + C_3)\gamma} \right) + \frac{C_3 V_3}{(C_{s3} + C_3)} \right) p_3 \\ & - \left(C_1 V_1 + \frac{C_{s2} C_2 V_2}{C_{s2} + C_2} + \frac{C_{s3} C_3 V_3}{C_{s3} + C_3} \right) \left(\frac{\beta}{3\gamma^4} \right) \left(\frac{C_{s3}}{C_{s3} + C_3} \right)^3 p_3^3. \end{aligned} \tag{2.19}$$

This expression shows that only the odd levels of the transmon (and the SQUIDs) are coupled to the transmission lines. For another choice of the capacitance behavior a different system may be obtained, e.g., a system that couples also the even levels of the transmon with the transmission lines[¶].

In the present system, there is also a term (H_4) that describes an exchange interaction between the transmon and the SQUIDs[‖].

[¶] But within these Hamiltonians, other terms that do not conserve the energy and the particle numbers would emerge.

[‖] All these expressions are obtained by expanding the x variables [defined in Eq. (2.15) together with the cosines] inside the Hamiltonian in Eq. (2.16).

$$H_4 = \sum_{n=1}^{3}\sum_{m=1}^{3}\left(B_{2nm}p_1^{2n-1}p_2^{2m-1} + B_{3nm}p_1^{2n-1}p_3^{2m-1}\right) - E_{J2}\sin\left(\frac{\varphi_1}{\varphi_0}\right)\sin\left(\frac{\varphi_2}{\varphi_0}\right) - E_{J3}\sin\left(\frac{\varphi_1}{\varphi_0}\right)\sin\left(\frac{\varphi_3}{\varphi_0}\right). \tag{2.20}$$

Again, the coefficients B_{2nm} and B_{3nm} are found in the Appendix B. The Hamiltonian H_5, displayed in Eq. (B.1), describes processes such as the annihilation of two excitations of the transmon and the creation of an excitation on one SQUID and an outgoing photon in the transmission lines. In such processes, the information contained in the photons is lost.

Finally, there is another expression that contains SQUID-SQUID and SQUID-SQUID-transmon exchange interactions. This expression is not included in the thesis due to its extension, but is not a relevant expression because a slightly different system will be introduced (in the following sections) that do not present this interactions. In the previous expressions the terms describing only the transmission lines have been omitted. They will be included a posteriori.

Although it contains the terms that are required for a quantum switch, this Hamiltonian presents some problems:

a) One of them is the Hamiltonian H_4. Within this expression, the sine functions can be tuned to make them cancel some of the terms, but not all of them. There are some undesired interactions left.

b) Another problematic expression is H_5. According to this expression, an excitation in the SQUID can decay into a lower excitation of the transmon plus an outgoing photon in the transmission lines. In this case, the outgoing photon would lose the information it contained and the device would not work properly due to the presence of an excitation where it should not be. The interaction strengths of these processes are too large –compared to those of H_3– to neglect them.

c) Finally, the SQUID-SQUID and SQUID-SQUID-transmon exchange interactions also threaten to give important errors. During the process of transmission of a photon it is important to control exactly which levels are excited and which are not.

The solution to these problems necessarily involves finding some variation of the circuit shown in FIG. 2.2 that cancels –or minimizes– H_4 and H_5 but preserves

H_1, H_2 and H_3 because these describe the correct operation of the quantum switch I am looking for. These solutions could be:

i) Regarding H_4, I can get rid of it by introducing some inductive elements between the SQUIDs, such as a pair of Josephson junctions or a coil. The Hamiltonian of these elements contains a cosine of the fluxes $\varphi_2 - \varphi_3$ (in the case of a Josephson junction) whose Taylor expansion will cancel H_4.

ii) The Hamiltonian H_5, on the other hand, is more tricky. Imagine that a photon is sent to the switch. This photon can have energies ω_1 or ω_2. I am only interested in two processes –considering now that there is only one outgoing transmission line– namely: either the incoming photon with frequency ω_1 (ω_2) is absorbed and reflected back with energy ω_1 (ω_2) or it is absorbed and transmitted forward with energy ω_1' (ω_2'). The expression H_5 describes other possibilities such as the emission of a photon with energy $\omega_1'' < \omega_1'$ with the subsequent loss of information because it is not possible to know what was the previous state of the photon before the interaction took place and is also not possible to know what interaction took place. To avoid these processes some kind of filters can be introduced in the transmission lines such that they only accept photons that have the right energy. In this way the processes contained in H_5 cannot happen. Special care has to be taken when introducing these new elements because they may modify the entire Hamiltonian.

2.4 Frequency filters in the transmission lines

Different kinds of filters can be found in the electronics literature [43]. Some of them contain resistors, other contain capacitors and inductors, etc. Given that the cQED elements used in this work are capacitors and inductors, these are the filters I am considering to use. The high pass LC filter, schematically drawn in FIG. 2.3 seems to be the adequate device: it does not allow photons with frequencies below ω_1 and photons with higher frequencies pass through.

The Hamiltonian describing the device in FIG. 2.3 is given by (see [30])

$$H_{hp} = \frac{1}{2(C_1+C_2)}p^2 + \frac{C_1V_1}{C_1+C_2}p + \frac{C_2V_2}{C_1+C_2}p - \frac{C_1C_2}{2(C_1+C_2)}(V_1+V_2)^2 + \frac{\varphi^2}{2L}. \tag{2.21}$$

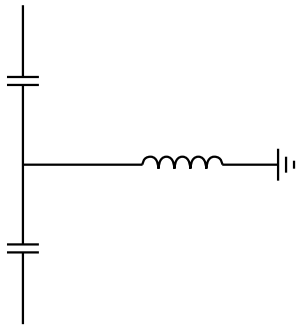

Figure 2.3: *Diagram of a high pass LC circuit containing two capacitors and an inductor. At one end of the circuit (e.g., at the top) there is the whole quantum switch and at the other end (bottom) there is one outgoing transmission line.*

Once quantized it reads**

$$H_{hp,q} = \omega_1 a^\dagger a + \int dp \left(\frac{b_1^\dagger a + a^\dagger b_1}{\sqrt{\pi\tau_1}} + \frac{b_2^\dagger a + a^\dagger b_2}{\sqrt{\pi\tau_2}} \right) + \int dp\, p \left(b_1^\dagger b_1 + b_2^\dagger b_2 \right). \tag{2.22}$$

According to this Hamiltonian, when a photon ($b^\dagger$) with frequency $\omega < \omega_1$ (ω_1 is the threshold frequency) goes in it is reflected, because it cannot excite the system. If the frequency is ω_1, then it excites the system ($a^\dagger$) and it decays into the outgoing transmission line. But if the frequency is larger than ω_1, it cannot transmit the whole photon: the information is lost.

Since the incoming photons may be in two different states, I need a cavity with two resonant frequencies that routes the photons forward. For this purpose a transmon or a system composed of two high pass LC filters can be used. In case a transmon is used, this must contain a non-linear capacitance so any of its energy levels can be selectively excited from the ground state. The problem with using a transmon is that three levels have to be considered, and the three excited levels may be coupled in the sense that an excitation in the third level can decay into the second level and emit a low energy photon in the transmission line. Thus, this does not solve the problems. Another problem that can arise when using a transmon is that due to the interaction between the inductive and the capacitive elements, the lifetime of its excited levels is larger than in the case of a simple filter.

**See Appendix A for the procedure followed for the quantization of a Hamiltonian.

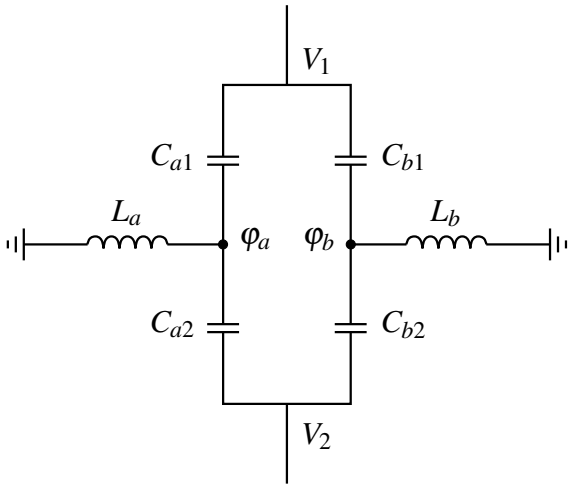

Figure 2.4: *Device proposed to act as a high pass filter. It will allow to transmit pulses of two definite frequencies. A pulse coming from the transmission line 1 (V_1) with frequency ω_a can excite the oscillator in the branch a and be transmitted into transmission line 2 (V_2). If the incoming photon has frequency ω_b the same will happen with the other branch, whereas if the frequency is neither ω_a nor ω_b, the pulse will not be transmitted.*

On the other hand, when using a system of high pass LC filters like the one shown in FIG. 2.4, with Hamiltonian

$$H_f = \frac{q_a^2}{2(C_{a1}+C_{a2})} + \frac{q_b^2}{2(C_{b1}+C_{b2})} + \frac{C_{a1}V_1 + C_aV_2}{C_{a1}+C_{a2}}q_a + \frac{C_{b1}V_1 + C_bV_2}{C_{b1}+C_{b2}}q_b - \frac{1}{2}\left(\frac{C_{a1}C_{a2}}{C_{a1}+C_{a2}} + \frac{C_{b1}C_{b2}}{C_{b1}+C_{b2}}\right)(V_1+V_2)^2 + \frac{\varphi_a^2}{2L_a} + \frac{\varphi_b^2}{2L_b}, \tag{2.23}$$

the resulting device has two levels that do not interact with each other. Since it does not contain a transmon inside, the lifetime of the excitations is small and the photons are transmitted fast. Nevertheless, there is a drawback in this system when compared to the transmon: in the transmon there is only one flux, whereas here there are two. Two fluxes mean two "artificial atoms". Two more atoms that have to be coherently coupled to the rest of the system.

2.5 An alternative solution

I could introduce any of these two elements (transmon or high pass LC filter) into the device, yielding a system with either five independent fluxes that represent five multilevel atoms or seven fluxes representing three multilevel atoms plus four

two-level atoms[††]. In both cases there are lots of possible excited levels –coming from the large number of fluxes and the large number of levels per atom– and thus, lots of sources of decoherence. Moreover, if I introduce these extra elements, the Hamiltonian will be modified, yielding a system where a photon has to interact with many elements before it can be transmitted and, probably, other processes that destroy the information contained in the photons may emerge from this new Hamiltonian. In order to simplify the system but introducing some elements that guarantee the proper operation of the quantum switch I propose a slightly different design from that of FIG. 2.2. Instead of two multilevel SQUIDs I use four modified high-pass filters. These elements, containing Josephson junctions instead of coils, are two-level SQUIDs. The new system is shown in FIG. 2.5. This reduction of the levels of the SQUIDs drastically reduces the amount of possible interactions between the different energy levels that give, as an output, an outgoing photon with the "wrong" energy (i.e., an outgoing photon with an energy different from that of the incoming photons. The device should not change the energy of the photons).

This device contains one multilevel transmon with a non-linear capacitor and four two-level SQUIDs. This translates into a flux with three excitations and four more fluxes with just one excitation each, as will be shown in Section 3.1.

With this setup, when a photon is absorbed by the transmon, the energy levels of the filters are modified due to the Josephson elements in the SQUIDs. With regular inductors this would not happen because their energy do not contain high enough powers of the fluxes involved in this interaction, as it is the case for the SQUIDs [28–30]. I expect that when a second photon comes in –after the first is absorbed by the transmon and the energy levels of all the SQUIDs are modified–, it excites the only SQUIDd available and is decays into one of the outgoing transmission lines. Since these SQUIDs are two-level systems, the information carried by the photons will not be lost by the same mechanism as it was with the previous design (see Section 2.3).

Now let us analyze the Hamiltonian for this device (FIG. 2.5). The Lagrangian

[††]Transmons and SQUIDs are always multilevel systems. Whenever the word *multilevel* is used, it refers to a system where the higher energy levels can be excited directly from the ground state. Moreover, the Hilbert space is conveniently limited and only the few energy levels needed are considered. Therefore, when I talk about a two-level system, what I mean is that only the ground state and the first excited state are considered, whereas the possibility of exciting higher levels is neglected. Whenever I talk about multilevel systems I am referring to systems where the higher energy levels are actually used.

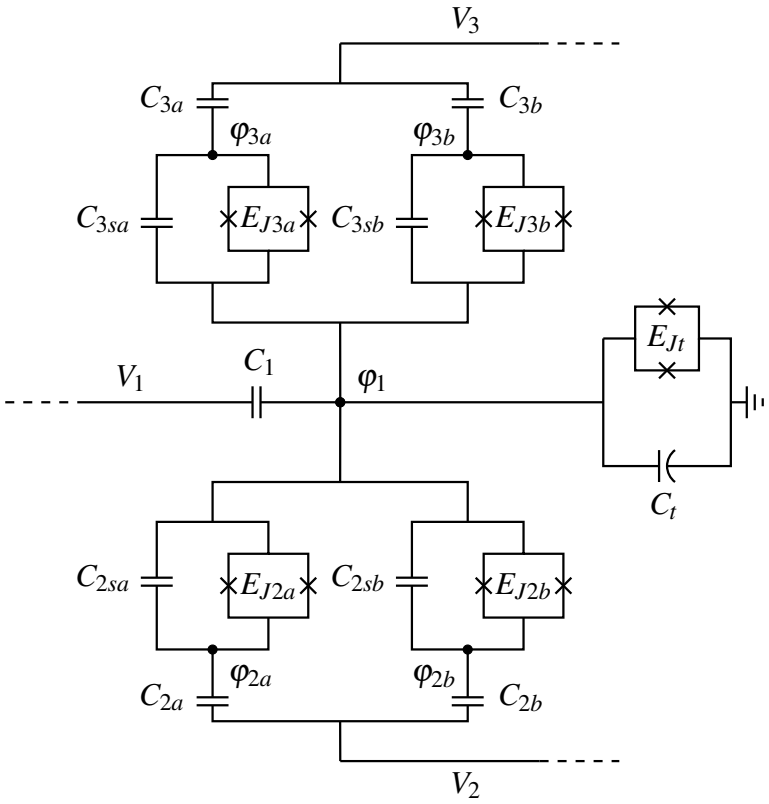

Figure 2.5: *This is the diagram of a device with two filters in the outgoing branches, containing two SQUIDs each. There are a total of five different fluxes –one at each node, black circles–, instead of the three of the previous design (FIG. 2.2), but in this case only the higher energy levels of the transmon are considered. I will treat the SQUIDs as two-level systems because I am not interested in exciting their higher energy levels.*

from which the Hamiltonian is derived is

$$\begin{aligned}
L =& \frac{C_{2a}}{2}(\dot{\varphi}_{2a}-V_2)^2+\frac{C_{2b}}{2}(\dot{\varphi}_{2b}-V_2)^2+\frac{C_{3a}}{2}(\dot{\varphi}_{3a}-V_3)^2+\frac{C_{3b}}{2}(\dot{\varphi}_{3b}-V_3)^2\\
&+\frac{C_{2sa}}{2}(\dot{\varphi}_1-\dot{\varphi}_{2a})^2+\frac{C_{2sb}}{2}(\dot{\varphi}_1-\dot{\varphi}_{2b})^2+\frac{C_{3sa}}{2}(\dot{\varphi}_1-\dot{\varphi}_{3a})^2+\frac{C_{3sb}}{2}(\dot{\varphi}_1-\dot{\varphi}_{3b})^2\\
&+\frac{C_1}{2}(\dot{\varphi}_1-V_1)^2+\frac{C_t}{2}\left(\dot{\varphi}_1^2+\alpha_t\dot{\varphi}_1^4\right)+E_{Jt}\cos\left(\frac{\varphi_1}{\varphi_0}\right)\\
&+E_{J2a}\cos\left(\frac{\varphi_1-\varphi_{2a}}{\varphi_0}\right)+E_{J2b}\cos\left(\frac{\varphi_1-\varphi_{2b}}{\varphi_0}\right)\\
&+E_{J3a}\cos\left(\frac{\varphi_1-\varphi_{3a}}{\varphi_0}\right)+E_{J3b}\cos\left(\frac{\varphi_1-\varphi_{3b}}{\varphi_0}\right).
\end{aligned} \tag{2.24}$$

The time derivative of the fluxes as a function of the momenta are

$$\begin{aligned}
\dot{\varphi}_{2a} =& \frac{p_{2a}+C_{2a}V_2+C_{2sa}\dot{\varphi}_1}{C_{2a}+C_{2sa}}\\
\dot{\varphi}_{2b} =& \frac{p_{2b}+C_{2b}V_2+C_{2sb}\dot{\varphi}_1}{C_{2b}+C_{2sb}},
\end{aligned} \tag{2.25}$$

with a similar expression for $\dot{\varphi}_{3a}$ and $\dot{\varphi}_{3b}$, and

$$\dot{\varphi}_1 = \frac{2^{1/3}\gamma}{f(x)}-\frac{f(x)}{2^{1/3}\beta}, \tag{2.26}$$

with

$$\gamma = C_1+C_t+\frac{C_{2a}C_{2sa}}{C_{2a}+C_{2sa}}+\frac{C_{2b}C_{2sb}}{C_{2b}+C_{2sb}}+\frac{C_{3a}C_{3sa}}{C_{3a}+C_{3sa}}+\frac{C_{3b}C_{3sb}}{C_{3b}+C_{3sb}} \tag{2.27}$$

$$\beta = 6C_t\alpha_t \tag{2.28}$$

$$\begin{aligned}
x =& p_1+C_1V_1+\frac{C_{2sa}}{C_{2a}+C_{2sa}}(p_{2a}+C_{2a}V_2)+\frac{C_{2sb}}{C_{2b}+C_{2sb}}(p_{2b}+C_{2b}V_2)\\
&+\frac{C_{3sa}}{C_{3a}+C_{3sa}}(p_{3a}+C_{3a}V_3)+\frac{C_{3sb}}{C_{3b}+C_{3sb}}(p_{3b}+C_{3b}V_3)
\end{aligned} \tag{2.29}$$

$$f(x) = \left(-3\beta^2x+\sqrt{4\beta^3\gamma^3+(3\beta^2x)^2}\right)^{1/3}. \tag{2.30}$$

These expressions are similar to the ones found before, so a similar Hamiltonian is expected. Previously I had to expand the flux $\dot{\varphi}_1$ in a power series of x up to $O(x^{12})$ [see Section 2.3, Eq. (2.16)]. Since now the SQUIDs contain only one excited level –the excitation of the SQUID $2a$ plays the role of the *first excitation*

and the excitation of the SQUID $2b$ plays the role of the *second excitation*– I only need to expand the flux up to $O(x^8)$. The Hamiltonian, up to this order, reads

$$\begin{aligned}
H =& -\frac{C_1 V_1^2}{2} + \frac{p_{2a}^2 + 2p_{2a}C_{2a}V_2 - C_{2sa}C_{2a}V_2^2}{2(C_{2a}+C_{2sa})} + \frac{p_{2b}^2 + 2p_{2b}C_{2b}V_2 - C_{2sb}C_{2b}V_2^2}{2(C_{2b}+C_{2sb})} \\
&+ \frac{p_{3a}^2 + 2p_{3a}C_{3a}V_2 - C_{3sa}C_{3a}V_3^2}{2(C_{3a}+C_{3sa})} + \frac{p_{3b}^2 + 2p_{3b}C_{3b}V_3 - C_{3sb}C_{3b}V_3^2}{2(C_{3b}+C_{3sb})} \\
&+ \frac{x^2}{2\gamma} - \frac{\beta x^4}{12\gamma^4} + \frac{\beta^2 x^6}{18\gamma^7} - \frac{\beta^3 x^8}{18\gamma^{10}} - E_{Jt}\cos\left(\frac{\varphi_1}{\varphi_0}\right) \\
&- E_{J2a}\cos\left(\frac{\varphi_1-\varphi_{2a}}{\varphi_0}\right) - E_{J2b}\cos\left(\frac{\varphi_1-\varphi_{2b}}{\varphi_0}\right) \\
&- E_{Ja}\cos\left(\frac{\varphi_1-\varphi_{3a}}{\varphi_0}\right) - E_{J3b}\cos\left(\frac{\varphi_1-\varphi_{3b}}{\varphi_0}\right).
\end{aligned} \tag{2.31}$$

This Hamiltonian has to be expanded, as before, in powers of the momenta to extract all the relevant interactions. To expand Eq. (2.31) I have imposed $C_{2a} > C_{2sa}$ and the same for the other three SQUIDs. I have also made C_1 small, but not necessarily as small as C_{s2a}. Previously I kept some powers of $C_{s2}/(C_2+C_{s2})$ because they were multiplying some expressions in the Taylor expansion of the Hamiltonian in Eq. (2.16) that I had to keep in order to give rise to interactions between higher SQUID energy levels, although these factors (and their powers) were small. Now I can be more strict and get rid of all the terms of order $(\frac{C_{2sa}}{C_{2a}+C_{2sa}})^3$ or smaller because now the SQUIDs are two-level systems. Taking into account these considerations, the Hamiltonian can be separated in seven different expressions, which I now discuss

$$\begin{aligned}
H_1 =& \frac{p_1^2}{2\gamma} - \frac{\beta p_1^4}{12\gamma^4} + \frac{\beta^2 p_1^6}{18\gamma^7} \\
&+ \frac{1}{2}\left(1 + \frac{C_{2sa}^2}{(C_{2a}+C_{2sa})\gamma}\right)\frac{p_{2a}^2}{C_{2a}+C_{2sa}} + \frac{1}{2}\left(1 + \frac{C_{2sb}^2}{(C_{2b}+C_{2sb})\gamma}\right)\frac{p_{2b}^2}{C_{2b}+C_{2sb}} \\
&+ \frac{1}{2}\left(1 + \frac{C_{3sa}^2}{(C_{3a}+C_{3sa})\gamma}\right)\frac{p_{3a}^2}{C_{3a}+C_{3sa}} + \frac{1}{2}\left(1 + \frac{C_{3sb}^2}{(C_{3b}+C_{3sb})\gamma}\right)\frac{p_{3b}^2}{C_{3b}+C_{3sb}} \\
&- (E_{Jt}+E_{J2a}+E_{J2b}+E_{J3a}+E_{J3b})\cos\left(\frac{\varphi_1}{\varphi_0}\right) \\
&- E_{J2a}\cos\left(\frac{\varphi_{2a}}{\varphi_0}\right) - E_{J2b}\cos\left(\frac{\varphi_{2b}}{\varphi_0}\right) \\
&- E_{J3a}\cos\left(\frac{\varphi_{3a}}{\varphi_0}\right) - E_{J3b}\cos\left(\frac{\varphi_{3b}}{\varphi_0}\right).
\end{aligned} \tag{2.32}$$

H_1 [Eq. (2.32)] contains information about the energy of the transmon and SQUID excitations. Just as before, the cosines have been separated and sorted into the different expressions that form the Hamiltonian.

The coupling between the different levels is contained in H_2.

$$H_2 = \sum_k \left(\sum_{i=1}^{3} A'_{ik} p_1^{2i} p_k^2 - E_{Jk} \left(\cos \frac{\varphi_1}{\varphi_0} - 1 \right) \left(\cos \frac{\varphi_k}{\varphi_0} - 1 \right) \right), \tag{2.33}$$

where $k \in \{2a, 2b, 3a, 3b\}$. The reader is referred to Appendix B (Section B.2) for a complete definition of all the coefficients in this expression.

The SQUIDs have to be coupled to the transmission lines. Actually they are coupled to all the transmission lines but, as expected, they are strongly coupled only to their nearest transmission line, whereas the transmon is weakly coupled to all the transmission lines. This makes its lifetime larger. This is expressed in the Hamiltonian H_3:

$$H_3 = \sum_{i=1}^{3} \left(B'_{i1} V_i p_1 + B'_{i3} V_i p_1^3 + \sum_k B'_{ik} V_i p_k \right), \tag{2.34}$$

with the coefficients B'_{ik} also found in the aforementioned Appendix. The Hamiltonian also contains some terms that describe the exchange of excitations between the transmon and the SQUIDs (H_4) and also between the SQUIDs ($H_{4.2}$):

$$\begin{aligned} H_4 = &\left(\frac{1}{\gamma} p_1 - \frac{\beta}{3\gamma^4} p_1^3 + \frac{\beta^2}{3\gamma^7} p_1^5 \right) \frac{C_{2sa}}{C_{2a} + C_{2sa}} p_{2a} \\ &- E_{J2a} \sin \left(\frac{\varphi_1}{\varphi_0} \right) \sin \left(\frac{\varphi_{2a}}{\varphi_0} \right) + \{2a \to 2b,\ 3a,\ 3b\}, \end{aligned} \tag{2.35}$$

$$\begin{aligned} H_{4.2} = &\frac{C_{2sa}}{C_{2a} + C_{2sa}} \frac{C_{2sb}}{C_{2b} + C_{2sb}} \frac{p_{2a} p_{2b}}{\gamma} + \frac{C_{3sa}}{C_{3a} + C_{3sa}} \frac{C_{3sb}}{C_{3b} + C_{3sb}} \frac{p_{3a} p_{3b}}{\gamma} \\ &+ \frac{C_{2sa}}{C_{2a} + C_{2sa}} \frac{C_{3sb}}{C_{3b} + C_{3sb}} \frac{p_{2a} p_{3b}}{\gamma} + \frac{C_{3sa}}{C_{3a} + C_{3sa}} \frac{C_{2sb}}{C_{2b} + C_{2sb}} \frac{p_{3a} p_{2b}}{\gamma} \\ &+ \frac{C_{2sa}}{C_{2a} + C_{2sa}} \frac{C_{3sa}}{C_{3a} + C_{3sa}} \frac{p_{2a} p_{3a}}{\gamma} + \frac{C_{2sb}}{C_{2b} + C_{2sb}} \frac{C_{3sb}}{C_{3b} + C_{3sb}} \frac{p_{2b} p_{3b}}{\gamma}. \end{aligned} \tag{2.36}$$

After quantizing H_4 and also $H_{4.2}$ (see Appendix A), terms would appear describing how an excitation in one of the SQUIDs can "jump" to another SQUID (e.g., from terms with $p_{2a} p_{2b}$).

Version of June 29, 2015– Created June 29, 2015 - 21:15

By choosing a suitable set of values for the energy of the Josephson junctions it is possible to make H_4 vanish. In order to cancel also $H_{4.2}$, more Josephson junctions –or just regular inductors– have to be introduced into the system. It is trivial to introduce them in the Hamiltonian because their energy does not depend on the derivative of the fluxes, and they do not create other interactions: these extra elements only cancel $H_{4.2}$ and increase the energy levels of the SQUIDs, slightly.

There are two more expressions that cannot be canceled but their contribution to the Hamiltonian is not much important, in contrast to the equivalent expressions for the previous device, from Section 2.3. These are H_5, in Eq. (B.2), and H_6, in Eq. (B.3), both in the Appendix B.

H_5 describes exchange of excitations between SQUIDs in the presence of an excited state in the transmon. This expression cannot be canceled in the same way as $H_{4.2}$. It is of the same order as H_2, but by comparing it with H_3 it can be seen that the excited SQUID will emit a photon into the transmission line rather than decay into another SQUID excitation. Regarding H_6, it describes two processes: the relaxation of a SQUID excited state with the emission of a photon into any transmission line in the presence of an excitation in the transmon and the relaxation of a SQUID state with the emission of a photon into a transmission line plus the excitation of two transmon energy levels. The amplitude of these processes is much smaller than those described in H_3, so these are not likely to happen. Also because of the discrete energy separation of the transmon and SQUID levels, not all the combinations that appear in these two Hamiltonians are possible, especially if the energy spectrum of the transmon and the SQUIDs dissuade such processes to happen.

The advantages of working with this design are that all the necessary interactions are contained in H_2 and H_3, and that the contributions of H_5 and H_6 to the total Hamiltonian is small compared to other similar terms. The inconvenience is that more elements have to be added in order to completely get rid of H_4. To cancel this expression I propose the device shown in FIG. 2.6. It contains six inductors that connect the four SQUID fluxes in all the possible ways. This cancels the SQUID-SQUID interaction, as will be shown in Section 3.1.

The Hamiltonian of these extra inductors is[‡‡]

$$\begin{aligned} H_i =& \frac{1}{2}\varphi_{3a}^2\left(\frac{1}{L_1}+\frac{1}{L_2}+\frac{1}{L_3}\right)+\frac{1}{2}\varphi_{3b}^2\left(\frac{1}{L_1}+\frac{1}{L_5}+\frac{1}{L_6}\right) \\ &+\frac{1}{2}\varphi_{2a}^2\left(\frac{1}{L_3}+\frac{1}{L_4}+\frac{1}{L_6}\right)+\frac{1}{2}\varphi_{2b}^2\left(\frac{1}{L_2}+\frac{1}{L_4}+\frac{1}{L_5}\right) \\ &-\frac{\varphi_{3a}\varphi_{3b}}{L_1}-\frac{\varphi_{3a}\varphi_{2b}}{L_2}-\frac{\varphi_{3a}\varphi_{2a}}{L_3}-\frac{\varphi_{2a}\varphi_{2b}}{L_4}-\frac{\varphi_{3b}\varphi_{2b}}{L_5}-\frac{\varphi_{3b}\varphi_{2a}}{L_6}. \end{aligned} \tag{2.37}$$

Now that all the necessary elements that form the quantum switch have been identified and that the Hamiltonian contains all the desired interactions, it can be quantized and conditions can be imposed on the still free parameters that are left to cancel the remaining undesired interactions. This will result in a functional model for a quantum switch: the central element for a quantum random access memory based on circuit-QED.

[‡‡]The energy of an inductor with inductance L is $\frac{1}{2}\Delta\varphi^2/L$, where $\Delta\varphi$ is the flux across the device. From this, the Lagrangian is obtained. Since it does not depend on the derivative of the flux, the Legendre transformation is trivial.

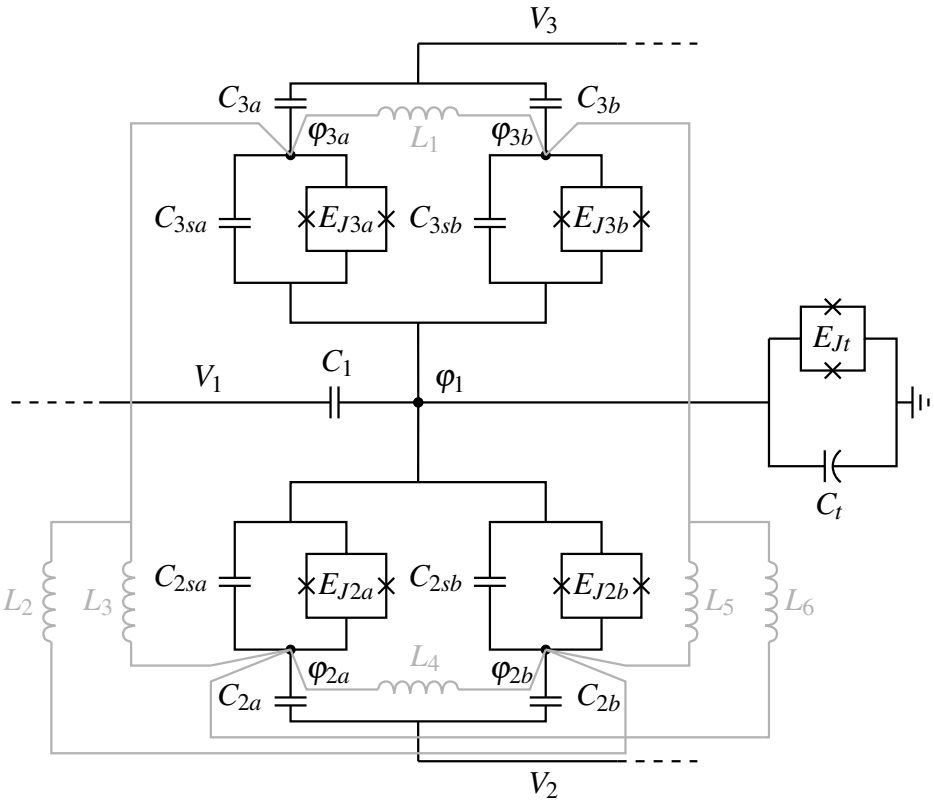

Figure 2.6: *This figure shows the same diagram as before but with the extra inductors in light gray. These six inductors connect the four SQUID fluxes in all the possible ways. It would also work if the inductors were substituted by Josephson junctions.*

Chapter 3

Analysis of the model and further considerations

The device schematically drawn in FIG. 2.6 is the definitive design for the quantum switch. This device gives rise to the desired interactions, described by H_1, H_2 and H_3 but it also produces processes that are unacceptable in a successfully operating quantum switch and, thus, have to be eliminated. These are H_4, $H_{4.2}$, H_5 and H_6. The last two expressions both contain exchange interactions. Compared to the other expression that contains this kind of interactions, the Hamiltonian H_3, the expressions in H_5 and H_6 describe very weak processes –the coefficients in front of each of the momenta are small, so these expressions lead to processes whose probability to happen are very small– and, thus, can be neglected. The way to deal with H_4 and $H_{4.2}$ consists of quantizing the Hamiltonian and imposing the necessary conditions on the free parameters (Josephson energies, capacitances and inductances) to make these expressions cancel.

3.1 Quantizing the Hamiltonian

The procedure for quantizing the Hamiltonian is the usual: impose $[p_i, \phi_i] = i\hbar/\varphi_0$* and cancel the expressions that should be canceled: the Hamiltonians H_4 and $H_{4.2}$ need to be strongly suppressed, so the only remaining expressions are H_1, H_2 and H_3. From these conditions the expressions for the momenta and the fluxes as a function of ladder operators are found. The flux ϕ_1 and the momentum

*The variables ϕ_i are defined as $\phi_i = \varphi_i/\varphi_0$. See Appendix A.

p_1 read

$$p_1 = -\frac{i\hbar}{2\varphi_0}\left(\frac{3}{2}\frac{\gamma^2}{\beta E_T}\right)^{1/4}(a_1 - a_1^\dagger) \tag{3.1}$$

$$\phi_1 = \left(\frac{2}{3}\frac{\beta E_T}{\gamma^2}\right)^{1/4}(a_1 + a_1^\dagger), \tag{3.2}$$

with $E_T = \frac{\hbar^2}{8\gamma\varphi_0^2}$. The ladder operators a_1 and $a_1^\dagger$ annihilate and create an excitation in the transmon. The other fluxes and momenta are defined as

$$p_{2a} = -\frac{i\hbar}{2\varphi_0}\left[E_{J2a}\frac{C_{2a}+C_{2sa}}{C_{2sa}}\left(\frac{\beta}{6\gamma^2 E_T}\right)^{1/2}\right]^{1/2}(a_{2a} - a_{2a}^\dagger) \tag{3.3}$$

$$\phi_{2a} = \left[\frac{1}{E_{J2a}}\frac{C_{2sa}}{C_{2a}+C_{2sa}}\left(\frac{6\gamma^2 E_T}{\beta}\right)^{1/2}\right]^{1/2}(a_{2a} + a_{2a}^\dagger), \tag{3.4}$$

with similar expressions for p_{2b}, p_{3a}, p_{3b} and the rest of the fluxes. In each of these pairs of equations, the ladder operators a_{2a} (and also $a_{2a}^\dagger$) act on the SQUID that contains φ_{2a}. With this transformation, the terms in H_4 [see Eq. (2.35)] containing $a^\dagger a$ vanish, whereas the terms containing aa and $a^\dagger a^\dagger$ disappear by making use of the rotating wave approximation. Now consider $H_{4.2}$ [displayed in Eq. (2.36)] together with H_i [in Eq. (2.37)]. In order to cancel them, the extra inductances must satisfy[†]

$$\begin{aligned}
L_1 &= \frac{4\gamma\varphi_0^4}{E_{J3a}E_{J3b}}\frac{6\gamma^2 E_T}{\hbar^2\beta} & L_2 &= \frac{4\gamma\varphi_0^4}{E_{J3a}E_{J2b}}\frac{6\gamma^2 E_T}{\hbar^2\beta}\\
L_3 &= \frac{4\gamma\varphi_0^4}{E_{J3a}E_{J2a}}\frac{6\gamma^2 E_T}{\hbar^2\beta} & L_4 &= \frac{4\gamma\varphi_0^4}{E_{J2a}E_{J2b}}\frac{6\gamma^2 E_T}{\hbar^2\beta}\\
L_5 &= \frac{4\gamma\varphi_0^4}{E_{J3b}E_{J2b}}\frac{6\gamma^2 E_T}{\hbar^2\beta} & L_6 &= \frac{4\gamma\varphi_0^4}{E_{J3b}E_{J2a}}\frac{6\gamma^2 E_T}{\hbar^2\beta}.
\end{aligned} \tag{3.5}$$

Once H_1 has been expanded using these equations, the resulting expression contains terms with $a^\dagger a$, but also a^2, $a^2 a^\dagger a$, a^4 and higher orders of a. Since it is not possible to get rid of all terms that do not conserve energy –interactions of the

[†]Boxed equations contain the conditions that must be imposed to the different parameters, i.e., Josephson energies, inductances, capacitances, etc.

kind aa, $(a^\dagger)^3 a$, etc–, the energies of the Josephson junctions have to be modified until some terms cancel and others become negligible. What can be canceled are the terms containing a^2 (and their hermitian conjugates). Consider the expressions in H_1 that contain information about the first energy level of the transmon. That is (the cosines have been expanded in a Taylor series), see Eq. (2.32),

$$H_{1.1} = \frac{p_1^2}{2\gamma} + \bar{E}_J \frac{\phi_1^2}{2}, \tag{3.6}$$

where $\bar{E}_J = E_{Jt} + E_{J2a} + E_{J2b} + E_{J3a} + E_{J3b}$. Expressed in the ladder operators, this becomes

$$H_{1.1} = -\left(\frac{3}{2}\frac{\gamma^2}{\beta}E_T\right)^{1/2}(a_1 - a_1^\dagger)^2 + \left(\frac{\bar{E}_J^2}{6}\frac{\beta}{\gamma^2}E_T\right)^{1/2}(a_1 + a_1^\dagger)^2. \tag{3.7}$$

By using Josephson energies that satisfy the condition

$$\bar{E}_J = \frac{3\gamma^2}{\beta}, \tag{3.8}$$

the expression for $H_{1.1}$ becomes a simpler equation containing only a particle density operator

$$H_{1.1} = 2\sqrt{2\bar{E}_J E_T}\, a_1^\dagger a_1. \tag{3.9}$$

The same procedure has to be applied to the other elements in H_1. After expanding them, some of the terms must be rearranged, since they may contribute to e.g. $H_{1.1}$. These other expressions become

$$H_{1.1} = \left(2\sqrt{2\bar{E}_J E_T} - 7E_T + 90E_T\sqrt{\frac{2E_T}{\bar{E}_J}}\right) a_1^\dagger a_1, \tag{3.10}$$

$$\begin{aligned} H_{1.2} \approx & -\frac{7}{2}E_T\, a_1^{\dagger 2} a_1^2 + 90E_T\sqrt{\frac{2E_T}{\bar{E}_J}}\, a_1^{\dagger 2} a_1^2 \\ & + \frac{5}{3}E_T\left(\left(a_1^\dagger a_1\right)a_1^2 + a_1^{\dagger 2}\left(a_1^\dagger a_1\right)\right) + \frac{5}{2}E_T\left(a_1^2 + a_1^{\dagger 2}\right), \end{aligned} \tag{3.11}$$

$$\begin{aligned} H_{1.3} \approx E_T\sqrt{\frac{2E_T}{\bar{E}_J}}\Big(& 20\left(a_1^{\dagger 3} a_1^3\right) - 45\left(a_1^{\dagger 2} + a_1^2\right) \\ & - 75\left(\left(a_1^\dagger a_1\right)a_1^2 + a_1^{\dagger 2}\left(a_1^\dagger a_1\right)\right) \\ & - 15\left(\left(a_1^{\dagger 2} a_1^2\right)a_1^2 + a_1^{\dagger 2}\left(a_1^{\dagger 2} a_1^2\right)\right)\Big). \end{aligned} \tag{3.12}$$

In all these expressions I already got rid of some terms that contained high powers of a and $a^\dagger$. In order to apply the rotating wave approximation, the prefactor of aa has to be smaller than the prefactor of $a^\dagger a$. It can be achieved by imposing $\bar{E}_J > E_T$. This implies that C_t is smaller than the other capacitances or that $\sqrt{\alpha_t}\,\hbar/\varphi_0$ is small compared to γ.

These simplifications and approximations result in an expression for H_1, the Hamiltonian that describes the energy levels of the transmon and SQUIDs, that only contains particle density operators ($a^\dagger a$ and powers of this operator).

$$\begin{aligned}
H_1 = &\left(2\sqrt{2\bar{E}_J E_T} - 7E_T + 90E_T\sqrt{\frac{2E_T}{\bar{E}_J}}\right) a_1^\dagger a_1 \\
&+ \left(90E_T\sqrt{\frac{2E_T}{\bar{E}_J}} - \frac{7}{2}E_T\right) a_1^{\dagger 2} a_1^2 + 20E_T\sqrt{\frac{2E_T}{\bar{E}_J}}\, a_1^{\dagger 3} a_1^3 \\
&+ \left(4\frac{E_{J2a}E_{2a}}{\sqrt{2\bar{E}_J E_T}} + 2\frac{E_{J2a}C_{2sa}}{C_{2a}+C_{2sa}}\left(\frac{2E_T}{\bar{E}_J}\right)^{1/2}\right) a_{2a}^\dagger a_{2a} \\
&+ \left(4\frac{E_{J2b}E_{2b}}{\sqrt{2\bar{E}_J E_T}} + 2\frac{E_{J2b}C_{2sb}}{C_{2b}+C_{2sb}}\left(\frac{2E_T}{\bar{E}_J}\right)^{1/2}\right) a_{2b}^\dagger a_{2b} \\
&+ \left(4\frac{E_{J3a}E_{3a}}{\sqrt{2\bar{E}_J E_T}} + 2\frac{E_{J3a}C_{3sa}}{C_{3a}+C_{3sa}}\left(\frac{2E_T}{\bar{E}_J}\right)^{1/2}\right) a_{3a}^\dagger a_{3a} \\
&+ \left(4\frac{E_{J3b}E_{3b}}{\sqrt{2\bar{E}_J E_T}} + 2\frac{E_{J3b}C_{3sb}}{C_{3b}+C_{3sb}}\left(\frac{2E_T}{\bar{E}_J}\right)^{1/2}\right) a_{3b}^\dagger a_{3b},
\end{aligned} \tag{3.13}$$

where the energies E_{2a}, E_{2b}, E_{3a} and E_{3b} are

$$\begin{aligned}
E_{2a} &= \frac{\hbar^2}{8C_{2sa}\varphi_0^2} & E_{2b} &= \frac{\hbar^2}{8C_{2sb}\varphi_0^2} \\
E_{3a} &= \frac{\hbar^2}{8C_{3sa}\varphi_0^2} & E_{3b} &= \frac{\hbar^2}{8C_{3sb}\varphi_0^2}.
\end{aligned} \tag{3.14}$$

Unlike in the case of the flux ϕ_1 and momentum p_1, for the SQUIDs it is possible to exactly cancel all the undesired expressions without making use of the rotating wave approximation. To do so, I had to impose

$$
\begin{aligned}
E_{J2a}E_{2a} &= (\bar{E}_J - E_{J2a} + E_{J2b} + E_{J3a} + E_{J3b})\,\frac{E_T C_{2sa}}{C_{2a}+C_{2sa}} \\
E_{J2b}E_{2b} &= (\bar{E}_J + E_{J2a} - E_{J2b} + E_{J3a} + E_{J3b})\,\frac{E_T C_{2sb}}{C_{2b}+C_{2sb}} \\
E_{J3a}E_{3a} &= (\bar{E}_J + E_{J2a} + E_{J2b} - E_{J3a} + E_{J3b})\,\frac{E_T C_{3sa}}{C_{3a}+C_{3sa}} \\
E_{J3b}E_{3b} &= (\bar{E}_J + E_{J2a} + E_{J2b} + E_{J3a} - E_{J3b})\,\frac{E_T C_{3sb}}{C_{3b}+C_{3sb}}.
\end{aligned}
\tag{3.15}
$$

Now, ideally, $E_{J2a} \sim E_{Jt}$ so the SQUIDs and the transmon have similar energy levels, but this equations tells that E_{J2a}, E_{J2b}, E_{J3a}, $E_{J3b} << E_{Jt}$ –recall that $\frac{C_{2sa}}{C_{2a}+C_{2sa}} < 1$.

Now I check whether these conditions are consistent with what is expected from H_2. This Hamiltonian contains the coupling between the transmon and the SQUIDs. Since all the couplings have the same form, by analyzing one of them the whole Hamiltonian can be easily found. Let me first study the coupling between the transmon and the SQUID $2a$:

$$
\begin{aligned}
H_{2.1} = &\left(-\frac{16\varphi_0^4 E_T^2}{\hbar^4 \bar{E}_J} p_1^2 + \frac{15\cdot 2^8 \varphi_0^6 E_T^3}{\hbar^6 \bar{E}_J^2} p_1^4 - \frac{42\cdot 2^{12}\varphi_0^8 E_T^4}{\hbar^8 \bar{E}_J^3} p_1^6 \right) \left(\frac{C_{2sa}}{C_{2a}+C_{2sa}} \right)^2 p_{2a}^2 \\
&- E_{J2a} \left(\frac{\phi_1^2}{4} - \frac{\phi_1^4}{48} + \frac{\phi_1^6}{1440} \right) \phi_{2a}^2.
\end{aligned}
\tag{3.16}
$$

Now ladder operators could be plugged inside the fluxes and momenta using Eq. (3.1) to (3.4), but it can be simplified if all the six terms are compared by pairs. Let us consider first the terms in Eq. (3.16) containing $p_1^2 p_{2a}^2$ and $\phi_1^2 \phi_{2a}^2$.

$$
-\frac{16\varphi_0^4 E_T^2}{\hbar^4 \bar{E}_J} \left(\frac{C_{2sa}}{C_{2a}+C_{2sa}} \right)^2 p_1^2 p_{2a}^2 = -\frac{E_T E_{J2a}}{2\bar{E}_J} \frac{C_{2sa}}{C_{2a}+C_{2sa}} \left(a_1 - a_1^\dagger \right)^2 \left(a_{2a} - a_{2a}^\dagger \right)^2, \tag{3.17}
$$

$$
-\frac{E_{J2a}}{4} \phi_1^2 \phi_{2a}^2 = -\frac{E_T}{2} \frac{C_{2sa}}{C_{2a}+C_{2sa}} \left(a_1 + a_1^\dagger \right)^2 \left(a_{2a} + a_{2a}^\dagger \right)^2. \tag{3.18}
$$

Since $E_{J2a} < \bar{E}_J$, the first line is negligible compared to the second. A similar

analysis of the other four terms yields

$$H_{2.1} \approx -\left(1-\left(180\frac{E_{J2a}}{\bar{E}_J}+\frac{1}{2}\right)\sqrt{\frac{2E_T}{\bar{E}_J}}+7560\frac{E_T E_{J2a}}{\bar{E}_J^2}\right)\frac{2E_T C_{2sa}}{C_{2a}+C_{2sa}}a_1^\dagger a_1 a_{2a}^\dagger a_{2a}$$
$$+\left(\left(90\frac{E_{J2a}}{\bar{E}_J}+\frac{1}{4}\right)\sqrt{\frac{2E_T}{\bar{E}_J}}+7560\frac{E_T E_{J2a}}{\bar{E}_J^2}\right)\frac{2E_T C_{2sa}}{C_{2a}+C_{2sa}}a_1^{\dagger 2}a_1^2 a_{2a}^\dagger a_{2a}$$
$$-1680\frac{E_T E_{J2a}}{\bar{E}_J^2}\frac{2E_T C_{2sa}}{C_{2a}+C_{2sa}}a_1^{\dagger 3}a_1^3 a_{2a}^\dagger a_{2a}. \tag{3.19}$$

To obtain this expression I have also used the rotating wave approximation. The full interaction Hamiltonian H_2 is constructed by doing the same analysis with the other SQUIDs.

Up to this point, the only free parameters that are left are the capacitances, all of them, but with the constraints $C_{2a} \sim C_{2b} \sim C_{3a} \sim C_{3b}$, $C_{2sa} \sim C_{2sb} \sim C_{3sa} \sim C_{3sb}$ and C_t, $C_{2a} > C_1 > C_{2sa}$. The parameters V_1, V_2 and V_3 are also still free but in principle, in order to make the system scalable, they have to be equal. Nevertheless, I will assume that they can be slightly different –to check whether the system can be improved by not making it scalable– and at the end of the calculations, if it is possible, they will be made equal. For these potentials I have assumed the following quantized form

$$V_1 = -\frac{i\hbar}{2\varphi_0}A_1^{1/4}(b_1 - b_1^\dagger) \tag{3.20}$$

$$V_2 = -\frac{i\hbar}{2\varphi_0}A_2^{1/4}(b_2 - b_2^\dagger) \tag{3.21}$$

$$V_3 = -\frac{i\hbar}{2\varphi_0}A_3^{1/4}(b_3 - b_3^\dagger). \tag{3.22}$$

To derive the quantized form of the Hamiltonian H_3 as a function of the ladder operators I have also used the rotating wave approximation.The final expression reads

$$H_3 = \sum_{i=1}^{3}\left(\left(\mu_{1a,i} - 3\mu_{1b,i}\right)a_1^\dagger b_1 + 3\mu_{1b,1}a_1^\dagger a_1^\dagger a_1 b_1 \right.$$
$$\left. + \mu_{1b,1}a_1^{\dagger 3}b_1 + \sum_k \mu_{k,i}a_k^\dagger b_i\right) + h.c. \tag{3.23}$$

Here the index k runs over $\{2a, 2b, 3a, 3b\}$. The most relevant coefficients $\mu_{i,j}$ that appear in this expression are displayed below. Those that are small enough to be

ignored are not shown.

$$\mu_{1a,1} = 2C_1 E_T A_1^{1/4} \left(\frac{\bar{E}_J}{2E_T}\right)^{1/4} \tag{3.24}$$

$$\mu_{1b,1} = 2C_1 E_T A_1^{1/4} \left(\frac{2E_T}{\bar{E}_J}\right)^{1/4} \tag{3.25}$$

$$\mu_{2a,1} = 2C_1 E_T A_1^{1/4} \left(\frac{\bar{E}_J}{2E_T}\right)^{1/4} \left(\frac{E_{J2a}}{\bar{E}_J}\frac{C_{2sa}}{C_{2a}+C_{2sa}}\right)^{1/2} \tag{3.26}$$

$$\mu_{2a,2} \approx 2C_{2a} E_{2a} A_2^{1/4} \left(\frac{\bar{E}_J}{2E_T}\right)^{1/4} \left(\frac{E_{J2a}}{\bar{E}_J}\frac{C_{2sa}}{C_{2a}+C_{2sa}}\right)^{1/2} \tag{3.27}$$

$$\mu_{2b,1} = 2C_1 E_T A_1^{1/4} \left(\frac{\bar{E}_J}{2E_T}\right)^{1/4} \left(\frac{E_{J2b}}{\bar{E}_J}\frac{C_{2sb}}{C_{2b}+C_{2sb}}\right)^{1/2} \tag{3.28}$$

$$\mu_{2b,2} \approx 2C_{2b} E_{2b} A_2^{1/4} \left(\frac{\bar{E}_J}{2E_T}\right)^{1/4} \left(\frac{E_{J2b}}{\bar{E}_J}\frac{C_{2sb}}{C_{2b}+C_{2sb}}\right)^{1/2} \tag{3.29}$$

$$\mu_{3a,1} = 2C_1 E_T A_1^{1/4} \left(\frac{\bar{E}_J}{2E_T}\right)^{1/4} \left(\frac{E_{J3a}}{\bar{E}_J}\frac{C_{3sa}}{C_{3a}+C_{3sa}}\right)^{1/2} \tag{3.30}$$

$$\mu_{3a,3} \approx 2C_{3a} E_{3a} A_3^{1/4} \left(\frac{\bar{E}_J}{2E_T}\right)^{1/4} \left(\frac{E_{J3a}}{\bar{E}_J}\frac{C_{3sa}}{C_{3a}+C_{3sa}}\right)^{1/2} \tag{3.31}$$

$$\mu_{3b,1} = 2C_1 E_T A_1^{1/4} \left(\frac{\bar{E}_J}{2E_T}\right)^{1/4} \left(\frac{E_{J3b}}{\bar{E}_J}\frac{C_{3sb}}{C_{3b}+C_{3sb}}\right)^{1/2} \tag{3.32}$$

$$\mu_{3b,3} \approx 2C_{3b} E_{3b} A_3^{1/4} \left(\frac{\bar{E}_J}{2E_T}\right)^{1/4} \left(\frac{E_{J3b}}{\bar{E}_J}\frac{C_{3sb}}{C_{3b}+C_{3sb}}\right)^{1/2}. \tag{3.33}$$

Previously I had to make the capacitances C_{2sa} smaller than C_{2a} [for the Taylor expansion of the Hamiltonian in Eq. (2.31)] and I found that the energies E_{J2a} and E_T are smaller than $\bar{E}_J$ [see Eq. (3.10) to (3.12) and also Eq. (3.15)]. Using these conditions the interaction strengths $\mu_{1a,2}$ and $\mu_{1a,3}$ become much smaller than $\mu_{1a,1}$, so they can be ignored. The same happens with $\mu_{1b,2}$ and $\mu_{1b,3}$. This means that the transmon is strongly coupled to the incoming transmission line but weakly coupled to the outgoing transmission lines, so a photon absorbed by the transmon will modify the energy levels of the SQUIDs –as described by H_2– but

will not be transmitted forward. Similarly, the interaction strength $\mu_{2a,3}$ is smaller than $\mu_{2a,1}$ and $\mu_{2a,2}$. This indicates that the SQUID $2a$ can absorb a photon from the incoming transmission line and emit it into its nearest transmission line, but not into the other. This is exactly the behavior expected for the quantum switch. For the other SQUIDs the same applies, so $\mu_{2a,3}$, $\mu_{2b,3}$, $\mu_{3a,2}$ and $\mu_{3b,2}$ can be disregarded.

3.2 Dynamics of operation and a problem with the transmon

In the previous sections I have introduced a model for a quantum switch using superconducting qubits. The proposed device (FIG. 2.6) consists of a semi-infinite incoming transmission line coupled to a system composed of four SQUIDs and a transmon. Two outgoing transmission lines couple the SQUIDs to the next quantum switch as incoming transmission lines in a tree-like network. The model I propose is described by a Hamiltonian that can be divided in three parts. The first part of that Hamiltonian [H_1, see Eq. (3.13)], describe the energy level of each of the artificial atoms. All the levels are supposed to have a different energy. The second part is more interesting [H_2, see Eq. (3.19)]. It describes a density-density interaction between the energy levels of different atoms. That is, when a transmon level is excited, this part of the Hamiltonian contributes to modify the energy levels of all the other atoms. Ideally, an incoming photon will have the energy to excite only the first or third level of the transmon (the second level is not coupled to the transmission lines, as shown by the third part of the Hamiltonian, H_3). If a second photon comes in, it will not be possible to excite further levels of the transmon –the photon will not have enough energy to do so. Instead, the photon will excite one of the SQUIDs. Since the excitation of the transmon modifies the energy spectrum of the SQUIDs, now this will be possible. We have to make sure that, if the first photon excites the first transmon level (or the third) the second only excites the SQUIDs leading to the second transmission lines (or the third). This way, the first photon decides which paths the other photons will follow.

Up to this point I have assumed that the lifetimes of the transmon excitations are large compared to those of the SQUIDs. Otherwise the transmon will decay to its ground state and the other photons will not be routed forward, but this is something that will be determined by H_3, the third and last part of the Hamiltonian [see Eq. (3.23)]. This last expression tells us that the transmon is only coupled to the incoming transmission lines (both levels) thus, a photon absorbed by the trans-

mon can only be reflected back into the incoming transmission line. It cannot be transmitted. The SQUIDs, on the other side, are coupled to both the incoming transmission lines and to the closest outgoing transmission line, but not the other. Therefore, the second photon –which cannot be absorbed by the transmon– will be absorbed by the SQUID. After some time this photon will be emitted into a transmission line, either back or forward to the next node in the network of switches. The constraints I have imposed before force the excited SQUID to emit a photon into the outgoing transmission lines.

3.2.1 Operation

The operation of the quantum switch is represented in FIG. 3.1. This scheme shows how a register of photons is routed by the device. In the ideal case, a register of photons sent through the incoming transmission line will arrive at the first node of the network, where the first photon of the register is absorbed by the transmon. The photons in the register can be in two different states (or a superposition), each with energies ω_a and ω_b. When the first photon arrives at the switch it encounters a system with the energy spectrum shown in the top left box (A). The switch is in the ground state, with the paths closed (i) and the first incoming photon can be absorbed by the device by exciting the first level of the transmon (red) if it has energy $\omega_a = \omega_{T1}$ or the third level (green) if it has energy $\omega_b = \omega_{T3}$. The other levels depicted in this box are not accessible for a photon that can only be in the states ω_a or ω_b. In the box (A), the left upright arrow contains the energy of the incoming photon. The levels next to it describe the spectrum of the transmon in the range of possible energies the incoming photons can have. The lowest level, labeled with $|GS\rangle$, is the ground state.

Once the transmon is excited, a new set of energies is accessible for the next incoming photons (B). Although $\omega_{2a} \neq \omega_{T1}$, the Hamiltonian H_2 gives an extra contribution to the energy levels ($J_{i,k}$) such that if the first level of the transmon is excited, an incoming photon with energy ω_a can be absorbed by the SQUID $2a$ (or the SQUID $3a$, if the third level of the transmon is excited) or by the SQUID $2b$ if the energy of the photon is ω_b. Thus, the transmon opens one or the other path (ii) according to the state of the first photon absorbed.

After being absorbed by the corresponding SQUID, the second photon is emitted into the open outgoing transmission line and the system goes back to the state with just one excited state (either $|\omega_{T1}\rangle$ or $|\omega_{T3}\rangle$), waiting for the next photon of the register. If the first incoming photon has energy ω_a, then all the successive photons will be absorbed by either $2a$ or $2b$ and will be transmitted through the

Version of June 29, 2015– Created June 29, 2015 - 21:15

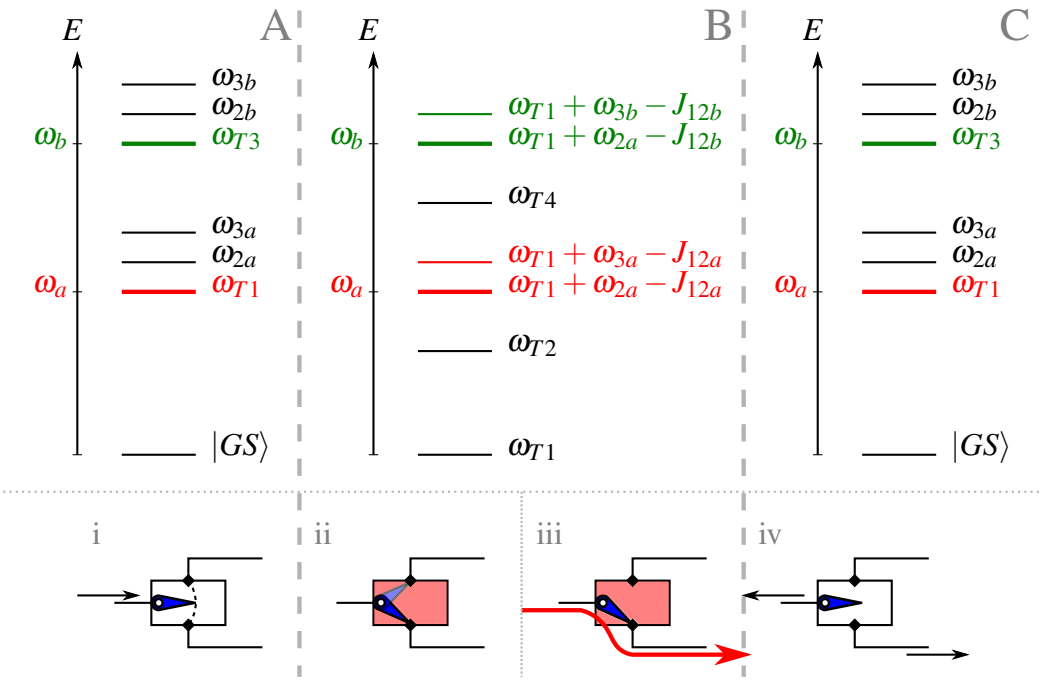

Figure 3.1: *In this figure I schematically show the expected behavior of the quantum switch based on the interactions contained in the Hamiltonians. The upper part of the figure contains a set of diagrams with the energy levels of the device at each step of the process of routing a register of photons. The lower part contains a graphic representation of the behavior of the device at each step of the process. In (A) the system is in its ground state and an incoming photon (i) comes in. This can excite any of the energy levels and "open" the path (ii) to any (or both) of the outgoing transmission lines. Once the transmon is excited, a second incoming photon can only excite a selection of states (B) and decay into the path opened by the transmon (iii). A third, fourth, etc. photon experiences the same process while the transmon is excited. At the end of the process (iv), when all the photons have gone through, the transmon emits a photon into the first transmission line (where the photons came in) and the system goes back to the ground state (C), waiting for the process to start over again. For a more detailed explanation see the text.*

same transmission line, independently of their state (iii).

In the inset (B), the third level of the transmon does not appear. This is because in order to excite this level –assuming that the first level of the transmon is already excited–, the photon would have to create two elemental excitations, but according to H_3, it can only create either one or three. That is why the second and a hypothetical fourth level is displayed. Nevertheless, these levels do not have enough energy to become excited.

Finally, when the whole register has gone through, the first photon is emitted into the ingoing transmission line and the rest of the register continues its way to the next quantum switch (iv). The device, after being relaxed, comes back to the ground state, with all the paths closed (iv), waiting for another register to come in (C).

During all of this process, if the first photon is in a superposition of states, say $\psi = (|\omega_a\rangle + |\omega_b\rangle)/\sqrt{2}$, then the photons that follow will all be forwarded through both the second and third outgoing transmission lines.

3.2.2 Scalability

In order to make a system composed of a tree-like network with one of these devices in each node, the transmon energy levels must coincide with those of the "open" SQUIDs ($\omega_{T1} = \omega_{2a} - J_{12a}$). Unfortunately, this is not the case with the present system. The energies of the transmon excitations are some orders of magnitude larger than the SQUID excitations and the energy separation is also larger. To solve this problem an external device can be added before each switch that increases the energy of only the first photon without measuring it. Another solution would be to add another element in the SQUIDs that increases the energy of its excitations. This could be a simple inductor connected to the point labeled as φ_{2a} in FIG. 2.6 on one end, and to the ground at the other end. Since it is an inductive element, it can be straightforwardly added to the Hamiltonian. This element will generate a term raising the energy of the SQUID, but also another term containing $a_{2a}^\dagger a_{2a}^\dagger$ and $a_{2a}a_{2a}$. These two last elements cannot be suppressed using the rotating wave approximation because they are large compared to the energy of the excited levels of the SQUID –the main contribution to its energy would come from this expression. Moreover, the density-density interaction strength (in the expression H_2) will be too small compared to the energy of the excitations.

Nevertheless, I will assume that a solution can be found to this drawback and

continue with the analysis (I will come back to this in Section 5.1). In the worst case, it will not be possible to construct a QRAM using a network of quantum switches, but a fully operational quantum switch that routes many-photons registers can still be found.

3.3 The final Hamiltonian

So far, a transmon-based quantum switch has been presented and his Hamiltonian has been analyzed, hypothesizing about its expected behavior in an idealized case. Nevertheless, the form of the Hamiltonian is not the most suitable to work with. It would be convenient to use a simpler notation. In previous chapters I have claimed that terms containing $a_1^\dagger a_1$ describe the first level of the transmon and terms with $(a_1^\dagger)^3 a_1^3$ describe the third level. The first statement is right, but the last in incomplete. $a_1^\dagger a_1$ acting on a ket that describes the third transmon excitation gives a non-zero contribution. The notation I use in this chapter makes a clear distinction between levels. From the resulting equations I have obtained the expressions for the energy of each of the excitations and the coupling strengths.

Let me start by writing the Hamiltonian as a sum of all the contributions found previously plus an expression describing the transmission lines

$$H = H_{sys} + H_J + H_C + H_T. \tag{3.34}$$

This is the full Hamiltonian that completely describes the routing device. In this expression H_{sys} is the part of the Hamiltonian that describes the energy levels, H_J contains the interaction between the energy levels, H_C describes the coupling to the transmission lines and H_T is the Hamiltonian of the transmission lines. The first part can be reduced to

$$\begin{aligned} H_{sys} =& \omega_{T1} a_{T1}^\dagger a_{T1} + \omega_{T2} a_{T2}^\dagger a_{T2} + \omega_{T3} a_{T3}^\dagger a_{T3} \\ &+ \omega_{2a} a_{2a}^\dagger a_{2a} + \omega_{2b} a_{2b}^\dagger a_{2b} + \omega_{3a} a_{3a}^\dagger a_{3a} + \omega_{3b} a_{3b}^\dagger a_{3b}. \end{aligned} \tag{3.35}$$

In this equation I have used three new (projection) operators. In a 4D Hilbert

space (only three excited levels) these are defined as

$$a_{T1}^{\dagger} = \frac{1}{6} a_1^2 a_1^{\dagger 3} = \begin{pmatrix} 0 & 0 & 0 & 0 \\ 0 & 0 & 0 & 0 \\ 0 & 0 & 0 & 1 \\ 0 & 0 & 0 & 0 \end{pmatrix}, \tag{3.36}$$

$$a_{T2}^{\dagger} = \frac{1}{3\sqrt{2}} a_1 a_1^{\dagger 3} = \begin{pmatrix} 0 & 0 & 0 & 0 \\ 0 & 0 & 0 & 1 \\ 0 & 0 & 0 & 0 \\ 0 & 0 & 0 & 0 \end{pmatrix}, \tag{3.37}$$

$$a_{T3}^{\dagger} = \frac{1}{\sqrt{6}} a_1^{\dagger 3} = \begin{pmatrix} 0 & 0 & 0 & 1 \\ 0 & 0 & 0 & 0 \\ 0 & 0 & 0 & 0 \\ 0 & 0 & 0 & 0 \end{pmatrix}. \tag{3.38}$$

They excite the first, second and third energy levels of the transmon, respectively, from the ground state. These operators do not satisfy the usual commutation relations. The reason to choose them is to simplify the notation and to easily identify the energy of each transmon level. The energy of each of these excitations is

$$\omega_{T1} = 2\sqrt{2\bar{E}_J E_T} - 7E_T + 90E_T \sqrt{\frac{2E_T}{\bar{E}_J}} \tag{3.39}$$

$$\omega_{T2} = 2\omega_{T1} + 2\left(90E_T \sqrt{\frac{2E_T}{\bar{E}_J}} - \frac{7}{2}E_T\right) \tag{3.40}$$

$$\omega_{T3} = 3\omega_{T2} - 3\omega_{T1} + 120E_T \sqrt{\frac{2E_T}{\bar{E}_J}} \tag{3.41}$$

$$\omega_{2a} = 4\frac{E_{J2a}E_{2a}}{\sqrt{2\bar{E}_J E_T}} + 2\frac{E_{J2a}C_{2sa}}{C_{2a}+C_{2sa}} \sqrt{\frac{2E_T}{\bar{E}_J}}, \tag{3.42}$$

and similar expressions for ω_{2b}, ω_{3a} and ω_{3b}. Using the same notation, the interaction Hamiltonian reads

$$H_J = -\sum_{i=1}^{3} \sum_{k} J_{ik} a_{Ti}^{\dagger} a_{Ti} a_k^{\dagger} a_k, \qquad \text{with } k \in \{2a, 2b, 3a, 3b\}, \tag{3.43}$$

with interaction strengths

$$J_{12a} = \left(1 - \left(180\frac{E_{J2a}}{\bar{E}_J} + \frac{1}{2}\right)\sqrt{\frac{2E_T}{\bar{E}_J}} + 7560\frac{E_T E_{J2a}}{\bar{E}_J^2}\right)\frac{2E_T C_{2sa}}{C_{2a}+C_{2sa}} \tag{3.44}$$

$$J_{22a} = 2J_{12a} - \left(\left(90\frac{E_{J2a}}{\bar{E}_J} + \frac{1}{4}\right)\sqrt{\frac{2E_T}{\bar{E}_J}} + 7560\frac{E_T E_{J2a}}{\bar{E}_J^2}\right)\frac{4E_T C_{2sa}}{C_{2a}+C_{2sa}} \tag{3.45}$$

$$J_{32a} = 3J_{22a} - 3J_{12a} + 20160\frac{E_T^2 E_{J2a}}{\bar{E}_J^2}\frac{C_{2sa}}{C_{2a}+C_{2sa}}. \tag{3.46}$$

The other nine expressions are found by substituting $2a$ by $2b$, $3a$ and $3b$ in Eq. (3.44) to (3.46). With the current set of capacitors, the interaction strengths are two orders of magnitude smaller that the energies of the SQUIDs, just like in other similar works [17].

The following is the Hamiltonian that describes the coupling to the transmission lines.

$$\begin{aligned} H_C = \int_{-\infty}^{\infty} dp \Bigg[& \frac{a_{T1}^\dagger b_1(p)}{\sqrt{\pi\tau_{T1}}} + \frac{a_{T3}^\dagger b_1(p)}{\sqrt{\pi\tau_{T3}}} \\ & + \left(\sqrt{\frac{3}{\pi\tau_{T1}}} - 3\sqrt{\frac{2}{\pi\tau_{T3}}}\right) a_{T3}^\dagger a_{T2} b_1 + \left(\sqrt{\frac{2}{\pi\tau_{T1}}} - \sqrt{\frac{3}{\pi\tau_{T3}}}\right) a_{T2}^\dagger a_{T1} b_1 \\ & + \frac{a_{2a}^\dagger b_1(p)}{\sqrt{\pi\tau_{2a,1}}} + \frac{a_{2a}^\dagger b_2(p)}{\sqrt{\pi\tau_{2a,2}}} + \frac{a_{2b}^\dagger b_1(p)}{\sqrt{\pi\tau_{2b,1}}} + \frac{a_{2b}^\dagger b_2(p)}{\sqrt{\pi\tau_{2b,2}}} \\ & + \frac{a_{3a}^\dagger b_1(p)}{\sqrt{\pi\tau_{3a,1}}} + \frac{a_{3a}^\dagger b_3(p)}{\sqrt{\pi\tau_{3a,3}}} + \frac{a_{3b}^\dagger b_1(p)}{\sqrt{\pi\tau_{3b,1}}} + \frac{a_{3b}^\dagger b_3(p)}{\sqrt{\pi\tau_{3b,3}}} + h.c. \Bigg]. \end{aligned} \tag{3.47}$$

Here I have introduced the parameters $\tau_{i,j}$ to stress that the exchange interaction strengths are related to the lifetime of the excitations. These $\tau_{i,j}$ are related to $\mu_{i,j}$ as (only for the transmon)

$$\frac{1}{\sqrt{\pi\tau_{T1}}} = \mu_{1a,1} - 3\mu_{1b,1} \tag{3.48}$$

$$\frac{1}{\sqrt{\pi\tau_{T3}}} = \sqrt{6}\mu_{1b,1}. \tag{3.49}$$

For the SQUIDs this relation is simpler:

$$\frac{1}{\sqrt{\pi\tau_{i,j}}} = \mu_{i,j}, \qquad \text{with } i \in \{2a, 2b, 3a, 3b\} \text{ and } j \in \{1,2,3\}. \tag{3.50}$$

Let me focus for a second on Eq. (3.47). In the second line there are two expressions with a different form. The first (actually its hermitian conjugate) implies that the third excited level of the transmon can decay into the second excited level and emit a photon. This process makes the switch stop working. The other expression is not that harmful. It says that an incoming photon can excite the second level of the transmon if the first is already excited, but this will not happen if the energy of the photon does not coincide withe the energy gap between the first and second levels of the transmon. The hermitian conjugate of this expression describes how the second level of the transmon decays into the first one by emitting a photon. Regarding this last process, since the second level cannot possibly be excited, it will just not happen. Moreover, if by any chance the second level is excited, the switch will not work, so there is no need to worry about this process.

Only one of the coefficients multiplying these two expressions can be canceled and, given the nature of the interactions I decided to cancel the first. I do not expect the second to affect the functioning of the device. In order to cancel it the lifetimes have to satisfy $\tau_{T3} = 6\tau_{T1}$ or, equivalently,

$$\frac{\alpha_t \hbar^2}{\varphi_0^2} = \frac{\gamma^3}{324\, C_t}. \tag{3.51}$$

This constraint on α_t implies that $\bar{E}_J > E_T$, which is a condition I already had to impose before. Moreover, in this way the lifetimes of both transmon levels are of the same order of magnitude, which is necessary for a device that does not make a distinction between left-steering or right-steering photons.

Finally, the Hamiltonian describing the transmission lines, derived assuming that the superconducting wires behave as the continuum limit of an infinite chain of LC oscillators[‡], reads

$$H_T = \int_{-\infty}^{\infty} dp\, p \left(b_1^\dagger(p) b_1(p) + b_2^\dagger(p) b_2(p) + b_3^\dagger(p) b_3(p) \right). \tag{3.52}$$

3.4 Relaxation and dephasing

In this chapter I derive the coupling of the system to an external bath following Ithier *et al.* [44] to take into account relaxation and dephasing processes. Recall

[‡] see the Appendix A.

that the Hamiltonian contains $\omega a^\dagger a$ and $\mu b^\dagger a + h.c$ [Eq. (3.35) and (3.47)]. For simplicity, let me consider its analogy to a two-level system. Consider the following Hamiltonian, which describes a two-level system not coupled to any external field.

$$H = \vec{n}(0)\cdot\vec{\sigma} = n_z\sigma_z + n_\perp\sigma_\perp, \tag{3.53}$$

where $\sigma_\perp$ contains σ_x and σ_y or σ_- and σ_+ and $\vec{n}$ is a field that contains information about how the system interacts with its environment. At $\vec{n}(0)$ it does not interact at all.

Let $\vec{n}$ be a function that depends on two parameters, $\vec{n}(\lambda,\rho)$, where λ is a variable related to the coupling to the transmission lines and ρ is a variable related to the coupling to an external source of decoherence. In the Hamiltonian, if the coupling of the transmon with the external bath is neglected, then $\vec{n}(0,0) = n_z$ and $n_\perp = 0$. A perturbation of the Hamiltonian by $\delta\lambda$ –but keeping $\rho = 0$– gives

$$\begin{aligned}\vec{n}(\delta\lambda,0) =& \vec{n}(0,0) + \frac{d\vec{n}}{d\lambda}\delta\lambda + O\left(\delta\lambda^2\right)\\ =& n_z(0,0) + \frac{dn_z}{d\lambda}\delta\lambda\cdot\hat{n}_z + \frac{dn_\perp}{d\lambda}\delta\lambda\cdot\hat{n}_\perp + O\left(\delta\lambda^2\right).\end{aligned} \tag{3.54}$$

During the derivation of the Hamiltonian the following quantities are obtained

$$\delta\lambda = b + b^\dagger \tag{3.55}$$

$$\frac{dn_\perp}{d\lambda} = \frac{1}{\sqrt{\pi\tau}} \tag{3.56}$$

$$\frac{dn_z}{d\lambda} = 0 \tag{3.57}$$

$$n_z(0,0) = \omega. \tag{3.58}$$

Now let's do the same with ρ and λ simultaneously. By perturbing our Hamiltonian, we obtain

$$\vec{n}(\delta\lambda,\delta\rho) = n_z(0,0) + \frac{dn_\perp}{d\lambda}\delta\lambda\cdot\hat{n}_\perp + \frac{dn_z}{d\rho}\delta\rho\cdot\hat{n}_z + \frac{dn_\perp}{d\rho}\delta\rho\cdot\hat{n}_\perp + O\left(\delta^2\right). \tag{3.59}$$

The first two terms of this expansion give the Hamiltonian previously found. The other two terms describe the interaction with the external bath. Let $\frac{d\vec{n}}{d\rho}$ be a bath coupling rate $\vec{K}(p)$ and $\delta\rho$ the operators that describe this decoherence in the form $d + d^\dagger$. The Hamiltonian describing the decoherence is given by

$$H_d = \int dp\ \left(K_z(p)(d+d^\dagger)\sigma_z + K_\perp(p)(d+d^\dagger)\sigma_\perp\right). \tag{3.60}$$

Let me analyze how this Hamiltonian acts on any state in the z-basis. The first term of the Hamiltonian acting on a state $|\uparrow\rangle$ ($|\downarrow\rangle$) gives a constant times $d^\dagger|\uparrow\rangle$ ($d^\dagger|\downarrow\rangle$). Thus the initial state is only modified by a phase change plus the creation or annihilation of an external bath mode. This term describes a dephasing process. The second term flips the initial state from $|\uparrow\rangle$ (or $|\downarrow\rangle$) to $|\downarrow\rangle$ (or $|\uparrow\rangle$) and also gives an external mode excitation. Thus, it describes the relaxation/excitation of the two-level system.

Now this has to be generalized to a multilevel system. In our proposed device, whose energy levels are schematically represented in FIG. 3.1, there are six possible processes involving the relaxation of the transmon. These are

$$\begin{aligned} |\omega_{T3}\rangle &\longrightarrow |\omega_{T2}\rangle & |\omega_{T2}\rangle &\longrightarrow |\omega_{T1}\rangle \\ |\omega_{T3}\rangle &\longrightarrow |\omega_{T1}\rangle & |\omega_{T2}\rangle &\longrightarrow |GS\rangle \\ |\omega_{T3}\rangle &\longrightarrow |GS\rangle & |\omega_{T1}\rangle &\longrightarrow |GS\rangle\,, \end{aligned}$$

where $|\omega_{T3}\rangle$, $|\omega_{T2}\rangle$ and $|\omega_{T1}\rangle$ are kets representing the third, second and third excited states of the transmon, respectively. $|GS\rangle$ is the ground state.

For simplicity, I only consider the process on the last row. The reason for introducing this extra Hamiltonian is to quantify the effect of an external bath on the successful operation of the device. By considering only two out of the six possible processes, nothing relevant is being omitted, because the relaxation ratio can be increased so that the relaxation of the excited states described by these two processes actually contains the sum of all the possible relaxation processes of these states. With this simplification, the information on what state the transmon decays into is lost, but I am not interested in the final state. I only want to know whether the device works (no relaxation) or it does not (relaxation).

The relaxation terms involve the creation of an external bath mode and an operator or product of operators that describe the annihilation of one excitation (and its hermitian conjugate). Other possible combinations are suppressed by the rotating wave approximation. The dephasing terms contain a creation of an external bath mode and a projector operator of an excited state. Furthermore, commutation of the dephasing and relaxation operators has to be imposed, since these elements belong to different Hilbert spaces. The resulting Hamiltonian is

$$\begin{aligned} H_d = \int dp \sum_i \Big[& K_{ri}(p) r_i^\dagger(p) a_i + K_{di}(p) d_i^\dagger(p) a_i^\dagger a_i \\ & + p\left(r_i^\dagger(p) r_i(p) + d_i^\dagger(p) d_i(p) \right) \Big], \end{aligned} \tag{3.61}$$

where $r(p)$ are the relaxation modes and $d(p)$ are the dephasing modes. Here the index i runs over $\{T1, T2, 2a, 2b, 3a, 3b\}$. It is important to notice that the vacuum $|0\rangle$ is still an eigenstate of the Hamiltonian with zero energy. The coupling functions $K(p)$ can be approximated as constants [45] (first Markov approximation).

$$K_r(p) \approx \sqrt{\frac{\gamma_r}{2\pi}} \tag{3.62}$$

$$K_d(p) \approx \sqrt{\frac{\gamma_d}{4\pi}}. \tag{3.63}$$

Up to this point I have derived all the formulas with all the factors of $\hbar$ although in some equations I have set implicitly $\hbar = 1$ –by giving to the frequencies ω_i units of energy. From now on I will consider $\hbar = 1$ to simplify the notation.

3.5 Equations of motion

In the previous sections we have found a Hamiltonian that describes a quantum switch including relaxation and dissipation processes. This Hamiltonian has been expressed in a quantized notation. The next step towards studying the dynamics of operation of the quantum switch consists of obtaining, from the Hamiltonian, the equations of motion. With these equations, the probabilities of reflection and transmission of photons are obtained and the performance of the device is evaluated. Since the Hamiltonian contains different operators, it is not easy to diagonalize, so working in the Schrödinger picture may not be the best option. Instead I work in the Heisenberg picture.

In this model, a photon comes in, interacts with something and a photon comes out. The only element that has to be computed to be sure that the device works is the probability of the photon being reflected or transmitted. What happens during the interaction is irrelevant. For this reason it is convenient to work with the *input/output* formalism [45, 46] (or just *in/out*). Within this formalism, a quantum state in the asymptotic limit $t \to \infty$ ($|\psi_{out}\rangle$) is related, by a unitary operator, to the same state in the opposite asymptotic limit $t \to -\infty$ ($|\psi_{in}\rangle$) [47, 48]. This formalism is very convenient when the photons can be considered as free particles in the limit $t \to \pm\infty$ –far away from the scattering center–, in the sense that they are not influenced by the interaction part of the Hamiltonian.

The *in/out* operators are defined by [17, 45, 48]

$$b_{1in/out}(p) = \lim_{t_0 \to \pm\infty} e^{-iHt_0} e^{iH_T t_0} b_1(p) e^{-iH_T t_0} e^{iHt_0}. \tag{3.64}$$

By making use of the Baker-Campbell-Hausdorff formula together with the Hamiltonian H_T from Eq. (3.52), this becomes

$$\begin{aligned} b_{1in/out}(p) &= \lim_{t_0\to\pm\infty} e^{-ipt_0}e^{-iHt_0}b_1(p)e^{iHt_0} \\ &= \lim_{t_0\to\pm\infty} e^{-ipt_0}b_{1H}(p,t_0), \end{aligned} \tag{3.65}$$

where $b_{1H}(p,t_0)$ is an initial value of the operator $b_{1H}(p,t)$ in the Heisenberg picture. In time space the *in/out* operators are related to the momentum space ladder operators as [17, 45, 48]

$$b_{1in/out}(t) = \frac{1}{\sqrt{2\pi}}\int dp\, b_{1H}(p,t_0)e^{-ip(t-t_{0/1})}, \tag{3.66}$$

where $t_0 \to -\infty$ and $t_1 \to \infty$. These *in/out* operators will be inserted in the equations of motion to facilitate the calculations.

The equation of motion of an operator $A(t)$ is found, in the Heisenberg picture, by using

$$\frac{d}{dt}A(t) = i\,[H,A(t)] + \frac{\partial A}{\partial t}. \tag{3.67}$$

The equations of motion of the transmission line modes are

$$\begin{aligned} \dot{b}_1(\omega) = &-i\omega b_1(\omega) - i\left(\frac{a_{T1}}{\sqrt{\pi\tau_{T1}}} + \frac{a_{T3}}{\sqrt{\pi\tau_{T3}}} + \left(\sqrt{\frac{2}{\pi\tau_{T1}}} - \sqrt{\frac{3}{\pi\tau_{T3}}}\right)a^\dagger_{T1}a_{T2}\right. \\ &\left. + \frac{a_{2a}}{\sqrt{\pi\tau_{2a,1}}} + \frac{a_{2b}}{\sqrt{\pi\tau_{2b,1}}} + \frac{a_{3a}}{\sqrt{\pi\tau_{3a,1}}} + \frac{a_{3b}}{\sqrt{\pi\tau_{3b,1}}}\right) \end{aligned} \tag{3.68}$$

$$\dot{b}_2(\omega) = -i\omega b_2(\omega) - i\left(\frac{a_{2a}}{\sqrt{\pi\tau_{2a,2}}} + \frac{a_{2b}}{\sqrt{\pi\tau_{2b,2}}}\right) \tag{3.69}$$

$$\dot{b}_3(\omega) = -i\omega b_3(\omega) - i\left(\frac{a_{3a}}{\sqrt{\pi\tau_{3a,3}}} + \frac{a_{3b}}{\sqrt{\pi\tau_{3b,3}}}\right). \tag{3.70}$$

From these differential equations the relation between the *in/out* operators is obtained by integrating them and introducing b_{in} and b_{out} in the initial conditions [46] using Eq. (3.64-3.66). A full derivation of these equations can be found

in Appendix C. Here I give the results:

$$b_{1out}(t) = b_{1in}(t) - i\sqrt{2}\left(\frac{a_{T1}}{\sqrt{\tau_{T1}}} + \frac{a_{T3}}{\sqrt{\tau_{T3}}} + \left(\sqrt{\frac{2}{\tau_{T1}}} - \sqrt{\frac{3}{\tau_{T3}}}\right) a_{T1}^{\dagger} a_{T2} + \frac{a_{2a}}{\sqrt{\tau_{2a,1}}} + \frac{a_{2b}}{\sqrt{\tau_{2b,1}}} + \frac{a_{3a}}{\sqrt{\tau_{3a,1}}} + \frac{a_{3b}}{\sqrt{\tau_{3b,1}}}\right) \tag{3.71}$$

$$b_{2out}(t) = b_{2in}(t) - i\sqrt{2}\left(\frac{a_{2a}}{\sqrt{\tau_{2a,2}}} + \frac{a_{2b}}{\sqrt{\tau_{2b,2}}}\right) \tag{3.72}$$

$$b_{3out}(t) = b_{3in}(t) - i\sqrt{2}\left(\frac{a_{3a}}{\sqrt{\tau_{3a,3}}} + \frac{a_{3b}}{\sqrt{\tau_{3b,3}}}\right). \tag{3.73}$$

Similar relations hold for the decoherence operators. Finally, the evolution of the ladder operators describing the transmon and the SQUIDs is also found by using the Heisenberg equation. For the operator a_{T1} this is

$$\begin{aligned}\dot{a}_{T1} = &-i\omega_{T1} a_{T1} + i\sum_k J_{1k} a_{T1} a_k^{\dagger} a_k \\ &+ i\int dp \left[\frac{\left(a_{T1}^{\dagger} a_{T1} - a_{T1} a_{T1}^{\dagger}\right) b_1(p)}{\sqrt{\pi\tau_{T1}}} + \frac{a_{T3}^{\dagger} a_{T1} b_1(p)}{\sqrt{\pi\tau_{T3}}}\right. \\ &\quad + \left(\sqrt{\frac{3}{\pi\tau_{T3}}} - \sqrt{\frac{2}{\pi\tau_{T1}}}\right) b_1^{\dagger}(p) a_{T2} \\ &\quad + \sqrt{\frac{\gamma_{rT1}}{2\pi}}\left(a_{T1}^{\dagger} a_{T1} - a_{T1} a_{T1}^{\dagger}\right) r_{T1}(p) + \frac{\gamma_{rT3}}{\sqrt{2\pi}} a_{T3}^{\dagger} a_{T1} r_{T3}(p) \\ &\quad \left. + -\sqrt{\frac{\gamma_{dT1}}{4\pi}}\left(a_{T1} d_{T1}(p) + d_{T1}^{\dagger}(p) a_{T1}\right)\right].\end{aligned} \tag{3.74}$$

The *input* operators are introduced in this equation by making use of Eq.(C.7) in the Appendix C. This gives a coupled equation of motion that contains the *input*

operators as well as all the other a_k ladder operators:

$$\begin{aligned}
\dot{a}_{T1} =& -\left(i\omega_{T1}+\frac{1}{\tau_{T1}}+\frac{1}{2}\gamma_{rT1}+\frac{1}{4}\gamma_{dT1}\right)a_{T1}-\frac{1}{\sqrt{\tau_{T1}\tau_{T3}}}a_{T3}+i\sum_k J_{1k}a_{T1}a_k^\dagger a_k \\
&+\frac{2}{\sqrt{\tau_{T1}}}\left(\sqrt{\frac{2}{\tau_{T1}}}-\sqrt{\frac{3}{\tau_{T3}}}\right)a_{T1}^\dagger a_{T2}+\frac{2}{\sqrt{\tau_{T3}}}\left(\sqrt{\frac{2}{\tau_{T1}}}-\sqrt{\frac{3}{\tau_{T3}}}\right)a_{T3}^\dagger a_{T2} \\
&+\left(\frac{1}{\sqrt{\tau_{T1}}}\left(a_{T1}^\dagger a_{T1}-a_{T1}a_{T1}^\dagger\right)+\frac{1}{\sqrt{\tau_{T3}}}a_{T3}^\dagger a_{T1}\right)\times \\
&\qquad\left(\frac{a_{2a}}{\sqrt{\tau_{2a,1}}}+\frac{a_{2b}}{\sqrt{\tau_{2b,1}}}+\frac{a_{3a}}{\sqrt{\tau_{3a,1}}}+\frac{a_{3b}}{\sqrt{\tau_{3b,1}}}\right) \\
&+\left(\sqrt{\frac{2}{\tau_{T1}}}-\sqrt{\frac{3}{\tau_{T3}}}\right)\left(\frac{a_{2a}^\dagger}{\sqrt{\tau_{2a,1}}}+\frac{a_{2b}^\dagger}{\sqrt{\tau_{2b,1}}}+\frac{a_{3a}^\dagger}{\sqrt{\tau_{3a,1}}}+\frac{a_{3b}^\dagger}{\sqrt{\tau_{3b,1}}}\right)a_{T2} \\
&+i\sqrt{\frac{2}{\tau_{T1}}}a_{T1}^\dagger a_{T1}b_{1in}(t)-i\sqrt{\frac{2}{\tau_{T1}}}a_{T1}a_{T1}^\dagger b_{1in}(t) \\
&+i\sqrt{\frac{2}{\tau_{T3}}}a_{T3}^\dagger a_{T1}b_{1in}(t)-i\sqrt{2}\left(\sqrt{\frac{2}{\tau_{T1}}}-\sqrt{\frac{3}{\tau_{T3}}}\right)b_{1in}^\dagger(t)a_{T2} \\
&+i\sqrt{\gamma_{rT1}}\left(a_{T1}^\dagger a_{T1}-a_{T1}a_{T1}^\dagger\right)r_{T1in}(t)+i\sqrt{\gamma_{rT3}}a_{T3}^\dagger a_{T1}r_{T3in}(t) \\
&-i\sqrt{\frac{\gamma_{dT1}}{2}}\left(a_{T1}d_{T1in}(t)+d_{T1in}^\dagger(t)a_{T1}\right).
\end{aligned} \tag{3.75}$$

Similarly, the other operators satisfy the equations:

$$\begin{aligned}
\dot{a}_{T2} =& -\left(i\omega_{T2}+\left(\sqrt{\frac{2}{\tau_{T1}}}-\sqrt{\frac{3}{\tau_{T3}}}\right)^2\right)a_{T2}+i\sum_k J_{2k}a_{T2}a_k^\dagger a_k \\
&+\left(\frac{1}{\sqrt{\tau_{T1}}}a_{T1}^\dagger a_{T2}+\frac{1}{\sqrt{\tau_{T3}}}a_{T3}^\dagger a_{T2}-\left(\sqrt{\frac{2}{\tau_{T1}}}-\sqrt{\frac{3}{\tau_{T3}}}\right)a_{T1}\right)\times \\
&\qquad\left(\frac{a_{2a}}{\sqrt{\tau_{2a,1}}}+\frac{a_{2b}}{\sqrt{\tau_{2b,1}}}+\frac{a_{3a}}{\sqrt{\tau_{3a,1}}}+\frac{a_{3b}}{\sqrt{\tau_{3b,1}}}\right) \\
&+i\sqrt{\frac{2}{\tau_{T1}}}a_{T1}^\dagger a_{T2}b_{1in}(t)+i\sqrt{\frac{2}{\tau_{T3}}}a_{T3}^\dagger a_{T2}b_{1in}(t) \\
&-i\sqrt{2}\left(\sqrt{\frac{2}{\tau_{T1}}}-\sqrt{\frac{3}{\tau_{T3}}}\right)a_{T1}b_{1in}(t) \\
&+i\sqrt{\gamma_{rT1}}a_{T1}^\dagger a_{T2}r_{T1in}(t)+i\sqrt{\gamma_{rT3}}a_{T3}^\dagger a_{T2}r_{T3in}(t)
\end{aligned} \tag{3.76}$$

$$\begin{aligned}
\dot{a}_{T3} =& -\left(i\omega_{T3}+\frac{1}{\tau_{T3}}+\frac{1}{2}\gamma_{rT3}+\frac{1}{4}\gamma_{dT3}\right)a_{T3}-\frac{1}{\sqrt{\tau_{T1}\tau_{T3}}}a_{T1}+i\sum_k J_{3k}a_{T3}a_k^\dagger a_k \\
&+\left(\frac{a_{T1}^\dagger a_{T3}}{\sqrt{\tau_{T1}}}+\frac{a_{T3}^\dagger a_{T3}-a_{T3}a_{T3}^\dagger}{\sqrt{\tau_{T3}}}\right)\left(\frac{a_{2a}}{\sqrt{\tau_{2a,1}}}+\frac{a_{2b}}{\sqrt{\tau_{2b,1}}}+\frac{a_{3a}}{\sqrt{\tau_{3a,1}}}+\frac{a_{3b}}{\sqrt{\tau_{3b,1}}}\right) \\
&+i\sqrt{\frac{2}{\tau_{T1}}}a_{T1}^\dagger a_{T3}b_{1in}(t)+i\sqrt{\frac{2}{\tau_{T3}}}\left(a_{T3}^\dagger a_{T3}-a_{T3}a_{T3}^\dagger\right)b_{1in}(t) \\
&+i\sqrt{\gamma_{rT1}}a_{T1}^\dagger a_{T3}r_{T1in}(t)+i\sqrt{\gamma_{rT3}}\left(a_{T3}^\dagger a_{T3}-a_{T3}a_{T3}^\dagger\right)r_{T3in}(t) \\
&-i\sqrt{\frac{\gamma_{dT3}}{2}}\left(a_{T3}d_{T3in}(t)+d_{T3in}^\dagger(t)a_{T3}\right) \qquad (3.77)
\end{aligned}$$

$$\begin{aligned}
\dot{a}_{2a} =& -\left(i\omega_{2a}+\frac{1}{\tau_{2a,1}}+\frac{1}{\tau_{2a,2}}+\frac{1}{2}\gamma_{r2a}+\frac{1}{4}\gamma_{d2a}\right)a_{2a}+i\sum_{j=1}^{3}J_{j2a}a_{Tj}^\dagger a_{Tj}a_{2a} \\
&-i\sqrt{\frac{2}{\tau_{2a,1}}}b_{1in}(t)-i\sqrt{\frac{2}{\tau_{2a,2}}}b_{2in}(t) \\
&-\left(\frac{1}{\sqrt{\tau_{2a,1}\tau_{2b,1}}}+\frac{1}{\sqrt{\tau_{2a,2}\tau_{2b,2}}}\right)a_{2b}-\frac{1}{\sqrt{\tau_{2a,1}\tau_{3a,1}}}a_{3a}-\frac{1}{\sqrt{\tau_{2a,1}\tau_{3b,1}}}a_{3b} \\
&-\frac{1}{\sqrt{\tau_{2a,1}}}\left(\sqrt{\frac{2}{\tau_{T1}}}-\sqrt{\frac{3}{\tau_{T3}}}\right)a_{T1}^\dagger a_{T2}-\frac{1}{\sqrt{\tau_{2a,1}\tau_{T1}}}a_{T1}-\frac{1}{\sqrt{\tau_{2a,1}\tau_{T3}}}a_{T3} \\
&-i\sqrt{\gamma_{r2a}}r_{2ain}(t)-i\sqrt{\frac{\gamma_{d2a}}{2}}\left(a_{2a}d_{2ain}(t)+d_{2ain}^\dagger(t)a_{2a}\right). \qquad (3.78)
\end{aligned}$$

Similar expressions hold for the operators a_{2b}, a_{3a} and a_{3b}. Eq. (3.75) to (3.78) are the Langevin equations for the transmon and SQUID operators [45]. Now the $b(t)$, $r(t)$ and $d(t)$ operators could be expressed as the inverse Fourier transformation of $b(p)$, $r(p)$ and $d(p)$. This will introduce an integral into our equations of motion, but the time dependence of the *in* and *out* operators will disappear. In some calculations this may be useful, but in others it may not, so I am leaving it as it is, by now.

Chapter 4

Dynamics of operation of the Quantum Switch

One of the advantages of studying a system analytically is that its analysis holds for any value of the parameters that appear in the equations. Thus, the values of these parameters can be obtained after the analytical calculations have been performed and can be chosen to give the desired results. Since at the time of writing this text I already knew which conditions these parameters had to satisfy, I have imposed some constraints during the derivation of the equations in the previous chapters. In this section I compute the scattering amplitudes of some relevant processes and announce the remaining constraints to be imposed to the parameters that, at this point, remain free.

4.1 Scattering of a single photon

The proposed quantum switch is a physical system that, in the first step, absorbs a single photon and modifies its own energy spectrum according to the state of the absorbed photon. Thus, it is convenient to start studying what happens when a single photon comes in. For a correct performance of the quantum device, an incoming photon should only be absorbed if it has the right energy –that is, ω_{T1} or ω_{T3}– and reflected if it does not. In case the photon is absorbed, it has to be emitted back, never forward. The probability of transmission and reflection are the functions that have to be minimized or maximized and their values will reveal whether the device works properly or not.

When a photon ($b^{\dagger}_{1in}(k)\,|0\rangle$) is sent in, the system can respond in four different ways:

1. The photon is absorbed and emitted back (or just reflected) as $b^\dagger_{1out}(k')\,|0\rangle$.
2. The photon is absorbed and emitted forward as $b^\dagger_{2out}(k')\,|0\rangle$ or $b^\dagger_{3out}(k')\,|0\rangle$.
3. The photon is absorbed but decays into an external bath mode (relaxation).
4. The photon is absorbed but the system experiences dephasing due to the coupling with the external bath.

The last two processes cannot be controlled by the experimentalist, so my efforts will be concentrated on the first two. The probability amplitude for an incoming photon with frequency k being reflected with frequency p is

$$S_1(p,k) = \langle 0|\, b_{1out}(p) b^\dagger_{1in}(k)\,|0\rangle\,. \tag{4.1}$$

Similarly, the probability amplitudes for an incoming photon being transmitted into the second and third transmission lines are, respectively,

$$S_2(p,k) = \langle 0|\, b_{2out}(p) b^\dagger_{1in}(k)\,|0\rangle\,, \tag{4.2}$$
$$S_3(p,k) = \langle 0|\, b_{3out}(p) b^\dagger_{1in}(k)\,|0\rangle\,. \tag{4.3}$$

Let me start for the first process. After making use of the *in/out* relations in Eq. (3.71), (3.72), (3.73) and introducing inverse Fourier transformations, the probability amplitude $S_1(p,k)$ can be transformed to an equation containing only the *in* operators and the time-dependent operators that describe the transmon and SQUIDs excitations. This expression reads

$$S_1(p,k) = \langle 0|\, b_{1in}(p) b^\dagger_{1in}(k)\,|0\rangle \tag{4.4.a}$$
$$- i\left(\frac{2}{\sqrt{\tau_{T1}}} - \sqrt{\frac{6}{\tau_T}}\right)\frac{1}{\sqrt{2\pi}}\int dt\, e^{ipt}\,\langle 0|\, a^\dagger_{T1}(t) a_{T2}(t) b^\dagger_{1in}(k)\,|0\rangle \tag{4.4.b}$$
$$- i\sqrt{\frac{2}{\tau_{T1}}}\frac{1}{\sqrt{2\pi}}\int dt\, e^{ipt}\,\langle 0|\, a_{T1}(t) b^\dagger_{1in}(k)\,|0\rangle \tag{4.4.c}$$
$$- i\sqrt{\frac{2}{\tau_{T3}}}\frac{1}{\sqrt{2\pi}}\int dt\, e^{ipt}\,\langle 0|\, a_{T3}(t) b^\dagger_{1in}(k)\,|0\rangle \tag{4.4.d}$$
$$- i\sqrt{\frac{2}{\tau_{2a,1}}}\frac{1}{\sqrt{2\pi}}\int dt\, e^{ipt}\,\langle 0|\, a_{2a}(t) b^\dagger_{1in}(k)\,|0\rangle \tag{4.4.e}$$
$$+ (2a \to 2b,\ 3a,\ 3b)\,.$$

The first element of this equation, Eq. (4.4.a), is $\delta(p-k)$. The second element, Eq. (4.4.a), vanishes because in this expression there is a creation operator acting

on the vacuum by the left-hand side. The other six terms have to be transformed into a differential equation and solved using the Langevin equations*. This gives

$$\begin{aligned}
S_1(p,k) = \delta(p-k) \\
&- \frac{\delta(p-k)\left(\frac{2}{\tau_{T1}} + \frac{2}{\tau_{T3}}\alpha_1(p)\right)}{T_1(p) + \frac{1}{\tau_{T1}} + \frac{\alpha_1(p)}{\tau_{T3}} + \left(\frac{1}{\tau_{2a,1}} + \frac{\alpha_2(p)}{\tau_{2b,1}}\right)\frac{T_1(p)}{T_2(p)} + \left(\frac{1}{\tau_{3a,1}} + \frac{\alpha_3(p)}{\tau_{3b,1}}\right)\frac{T_1(p)}{T_3(p)}} \\
&- \frac{\delta(p-k)\left(\frac{2}{\tau_{2a,1}} + \frac{2}{\tau_{2b,1}}\alpha_2(p)\right)}{T_2(p) + \frac{1}{\tau_{2a,1}} + \frac{\alpha_2(p)}{\tau_{2b,1}} + \left(\frac{1}{\tau_{T1}} + \frac{\alpha_1(p)}{\tau_{T3}}\right)\frac{T_2(p)}{T_1(p)} + \left(\frac{1}{\tau_{3a,1}} + \frac{\alpha_3(p)}{\tau_{3b,1}}\right)\frac{T_2(p)}{T_3(p)}} \\
&- \frac{\delta(p-k)\left(\frac{2}{\tau_{3a,1}} + \frac{2}{\tau_{3b,1}}\alpha_3(p)\right)}{T_3(p) + \frac{1}{\tau_{3a,1}} + \frac{\alpha_3(p)}{\tau_{3b,1}} + \left(\frac{1}{\tau_{T1}} + \frac{\alpha_1(p)}{\tau_{T3}}\right)\frac{T_3(p)}{T_1(p)} + \left(\frac{1}{\tau_{2a,1}} + \frac{\alpha_2(p)}{\tau_{2b,1}}\right)\frac{T_3(p)}{T_2(p)}},
\end{aligned} \tag{4.5}$$

with

$$T_1(p) = i(\omega_{T1} - p) + \frac{\gamma_{rT1}}{2} + \frac{\gamma_{dT1}}{4} \tag{4.6}$$

$$T_2(p) = i(\omega_{2a} - p) + \frac{1}{\tau_{2a,2}} + \sqrt{\frac{\tau_{2a,1}}{\tau_{2b,1}\tau_{2a,2}\tau_{2b,2}}}\alpha_2(p) + \frac{\gamma_{r2a}}{2} + \frac{\gamma_{d2a}}{4} \tag{4.7}$$

$$T_3(p) = i(\omega_{3a} - p) + \frac{1}{\tau_{3a,3}} + \sqrt{\frac{\tau_{3a,1}}{\tau_{3b,1}\tau_{3a,3}\tau_{3b,3}}}\alpha_3(p) + \frac{\gamma_{r3a}}{2} + \frac{\gamma_{d3a}}{4}, \tag{4.8}$$

and

$$\alpha_1(p) = \frac{i(\omega_{T1} - p) + \frac{\gamma_{rT1}}{2} + \frac{\gamma_{dT1}}{4}}{i(\omega_{T3} - p) + \frac{\gamma_{rT3}}{2} + \frac{\gamma_{dT3}}{4}} \tag{4.9}$$

$$\alpha_2(p) = \frac{i(\omega_{2a} - p) + \frac{1}{\tau_{2a,2}} - \sqrt{\frac{\tau_{2b,1}}{\tau_{2a,1}\tau_{2a,2}\tau_{2b,2}}} + \frac{\gamma_{r2a}}{2} + \frac{\gamma_{d2a}}{4}}{i(\omega_{2b} - p) + \frac{1}{\tau_{2b,2}} - \sqrt{\frac{\tau_{2a,1}}{\tau_{2b,1}\tau_{2a,2}\tau_{2b,2}}} + \frac{\gamma_{r2b}}{2} + \frac{\gamma_{d2b}}{4}} \tag{4.10}$$

$$\alpha_3(p) = \frac{i(\omega_{3a} - p) + \frac{1}{\tau_{3a,3}} - \sqrt{\frac{\tau_{3b,1}}{\tau_{3a,1}\tau_{3a,3}\tau_{3b,3}}} + \frac{\gamma_{r3a}}{2} + \frac{\gamma_{d3a}}{4}}{i(\omega_{3b} - p) + \frac{1}{\tau_{3b,3}} - \sqrt{\frac{\tau_{3a,1}}{\tau_{3b,1}\tau_{3a,3}\tau_{3b,3}}} + \frac{\gamma_{r3b}}{2} + \frac{\gamma_{d3b}}{4}}. \tag{4.11}$$

*For the complete derivation, see Appendix D.

Similarly, the other two amplitudes are given by

$$S_2(p,k) = -\frac{\delta(p-k)\left(\frac{2}{\sqrt{\tau_{2a,1}\tau_{2a,2}}}+\frac{2}{\sqrt{\tau_{2b,1}\tau_{2b,2}}}\alpha_2(p)\right)}{T_2(p)+\frac{1}{\tau_{2a,1}}+\frac{\alpha_2(p)}{\tau_{2b,1}}+\left(\frac{1}{\tau_{T1}}+\frac{\alpha_1(p)}{\tau_{T3}}\right)\frac{T_2(p)}{T_1(p)}+\left(\frac{1}{\tau_{3a,1}}+\frac{\alpha_3(p)}{\tau_{3b,1}}\right)\frac{T_2(p)}{T_3(p)}}, \tag{4.12}$$

$$S_3(p,k) = -\frac{\delta(p-k)\left(\frac{2}{\sqrt{\tau_{3a,1}\tau_{3a,3}}}+\frac{2}{\sqrt{\tau_{3b,1}\tau_{3b,3}}}\alpha_3(p)\right)}{T_3(p)+\frac{1}{\tau_{3a,1}}+\frac{\alpha_3(p)}{\tau_{3b,1}}+\left(\frac{1}{\tau_{T1}}+\frac{\alpha_1(p)}{\tau_{T3}}\right)\frac{T_3(p)}{T_1(p)}+\left(\frac{1}{\tau_{2a,1}}+\frac{\alpha_2(p)}{\tau_{2b,1}}\right)\frac{T_3(p)}{T_2(p)}}. \tag{4.13}$$

The amplitude in Eq. (4.5) contains information about three processes: (1) the photon is absorbed by the transmon and is reflected, (2) the photon is absorbed by the SQUIDs in the second branch and is reflected, (3) the photon is absorbed by the SQUIDs in the third branch and is reflected. The first possible process is described by the second line together with the first. We neglect, for a moment, the decoherence parameters γ_r and γ_d. If, in addition, $\tau_{2a,1} = \tau_{2b,1}$ and $\tau_{2a,2} = \tau_{2b,2}$ (likewise for $3a$, $3b$) and also $\tau_{2a,1} = \tau_{2a,2}$, these amplitudes become much simpler and relevant information can be obtained. In this scenario, near $p = \omega_{T1}$ (p is the momentum of the photon), α_1 and T_1 go to zero and S_1 goes to 1, thus the photon is reflected. The contributions of the processes (2) and (3) are very small because the denominator in the third and four lines are large when $p \neq \omega_{2a}, \omega_{3a}$. In case the incoming photon has energy ω_{T3}, then α_1 diverges and the amplitude goes to $1 - \frac{2\alpha_1/\tau_{T3}}{\alpha_1/\tau_{T3}} = -1$ again (the amplitude squared goes to 1).

Near $p = \omega_{2a}$ [this is the process (2)], the second and fourth line do not contribute, thus the amplitude is given by the first and third lines. In this region of the momentum space, α_2 goes to zero and so does the amplitude ($S_1 \sim 1 - \frac{2/\tau_{2a,1}}{1/\tau_{2a,1}+1/\tau_{2a,2}}$). Something similar happens with ω_{2b}, ω_{3a} and ω_{3b}. In any other case, when the momentum is far from any of the energies of the excited levels, the three denominators in Eq. (4.5) grow and the amplitude goes to 1.

All this means that, in the ideal case where there is no decoherence and any value can be imposed on the lifetimes of the excitations, a photon that has momentum

- $p = \omega_{T1}$ or $p = \omega_{T3}$ is always reflected,
- $p = \omega_{2a}, \omega_{2b}, \omega_{3a}, \omega_{3b}$ is never reflected,
- p that do not coincide with the energy of any excitation is always reflected.

4.1.1 Probability

The amplitude itself is not an observable and, therefore, is not suitable for determining the performance of the quantum switch. The probability, on the other hand, is a real number and its values can be contrasted to the results of experimental realizations. The probability is the quantity that has to be maximized (or minimized) to obtain a proper quantum switch and is derived from the scattering amplitudes.

The scattering amplitudes computed in the previous section (and the ones that will be computed next) are valid for an incoming photon with any frequency, but these photons are sent with a definite momentum (or a superposition). I will assume that the incoming photons have a frequency distribution given by a Lorentzian centered at $k = \omega_t$ and with width $1/\tau_t$ (just like in similar works [17]). Hence, given an amplitude $S(p,k)$ describing any single-photon process involving an incoming particle with momentum k and an outgoing particle with momentum p, $\beta(p)$ refers to the convolution of the Lorentzian frequency distribution of the incoming photon with the amplitude of the process $S(p,k)$.

$$\beta(p) = \int \frac{dk}{\sqrt{\pi\tau_t}} \frac{1}{i(\omega_t - k) + \frac{1}{\tau_t}} S(p,k). \tag{4.14}$$

Now the incoming photon has a definite frequency –not just any– given by a Lorentzian curve in momentum space. With this, the probability of a process with an amplitude given by $\beta(p)$ is

$$P = \int dp\, |\beta(p)|^2 . \tag{4.15}$$

The probabilities of the single-photon processes discussed previously cannot be obtained analytically and will be evaluated numerically in Sections 4.3.1 and 4.3.2.

4.2 Two-photon processes

Once the first photon is absorbed, the second step in the operation of the quantum switch consists of absorbing a second photon and forwarding it into an outgoing transmission line, according to the state of the first absorbed photon. The first photon must remain in the device (the transmon must remain excited) until the full process has finished and only then it can be emitted back to the incoming transmission line, where it came from. The amplitude of this scattering process,

where a photon is transmitted to the second outgoing transmission line, is given by

$$S_{12}(p_1,p_2,k_1,k_2) = \langle 0|\, b_{1out}(p_1) b_{2out}(p_2) b^{\dagger}_{1in}(k_2) b^{\dagger}_{1in}(k_1)\, |0\rangle\,, \tag{4.16}$$

that is, two photons come in and one of them is reflected and the other is transmitted. Since the two photons are not sent in at the same time, some delay between the incoming pulses have to be imposed onto these equations. This delay Δt between pulses can be taken into account by introducing the Heaviside function $\Theta(t_2' - (t_1' + \Delta t))$. That is, the operators $b^{\dagger}_{1in}(k_1)$ and $b^{\dagger}_{2in}(k_2)$ would become

$$b^{\dagger}_{1in}(k_2) = \frac{1}{\sqrt{2\pi}} \int dt_2' e^{-ik_2 t_2'} b^{\dagger}_{1in}(t_2') \Theta(t_2' - (t_1' + \Delta t)), \tag{4.17}$$

$$b^{\dagger}_{1in}(k_1) = \frac{1}{\sqrt{2\pi}} \int dt_1' e^{-ik_1 t_1'} b^{\dagger}_{1in}(t_1'). \tag{4.18}$$

To evaluate $S_{12}(p_1,p_2,k_1,k_2)$, I have tried to follow the same procedure as in the previous section, but the complexity of the equations to be evaluated made it impossible to find the scattering amplitude by using the Langevin equations. I have tried different methods to solve the problem:

1. In the first place, I tried to solve the system numerically, but the dimension of the Hilbert space and also the form of the differential equations made this attempt fruitless. This attempt is expanded in the Appendix E.

2. I have also tried to use propagators and Green's functions to evaluate the expression in brackets that gives the scattering amplitude, but without success. Appendix F contains all the steps I have followed in this attempt to derive the scattering amplitude.

3. Another failed attempt to derive the scattering amplitude is described in the Appendix G, where I have made use of quantum field theory techniques to obtain the desired propagators. In this appendix, I derived the Feynman rules for the Hamiltonian I have proposed, but the results were not good either.

4. Finally, I have decided to assume that the lifetime of the transmon excitations is infinite and I have computed the scattering amplitude following the procedure described in the previous section. The validity of this assumption is discussed in Chapter 5.

A transmon excitation fixed in time implies that the transmon operators a_{T1}, a_{T2} and a_{T3} (together with their hermitian conjugate) are constant and, thus, the

Langevin equations do not satisfy the same differential equations as before. The transmon excitations cannot decay into an outgoing photon in the transmission lines anymore so, in this case, $b_{1in}(t)$ and $b_{1out}(t)$ do not depend explicitly on a_{T1}, a_{T2} and a_{T3} anymore. This assumption makes sense if the lifetime of the transmon is larger than that of the SQUIDs, which is required for a good performance of the quantum switch[†]. With this assumption, now the $b_{1in}(t)$ and $b_{1out}(t)$ operators become

$$b_{1out}(t) = b_{1in}(t) - i\sqrt{2}\left(\frac{a_{2a}}{\sqrt{\tau_{2a,1}}} + \frac{a_{2b}}{\sqrt{\tau_{2b,1}}} + \frac{a_{3a}}{\sqrt{\tau_{3a,1}}} + \frac{a_{3b}}{\sqrt{\tau_{3b,1}}}\right), \tag{4.19}$$

$$\begin{aligned} b_{1in}(t) =& \frac{1}{\sqrt{2\pi}}\int dp\, b_1(p) \\ &+ \frac{i}{\sqrt{2}}\left(\frac{a_{2a}}{\sqrt{\tau_{2a,1}}} + \frac{a_{2b}}{\sqrt{\tau_{2b,1}}} + \frac{a_{3a}}{\sqrt{\tau_{3a,1}}} + \frac{a_{3b}}{\sqrt{\tau_{3b,1}}}\right). \end{aligned} \tag{4.20}$$

Nevertheless, the transmon has to be coupled to the SQUIDs, otherwise it will disappear completely from the system. The modified equations of motion of the transmon and the SQUIDs once the transmon has been decoupled from the transmission lines read

$$\dot{a}_{T1} = \dot{a}_{T2} = \dot{a}_{T3} = 0 \tag{4.21}$$

$$\begin{aligned} \dot{a}_{2a} =& -\left(i\omega_{2a} + \frac{1}{\tau_{2a,1}} + \frac{1}{\tau_{2a,2}} + \frac{\gamma_{r2a}}{2} + \frac{\gamma_{d2a}}{4}\right) a_{2a} + i\sum_{j=1}^{3} J_{j2a} a_{Tj}^{\dagger} a_{Tj} a_{2a} \\ &- i\sqrt{\frac{2}{\tau_{2a,1}}}\, b_{1in}(t) - i\sqrt{\frac{2}{\tau_{2a,2}}}\, b_{2in}(t) \\ &- \left(\frac{1}{\sqrt{\tau_{2a,1}\tau_{2b,1}}} + \frac{1}{\sqrt{\tau_{2a,2}\tau_{2b,2}}}\right) a_{2b} - \frac{1}{\sqrt{\tau_{2a,1}\tau_{3a,1}}} a_{3a} - \frac{1}{\sqrt{\tau_{2a,1}\tau_{3b,1}}} a_{3b} \\ &- i\sqrt{\gamma_{r2a}}\, r_{2ain}(t) - i\sqrt{\frac{\gamma_{d2a}}{2}}\left(a_{2a} d_{2ain}(t) + d_{2ain}^{\dagger}(t) a_{2a}\right). \end{aligned} \tag{4.22}$$

The expressions for $2b$, $3a$ and $3b$ can be easily deduced from Eq. (4.22).

In the case that the transmon is already excited, the probability amplitude for a photon with momentum k being transmitted through the second transmission line

[†]The last $n-1$ photons of a n-photon register have to interact with the device while the transmon is excited.

with momentum p is

$$\begin{aligned} S_{12}(p,k) &= \langle 0|\, a_{T1} b_{2out}(p) b^\dagger_{1in}(k) a^\dagger_{T1}\,|0\rangle \\ &= \langle 0|\, a_{T1} b_{2in}(p) b^\dagger_{1in}(k) a^\dagger_{T1}\,|0\rangle \\ &\quad - i\sqrt{\frac{2}{\tau_{2a,2}}}\frac{1}{\sqrt{2\pi}}\int dp\, e^{ipt}\,\langle 0|\, a_{T1} a_{2a}(t) b^\dagger_{1in}(k) a^\dagger_{T1}\,|0\rangle \\ &\quad - i\sqrt{\frac{2}{\tau_{2b,2}}}\frac{1}{\sqrt{2\pi}}\int dp\, e^{ipt}\,\langle 0|\, a_{T1} a_{2b}(t) b^\dagger_{1in}(k) a^\dagger_{T1}\,|0\rangle\,. \end{aligned} \tag{4.23}$$

The second line gives zero because the two operators describing the incoming photons (in two different transmission lines) commute and, since a_{T1} is not coupled to the transmission lines, b_{2in} cannot annihilate a transmon excitation. It acts on the vacuum instead, giving $b_{2in}\,|0\rangle = 0$.

A simple way to see how the second line in Eq. (4.23) vanishes is the following: as I said before [in Section 3.5, Eq. (3.66)], the $b_{1in}(t)$ operator –and the same for b_{2in} and b_{3in}– is defined as

$$b_{1in}(t) = \int_{-\infty}^{\infty} dp\, e^{-ip(t-t_0)} b_1(p,t_0), \tag{4.24}$$

where b_1 is evaluated at some t_0 such that $[a_{T1}, b_1] = 0$, thus, the following relations are obtained:

$$[a_{T1}, b_{1in}] = \left[a^\dagger_{T1}, b^\dagger_{1in}\right] = 0 \tag{4.25}$$

$$[a_{T1}, b_{2in}] = \left[a^\dagger_{T1}, b^\dagger_{2in}\right] = 0 \tag{4.26}$$

$$[a_{T1}, b_{2in}] = \left[a^\dagger_{T1}, b^\dagger_{3in}\right] = 0, \tag{4.27}$$

and the same for a_{T2} and a_{T3}. Using these relations and following the same procedure as in the previous section (see also Appendix D) the scattering amplitude becomes

$$S_{12}(p,k) = -\frac{\delta(p-k)\left(\frac{2}{\sqrt{\tau_{2a,1}\tau_{2a,2}}} + \frac{2}{\sqrt{\tau_{2b,1}\tau_{2b,2}}}\alpha'_2(p)\right)}{T'_2(p) + \frac{1}{\tau_{2a,1}} + \frac{\alpha'_2(p)}{\tau_{2b,1}} + \left(\frac{1}{\tau_{3a,1}} + \frac{\alpha'_3(p)}{\tau_{3b,1}}\right)\frac{T'_2(p)}{T'_3(p)}}, \tag{4.28}$$

where now, the α' and T' operators are

$$T'_2(p) = i\,(\omega_{2a} - J_{12a} - p) + \frac{1}{\tau_{2a,2}} + \sqrt{\frac{\tau_{2a,1}}{\tau_{2b,1}\tau_{2a,2}\tau_{2b,2}}}\alpha'_2(p) + \frac{\gamma_{r2a}}{2} + \frac{\gamma_{d2a}}{4} \tag{4.29}$$

$$T'_3(p) = i\,(\omega_{3a} - J_{13a} - p) + \frac{1}{\tau_{3a,3}} + \sqrt{\frac{\tau_{3a,1}}{\tau_{3b,1}\tau_{3a,3}\tau_{3b,3}}}\alpha'_3(p) + \frac{\gamma_{r3a}}{2} + \frac{\gamma_{d3a}}{4} \tag{4.30}$$

and

$$\alpha_2'(p) = \frac{i(\omega_{2a} - J_{12a} - p) + \frac{1}{\tau_{2a,2}} - \sqrt{\frac{\tau_{2b,1}}{\tau_{2a,1}\tau_{2a,2}\tau_{2b,2}}} + \frac{\gamma_{r2a}}{2} + \frac{\gamma_{d2a}}{4}}{i(\omega_{2b} - J_{12b} - p) + \frac{1}{\tau_{2b,2}} - \sqrt{\frac{\tau_{2a,1}}{\tau_{2b,1}\tau_{2a,2}\tau_{2b,2}}} + \frac{\gamma_{r2b}}{2} + \frac{\gamma_{d2b}}{4}} \tag{4.31}$$

$$\alpha_3'(p) = \frac{i(\omega_{3a} - J_{13a} - p) + \frac{1}{\tau_{3a,3}} - \sqrt{\frac{\tau_{3b,1}}{\tau_{3a,1}\tau_{3a,3}\tau_{3b,3}}} + \frac{\gamma_{r3a}}{2} + \frac{\gamma_{d3a}}{4}}{i(\omega_{3b} - J_{13b} - p) + \frac{1}{\tau_{3b,3}} - \sqrt{\frac{\tau_{3a,1}}{\tau_{3b,1}\tau_{3a,3}\tau_{3b,3}}} + \frac{\gamma_{r3b}}{2} + \frac{\gamma_{d3b}}{4}}. \tag{4.32}$$

A similar expression holds for the case where the photon is emitted into the third transmission line and also in the case where the third level of the transmon is excited.

The expression for the transmission of a photon when the transmon is excited is very similar to that of the transmission of a photon where the transmon is not excited, shown in Eq. (4.12), the main difference being the frequency threshold at which the photon is absorbed. In this case, due to the presence of a transmon excitation, the second photon can be absorbed by one of the SQUIDs (if it has the right energy) and be transmitted forward whereas, in the previous case (no transmon excitation) a photon with the very same energy cannot be absorbed and, thus, is reflected. For a more detailed analysis of this result, the reader is referred to the following section, where numerical results have been obtained and the two cases (presence and absence of a transmon excitation) are compared.

4.3 Numerical integration

Analytical expressions have been found –not free from approximations– for the scattering amplitudes of one and two photons. These amplitudes, once convoluted with the pulse shape in Eq. (4.14), give the probability of transmission of a photon within the different processes that can occur. However, these probabilities cannot be obtained analytically. Instead, some numerical values have to be introduced in the equations in order to make them numerically integrable. In this section I compute the squared amplitude (real numbers) of the different processes discussed previously and I also evaluate the probability that these processes take place.

The free parameters that are left in the equations derived in the previous sections are the capacitances, although some constraints have to be imposed on them. The values they take must satisfy:

a) $C_{2sa} < C_{2a}$. This condition is used to impose a cutoff in the Taylor expansion of the Hamiltonian, to ensure that the rotating wave approximation holds and to decouple the transmon to the outgoing transmission lines.

b) $\tau_{T3} = 6\tau_{T1}$. This condition is already satisfied if $\hbar^2\alpha_t/\varphi_0^2 = \gamma^3/(324C_t)$ is imposed.

c) Similarly, $\tau_{2a,1} = \tau_{2b,1}$ (and the same for $3a$, $3b$). With these conditions, the scattering amplitude for a photon being transmitted –when it has the right energy– is maximized.

d) For the same reason, $\tau_{2a,1} = \tau_{2a,2}$ has also to be imposed.

e) τ_{T1} and τ_{T3} have to be much larger than the lifetimes of the SQUIDs.

f) Finally, and possibly more important, the energy of the SQUID levels and the coupling strengths have to be such that $\omega_{2a} - J_{12a} = \omega_{3a} - J_{33a}$ and also $\omega_{2b} - J_{12b} = \omega_{3b} - J_{33b}$. They also have to satisfy $\omega_{2a} \neq \omega_{2b} \neq \omega_{3a} \neq \omega_{3b}$.

With these conditions is not possible to obtain an explicit set of values for the capacitances. Multiple choices can be made, but none of them completely satisfies these constraints. The set of capacitances I propose is

$$\begin{aligned} C_t &= 0.1\, C_1 & & \\ C_{2a} &= 1.2\, C_1 & C_{2sa} &= 0.1824\, C_1 \\ C_{2b} &= 1.1\, C_1 & C_{2sb} &= 0.1934\, C_1 \\ C_{3a} &= C_1 & C_{3sa} &= 0.1650\, C_1 \\ C_{3b} &= C_1 & C_{3sb} &= 0.1799\, C_1, \end{aligned} \tag{4.33}$$

with $C_1 = 10^{-9}\frac{e^2}{h}\ F$. So the capacitances take values of the order of picofarads and femtofarads, which are realizable values [49]. With this set of variables, the energies of the transmon excitations are

$$\omega_{T1} = 7.18884 \cdot 10^9\ Hz \tag{4.34}$$
$$\omega_{T2} = 1.43829 \cdot 10^{10}\ Hz \tag{4.35}$$
$$\omega_{T3} = 2.19266 \cdot 10^{10}\ Hz, \tag{4.36}$$

and for the SQUIDs, the excitation energies are

$$\omega_{2a} = 1.0277 \cdot 10^9\ Hz \tag{4.37}$$
$$\omega_{2b} = 1.1615 \cdot 10^9\ Hz \tag{4.38}$$
$$\omega_{3a} = 1.05288 \cdot 10^9\ Hz \tag{4.39}$$
$$\omega_{3b} = 1.18562 \cdot 10^9\ Hz. \tag{4.40}$$

Version of June 29, 2015– Created June 29, 2015 - 21:15

The coupling strengths are also obtained from the capacitances

$$\begin{array}{lll} J_{12a} = 1.85615 \cdot 10^7\, Hz & J_{22a} = 3.14956 \cdot 10^7\, Hz & J_{32a} = 4.09808 \cdot 10^7\, Hz \\ J_{12b} = 2.09586 \cdot 10^7\, Hz & J_{22b} = 3.43797 \cdot 10^7\, Hz & J_{32b} = 4.32139 \cdot 10^7\, Hz \\ J_{13a} = 1.90274 \cdot 10^7\, Hz & J_{23a} = 3.29556 \cdot 10^7\, Hz & J_{33a} = 4.37402 \cdot 10^7\, Hz \\ J_{13b} = 2.13998 \cdot 10^7\, Hz & J_{23b} = 3.54703 \cdot 10^7\, Hz & J_{33b} = 4.50719 \cdot 10^7\, Hz. \end{array}$$

The values of the energies are in a range common in the related literature [49–51] and the values of the coupling strengths, two orders of magnitude smaller than the energies of the SQUID excitations, are also usual in other similar works (see, e.g., Neumeier *et al.* [17]). These values of the capacitances also satisfy:

i) $C_{2sa} \approx C_{2a}/5$. If the difference were larger, then the lifetime of the transmon would be much smaller than it is now. In this case, the transmon might also be coupled to the outgoing transmission lines.

ii) $\tau_{2a,1} \approx 400\tau_{T1}$. This is exactly the opposite of the expected behavior. To obtain this relation between $\tau_{2a,1}$ and τ_{T1} I have assumed that V_1 –and thus, A_1– are the same for any incoming pulse, but they may depend on the frequency of the pulse and also on other quantities, such as the cavity quality factor Q of the transmission line, related to the Purcell effect [52]. Although I do not expect this relation to be much different after considering a non constant A_1, I will consider that, in the case of the two-photon scattering, the lifetime of the transmon is infinitely larger than that of the SQUIDs. This assumption simplifies the calculations.

iii) $\tau_{2a,1} \approx \frac{4}{3}\tau_{2b,1}$. This is because different capacitances have to be given to the SQUID's capacitors. Otherwise they all would have the same energy. This small difference does not have a big influence in the scattering amplitudes, as will be shown in the next sections.

iv) The last condition is identically satisfied: $\omega_{2a} - J_{12a} = \omega_{3a} - J_{33a}$ and also $\omega_{2b} - J_{12b} = \omega_{3b} - J_{33b}$. Although it may seem that the energy of the SQUID excitations are similar, they are different enough , as will be seen during the numerical integration.

Regarding the relation between $\tau_{2a,1}$ and $\tau_{2a,2}$, it can be imposed by hand because they are independent, but their values have to be chosen wisely. Recall that, from Eq. (3.24) to (3.33), the lifetimes depend on some variables A_1, A_2 and A_3. If we want to make the system scalable, these have to be the same. Imagine that they are not, and imagine that the lifetimes satisfy $\tau_{2a,2} = \rho\,\tau_{2a,1}$ for some ρ which, in case the system is scalable, is $\rho \approx 25$ [with the capacitances given in Eq. (4.33)].

Near $p = \omega_{2a}$, the scattering amplitude for the transmission of a photon would go as $S \sim 2\frac{\sqrt{\rho}}{\rho+1}$, which goes to 0.38 for $\rho \approx 25$. In the following calculations, I will consider $\rho = 1$, so the amplitude will be maximized.

The values I have taken for the lifetimes are

$$\tau_{T1} = 1 \cdot 10^{-7}\, s \tag{4.41}$$

$$\tau_{T3} = 6 \cdot 10^{-7}\, s \tag{4.42}$$

$$\tau_{2a,1} = \tau_{2a,2} = \tau_{3a,1} = \tau_{3a,3} = 4 \cdot 10^{-5}\, s \tag{4.43}$$

$$\tau_{2b,1} = \tau_{2b,2} = \tau_{3b,1} = \tau_{3b,3} = 3 \cdot 10^{-5}\, s. \tag{4.44}$$

These values –both their magnitude and their ratio to the energy of the excitations– are common in the related literature [49–51].

Now that a choice for the capacitances and, thus, the energies and all the other parameters of the system have been presented, the scattering amplitudes can be evaluated numerically and their behavior as a function of the momentum of the photons can be analyzed. Besides these amplitudes, the probabilities are also obtained in the next sections.

4.3.1 Without decoherence

For the sake of simplicity, I will first consider an ideal case where decoherence is not present in the system. The following figures contain the probability amplitude squared (to make it real) without being convoluted with the Lorentzian pulse shape, but I do have considered that the momentum of the incoming photon is equal to the momentum of the outgoing photon[‡].

Reflection

When a photon is sent through the transmission line 1, it can be either transmitted or reflected, as show the Hamiltonian previously derived. Let us focus on the case where the photon is reflected. It can be reflected in two different ways: the photon can reach the end of the transmission line and come back or it can be absorbed by the device and be emitted into the transmission line again. In order to study the two different cases, the incoming transmission line can be split (or unfolded) is such a way that it is extended from $-\infty$ to ∞, as in FIG. 4.1.

[‡]This comes from the momentum conservation imposed by the Dirac delta function in the scattering amplitudes.

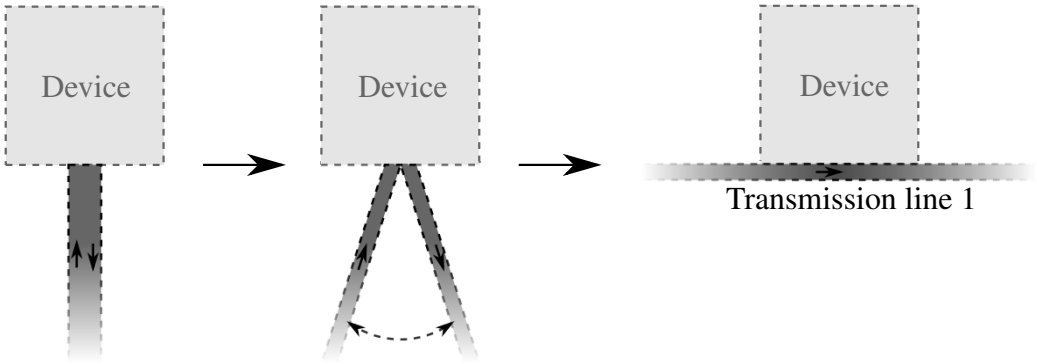

Figure 4.1: *This figure shows how the transmission line have to be transformed. The first picture represents the actual device introduced in the previous chapters and, in the incoming transmission line, the arrows show the path followed by a right-moving photon that is reflected without being absorbed. The transmission lines have to be split (symbolically, not physically) in the way shown by the second and third pictures. This way, a right-moving photon that is reflected without being absorbed always goes to the right whereas a right-moving photon that is reflected after being absorbed, first go to the right, is absorbed and then is emitted back as a left-moving photon (and goes to the left).*

An incoming photon that is reflected without interacting with the device goes, in this new representation, from $-\infty$ to ∞, whereas a photon that is reflected by the device goes from $-\infty$ to 0 (the position of the device), is absorbed and then is emitted back into the transmission line heading to $-\infty$ again. This is realized by considering "left-moving" and "right-moving" modes within the incoming pulse: $b_{1in}(k) = (r_{1in}(k) + l_{1in}(-k))/\sqrt{2}$ [48], where r_{1in} stands for incoming, right-moving mode in the first transmission line (not to be confused with the relaxation operators) and l_{1in} stands for left-moving. The amplitude for a photon that is absorbed and emitted back in the same transmission line is

$$\begin{aligned} S_{1I}(p,k) = &- \frac{\delta(p-k)\left(\frac{1}{\tau_{T1}} + \frac{1}{\tau_{T3}}\alpha_1(p)\right)}{T_1(p) + \frac{1}{\tau_{T1}} + \frac{\alpha_1(p)}{\tau_{T3}} + \left(\frac{1}{\tau_{2a,1}} + \frac{\alpha_2(p)}{\tau_{2b,1}}\right)\frac{T_1(p)}{T_2(p)} + \left(\frac{1}{\tau_{3a,1}} + \frac{\alpha_3(p)}{\tau_{3b,1}}\right)\frac{T_1(p)}{T_3(p)}} \\ &- \frac{\delta(p-k)\left(\frac{1}{\tau_{2a,1}} + \frac{1}{\tau_{2b,1}}\alpha_2(p)\right)}{T_2(p) + \frac{1}{\tau_{2a,1}} + \frac{\alpha_2(p)}{\tau_{2b,1}} + \left(\frac{1}{\tau_{T1}} + \frac{\alpha_1(p)}{\tau_{T3}}\right)\frac{T_2(p)}{T_1(p)} + \left(\frac{1}{\tau_{3a,1}} + \frac{\alpha_3(p)}{\tau_{3b,1}}\right)\frac{T_2(p)}{T_3(p)}} \\ &- \frac{\delta(p-k)\left(\frac{1}{\tau_{3a,1}} + \frac{1}{\tau_{3b,1}}\alpha_3(p)\right)}{T_3(p) + \frac{1}{\tau_{3a,1}} + \frac{\alpha_3(p)}{\tau_{3b,1}} + \left(\frac{1}{\tau_{T1}} + \frac{\alpha_1(p)}{\tau_{T3}}\right)\frac{T_3(p)}{T_1(p)} + \left(\frac{1}{\tau_{2a,1}} + \frac{\alpha_2(p)}{\tau_{2b,1}}\right)\frac{T_3(p)}{T_2(p)}}, \end{aligned} \tag{4.45}$$

whereas the amplitude for a photon being reflected without interaction is

$$S_{1N}(p,k) = \delta(p-k) + S_{1I}(p,k) \tag{4.46}$$

with the α's and T's the same as before. The difference between these expressions and the full scattering amplitude with only even modes (b_{1in}) is that, in these two expressions, the factors of two in the numerators have disappeared.

The total amplitude for a photon being transmitted, independently of how this happens, is $S_1 = S_{1N} + S_{1I}$. The curves in FIG. 4.2 and FIG. 4.3 show the momentum dependence of S_1 and also S_{1I}. In the first figure, the red curve shows the amplitude for a photon with energy around ω_{T1} and ω_{T3} being reflected (in any way). The green curve shows the probability that the photon is absorbed and reflected. The data in red is completely flat whereas the data in green is zero everywhere except for two peaks that go up to 1. This means that if a photon with energies around ω_{T1} and ω_{T3} but not exactly ω_{T1} or ω_{T3} is sent to the switch it will just be reflected without interacting with the device. If the photon has energy ω_{T1} or ω_{T3}, it will always be absorbed by the transmon. Moreover, this also shows that if the photon is absorbed by the transmon, it is always reflected.

Consider an incoming pulse shaped as a Lorentzian curve (in momentum space) with width $1/\tau_1$ and momentum ω_1. If τ_1 is much larger than τ_{T1} –it can be up to three or four orders of magnitude larger, with the numbers I have introduced[§] – then the integral of the product of the Lorentzian times the curve S_{1I} –that is, the probability that a photon is absorbed and reflected– goes to one.

Take a look at Eq. (4.45). Near $p \to \omega_{T1}$ the amplitude goes to one, but near $p \to \omega_{T3}$ it only goes to one if $\tau_{T3} = 6\tau_{T1}$. Something similar happens with all the other lifetimes. This is the reason why the constraints (b), (c) and (d) had to be imposed

In FIG. 4.3 the behavior is quite different. The red curve tells us that the photon will be reflected as long as its energy does not coincide with the excited state of the SQUIDs (ω_{2a}, ω_{2b}, ω_{3a} or ω_{3b}). If it coincides with one of these energies, the incoming photon will not be reflected. That means that it will be absorbed by the SQUIDs and transmitted forward into one of the outgoing transmission lines.

Regarding the green curve, its explanation is more complex. In FIG. 4.3, 4.4 and 4.5 the red curve shows that a photon with enough energy to excite any of

[§] A single photon pulse of these characteristics can be obtained by the emission of a photon by a single-mode cavity with resonant frequency ω_t and spontaneous emission lifetime comparable to τ_t [53]. Artificial atoms with this lifetime have been recently demonstrated [49, 50].

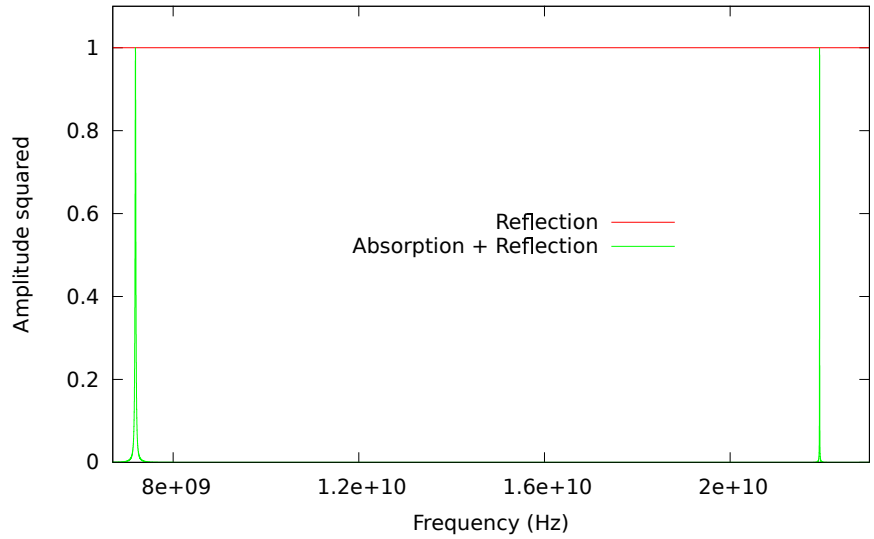

Figure 4.2: *These curves describe the probability amplitude squared for the reflection of a photon by the proposed device in the high energy range (around ω_{T1} and ω_{T3}). The red line gives the probability of reflection of an incoming photon as a function of the momentum, and the green curve gives the probability that a photon is absorbed by the transmon and reflected back.*

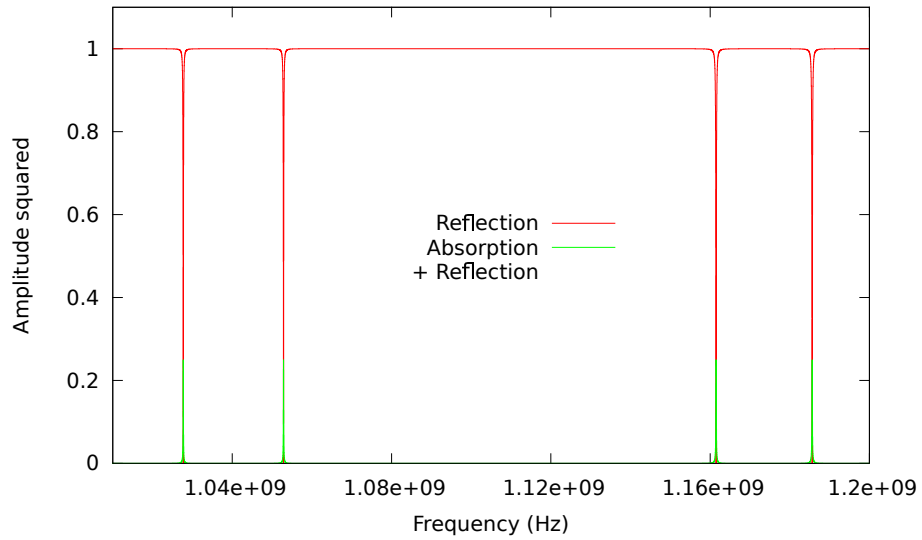

Figure 4.3: *This figure describes the reflection of a photon by the quantum switch in the low energy range (around ω_{2a}, ω_{2b}, ω_{3a} and ω_{3b}). The red line gives the probability of reflection of an incoming photon as a function of the momentum, and the green curve gives the probability that a photon is absorbed by the SQUIDs and reflected back (only right-moving or left-moving modes).*

the SQUIDs is never reflected. The same figures also tell us (green curves) that if the transmission line is split in a way such that right- and left-moving photons can be considered, if a left-moving photon –or a right-moving photon– is sent to the device there is a non-vanishing probability that the photon is reflected. This seems to contradict the previous statement, but it does not. In the first case an even photon, defined by $b^\dagger_{in} = (r^\dagger_{in} + l^\dagger_{in})/\sqrt{2}$ is absorbed, and the amplitude probability squared of obtaining a reflected even photon is computed. In the second case, a right-moving photon $r^\dagger_{in}$ is absorbed and the amplitude probability squared of obtaining a reflected right-moving photon is computed. This amplitude, before squaring, is 0.5. The amplitude for a left-moving photon being obtained after sending a right moving photon gives -0.5. The total amplitude of reflection is the sum of the two processes, which gives identically zero, but the figure only shows the square of one of the processes.

Hence, we can conclude that if an incoming photon has enough energy to excite a SQUID, it is always transmitted as long as it is described by an even mode, otherwise there is a probability of being reflected. In the case of an odd mode $b^\dagger_{in} = (r^\dagger_{in} - l^\dagger_{in})/\sqrt{2}$ [48], the photon is always reflected.

The curves in FIG. 4.4 and FIG. 4.5 show the same as those in FIG. 4.3 but with a closer look at the energies ω_{2a} and ω_{3a} in the first of the figures, and around ω_{2b} and ω_{3b} in the second. In all these figures, and also the ones that follow, it is very important to notice that there is no overlap between the peaks in the amplitudes, except in the case when a perfect overlap is needed (last figures). This means that the separation between the energy levels is just right and that a photon that is meant to excite one definite energy level will not excite any other than that.

Transmission

FIG. 4.6 and FIG. 4.7 show the probability amplitude of a photon being transmitted to the second (and third) transmission line in three different cases. In the first case (red line) the photon is transmitted only if its energy is ω_{2a} or ω_{2b} (ω_{3a} or ω_{3b}). In the second case (green line), the first level of the transmon is excited and, because of this, the photon can only be transmitted if its energy is $\omega_{2a} - J_{12a}$ or $\omega_{2b} - J_{12b}$ ($\omega_{3a} - J_{13a}$ or $\omega_{3b} - J_{13b}$, for the other figure). In the third case (blue line), the third level of the transmon is excited and, because of this, the photon can only be transmitted if its energy is $\omega_{2a} - J_{32a}$ or $\omega_{2b} - J_{32b}$ ($\omega_{3a} - J_{33a}$ or $\omega_{3b} - J_{33b}$).

The most interesting curves are those in FIG. 4.8 and FIG. 4.9. When a photon

Version of June 29, 2015– Created June 29, 2015 - 21:15

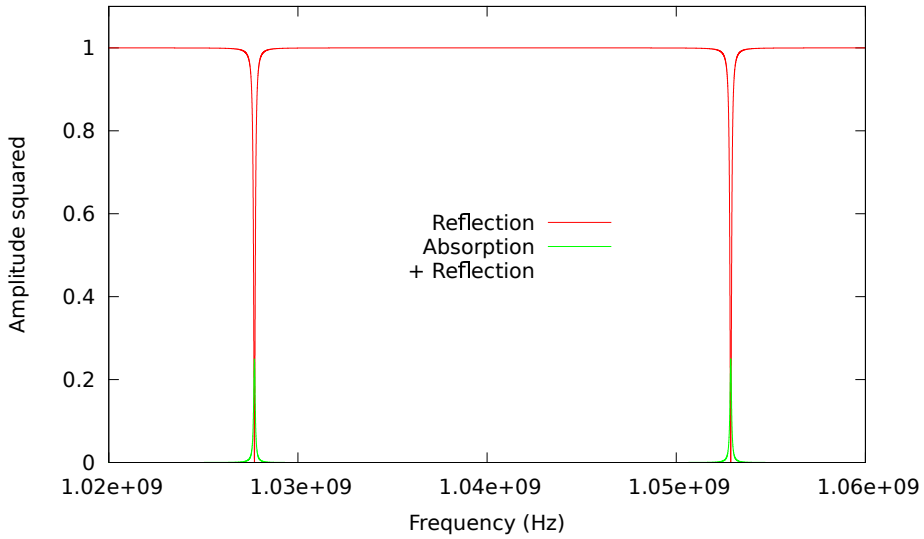

Figure 4.4: *Reflection of a photon by the quantum switch in the low energy range. In this case the probability amplitude ranges within energies around which the SQUIDs labeled with an a are excited (ω_{2a} and ω_{3a}).*

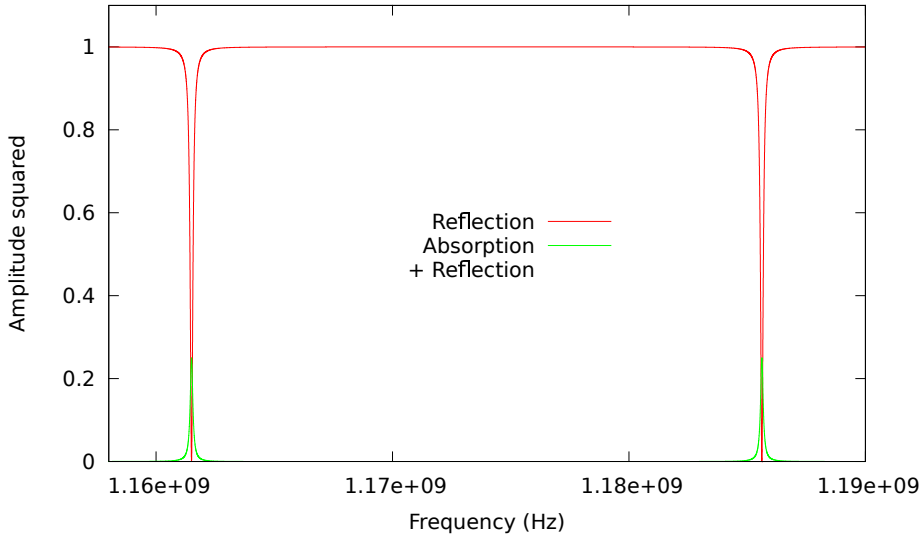

Figure 4.5: *Reflection of a photon by the quantum switch in the low energy range. In this case the probability amplitude ranges within energies around which the SQUIDs labeled with a b are excited (ω_{2b} and ω_{3b}).*

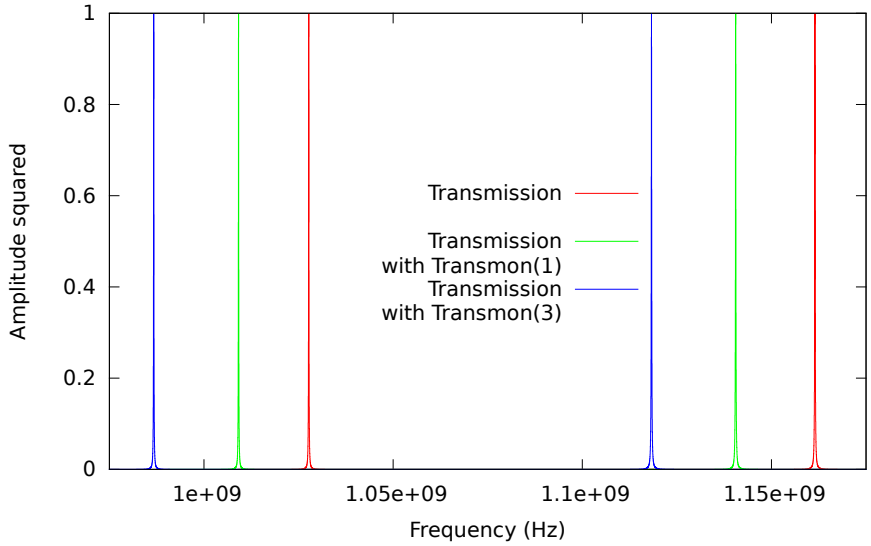

Figure 4.6: *The probability amplitude for the transmission of a photon to the second transmission line is plotted in this figure. The red curve gives the probability of transmission of an incoming photon as a function of the momentum, the green curve gives the probability of transmission when the first transmon level is excited and the blue curve gives the probability of transmission when the third level of the transmon is excited.*

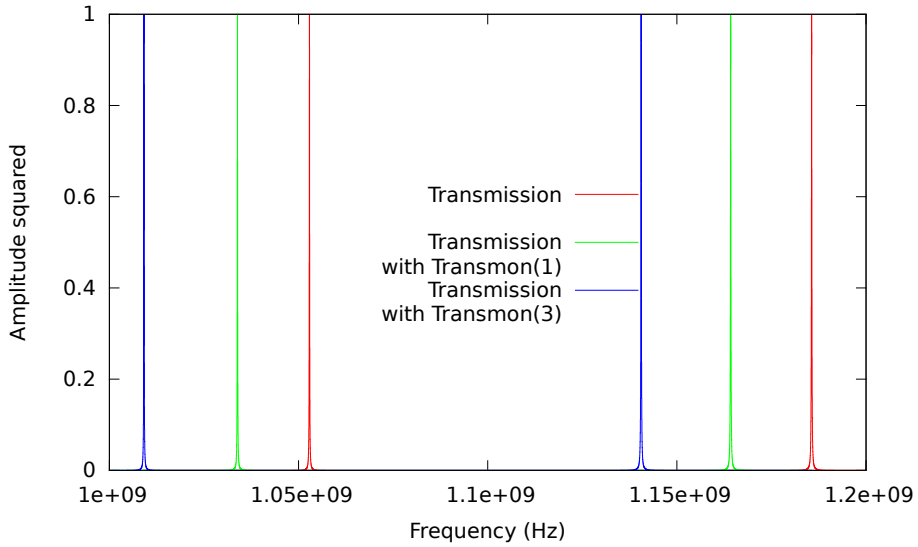

Figure 4.7: *The probability amplitude for the transmission of a photon to the third transmission line is plotted in this figure. The red curve gives the probability of transmission of an incoming photon as a function of the momentum, the green curve gives the probability of transmission when the first transmon level is excited and the blue curve gives the probability of transmission when the third level of the transmon is excited.*

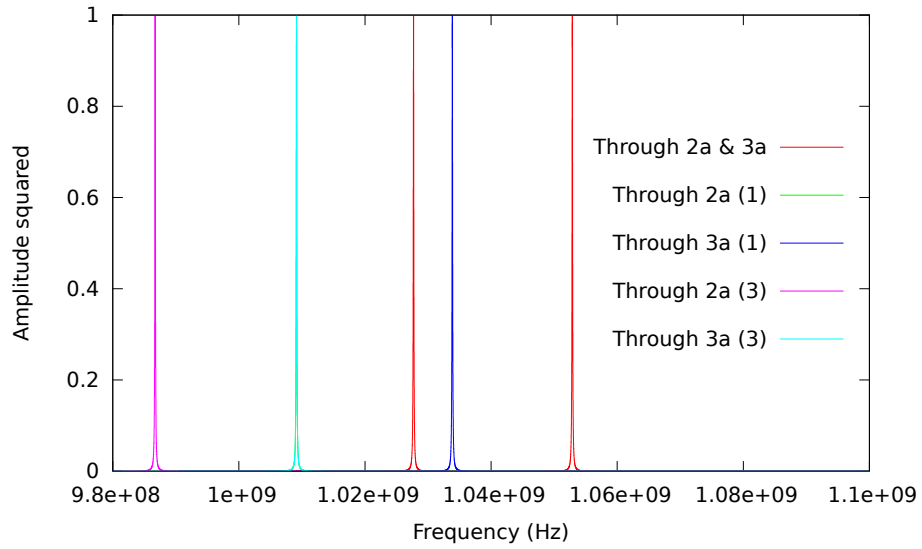

Figure 4.8: *The probability amplitude for the transmission of a photon to the second and third transmission lines through the SQUIDs labeled by a is shown in this figure. The red curve gives the probability of transmission of an incoming photon as a function of the momentum, the green curve gives the probability of transmission through $2a$ when the first transmon level is excited, the dark blue curve gives the probability of transmission through $3a$ when the first level of the transmon is excited, the magenta curve gives the probability of transmission through $2a$ when the third level of the transmon is excited and the cyan curve gives the probability of transmission through $3a$ when the third level of the transmon is excited. The green curve cannot be seen because it is behind the cyan curve (full overlap).*

is sent in, it can be sent with only four different frequencies: if it has frequencies ω_{T1} or ω_{T3} the photon will excite the first or third energy levels of the transmon; if we want them to be transmitted the photon has to be sent with enough energy to excite either the SQUIDs labeled with a or the SQUIDs labeled with b. The device is designed in such a way that the energy needed to send a photon through $2a$ when the first level of the transmon is excited is exactly the same as the energy needed to send a photon through $3a$ when the third level is excited. This way it is the transmon –or the first photon, which is absorbed by the transmon– who decides to which transmission line the following photons are transmitted.

Let me consider first FIG. 4.8. In this figure there is a red curve that shows the probability amplitude for a photon being transmitted through a to the second or third transmission line. There is also a green line that shows the probability for a photon being transmitted through a to the second transmission line when the first level of the transmon is excited. The blue line gives the probability that a photon

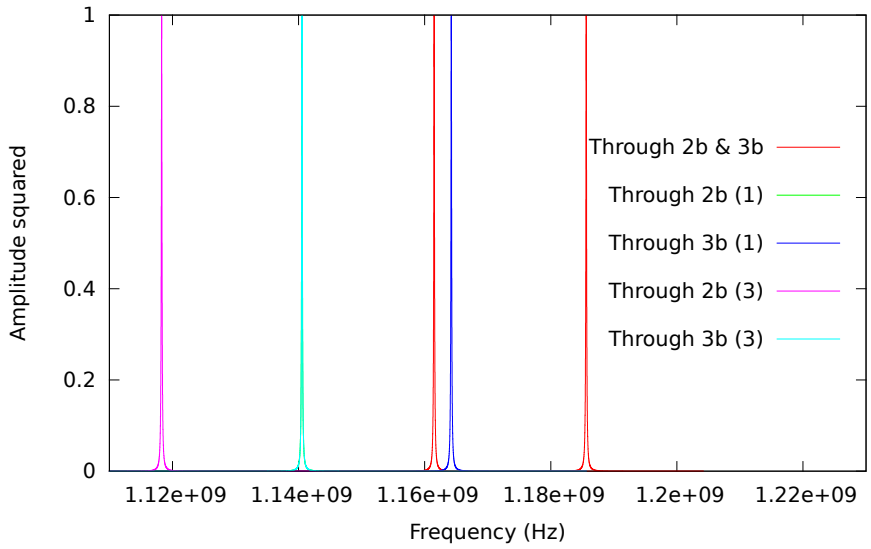

Figure 4.9: *Transmission of a photon to the second and third transmission lines through the SQUIDs labeled by b. The lines represent the same as in the previous figure. The green curve cannot be seen because it is behind the cyan curve.*

is transmitted through a to the third transmission line while the first level of the transmon is excited. There is also a magenta line that gives the probability for a photon being transmitted through a to the second transmission line while the third level of the transmon is excited. Finally, the cyan curve shows the probability that a photon is transmitted through a to the third transmission line when the third energy level of the transmon is excited. The cyan and the green curve are perfectly overlapping.

Imagine that an incoming photon (the second) is absorbed, and that this photon is supposed to excite the first level of the transmon on the next node of the network. This means that it has to be transmitted through either the low energy SQUID that leads to the second transmission line or the low energy SQUID that leads to the third transmission line. This is, the SQUIDs labeled with a, so this photon is sent with some energy ω_a. In this plot we expect to see two red, separated peaks that must not be excited. These have energy ω_{2a} and ω_{3a}. We also expect to see a blue and a magenta peak, separated as well. They have energy $\omega_{3a} - J_{13a}$ and $\omega_{2a} - J_{32a}$, respectively. These are not supposed to be excited either. Finally, we expect to see two overlapping peaks (green and cyan) with energy $\omega_a = \omega_{2a} - J_{12a} = \omega_{3a} - J_{33a}$ corresponding to the energy of the SQUID $2a$ when the first transmon level is excited (green) and to the energy of the SQUID $3a$ when the third transmon level is excited (cyan). Summarizing, when an incoming

photon (the second) goes to the switch with energy ω_a it is transmitted through $2a$ if the first energy level of the transmon is excited or through $3a$ if the second level of the transmon is excited. The last figure displays the same behavior but with the other two SQUIDs.

As I said before, the probability is found by calculating the convolution of these curves together with a Lorentzian curve centered at ω_t and with width $1/\tau_t$. For the variable τ_t I have taken $\tau_t = 10^{-4}\ s$, which is a realizable value [49, 50, 53]. With this value, which is much larger that the lifetimes of the excitations, the shape of the incoming pulse is a curve much narrower than those in the FIG. 4.2 to 4.9, so the convolution will give a probability as large (or small) as the value the scattering amplitude (squared) takes for the frequency ω_t of the incoming photon. In the next section, where dephasing is considered, the probabilities are computed to give the exact value they take (not just one or zero, as in this section) for each possible process.

4.3.2 With decoherence

The decoherence processes are present in the expressions for the scattering amplitudes with the parameters γ_r, γ_d (relaxation and dephasing). I have assumed that both take the same value $\gamma = 10^4\ s^{-1}$, for the transmon excitations and $\gamma = 10^3\ s^{-1}$, for the SQUID excitations. These are realizable values in systems with similar energy scales [51, 54]. Moreover, I have considered $\tau_{T3} = 3\tau_{T1}$ to account for all the possible relaxation processes that may experience the third excited level of the transmon (see Section 3.4).

The scattering amplitudes computed before [in Eq. (4.5) and (4.28)] become, in the presence of dephasing and relaxation processes and near $\omega_{T1} - p \to 0$ and $\omega_{2a} - p \to 0$,

$$S_1 \sim -\frac{1 - \frac{3}{4}\gamma\tau_{T1}}{1 + \frac{3}{4}\gamma\tau_{T1}} \tag{4.47}$$

$$S_{12} \sim \frac{1}{1 + \frac{3}{8}\gamma\tau_{2a,1}}. \tag{4.48}$$

If we consider a transmission line split like in Fig. 4.1, then Eq. (4.46) and (4.45)

become (near $\omega_{T1} - p \to 0$, as well):

$$S_{1N} \sim \frac{\frac{3}{4}\gamma\tau_{T1}}{1+\frac{3}{4}\gamma\tau_{T1}} \tag{4.49}$$

$$S_{1I} \sim -\frac{1}{1+\frac{3}{4}\gamma\tau_{T1}}. \tag{4.50}$$

The full scattering amplitude for all these processes will not be derived again. These are just the same as in the previous section (see FIG. 4.2 to 4.9) but with smaller peaks (and slightly wider). Instead, in this section, the probability of reflection and transmission of photons through the quantum switch in a few different cases is computed. These probabilities now include the possible decoherence processes.

Single-photon processes

The probability $p_{1,T1}$ for an incoming photon with frequency $\omega_t = \omega_{T1}$ being reflected by the quantum switch is expected to go to one. The same behavior is expected for a photon with frequency $\omega_t = \omega_{T3}$, both in the case the photons are even modes or just right- or left-moving particles. However, with the introduction of the dephasing processes, these probabilities are slightly different. The probabilities $p_{1,T1}$ and $p_{1,T3}$ are, for even modes,

$$p_{1,T1} = 0.997 \tag{4.51}$$

$$p_{1,T3} = 0.947. \tag{4.52}$$

This is the total probability: it accounts for the process where the photon is absorbed and reflected and also for the process where the photon is just reflected without being absorbed. If the incoming photon is a right- or a left-moving mode, these probabilities are slightly larger:

$$p_{1,T1} = 0.998 \tag{4.53}$$

$$p_{1,T3} = 0.973. \tag{4.54}$$

Thus, even modes are more likely to experience a decoherence process. Nevertheless, these are quite large values, if we take into account that the dephasing ratios have been taken larger than usual.

If the incoming photon has enough energy to excite a SQUID (without the presence of a transmon excitation), that is $\omega_t = \omega_{2a}$, the probabilities that it is

reflected by the device ($p_{1,2a,e}$) as an even mode or absorbed and reflected ($p_{1,2a,l}$) as a left-moving or right-moving mode are

$$p_{1,2a,e} = 1.92 \cdot 10^{-2} \tag{4.55}$$
$$p_{1,2a,l} = 0.238. \tag{4.56}$$

Photons with enough energy to excite the SQUIDs should not be reflected, so it is advisable to work with only even modes, although this makes the probability of reflection of the photons with larger energy (ω_{T1} or ω_{T3}) smaller.

In our scheme, the incoming photons can have energy ω_{T1} or ω_{T3} if they are the first to arrive at the switch, and energies $\omega_a = \omega_{2a} - J_{12a} = \omega_{3a} - J_{33a}$ or $\omega_b = \omega_{2b} - J_{12b} = \omega_{3b} - J_{33b}$ for the rest of the photons. Therefore, we have to make sure that a photon with energies ω_a or ω_b are not transmitted if the transmon is not excited. The probabilities of transmission of a photon with energy ω_a being emitted into the second transmission line ($p_{2,a}$) or into the third transmission line ($p_{3,a}$) are

$$p_{2,a} = 9.80 \cdot 10^{-6} \tag{4.57}$$
$$p_{3,a} = 2.31 \cdot 10^{-6}. \tag{4.58}$$

These are virtually zero.

Two-photon processes

More interesting is the case where the transmon is excited, either its first level or the third. In the case the first level of the transmon is excited, the next incoming photon must be transmitted only into the second outgoing transmission line, independently of whether its energy is ω_a or ω_b. The probabilities for the transmission of a photon in any possible case where the first transmon level is excited are

$$p_{2,a}(T1) = 0.952 \tag{4.59}$$
$$p_{2,b}(T1) = 0.964 \tag{4.60}$$
$$p_{3,a}(T1) = 1.63 \cdot 10^{-6} \tag{4.61}$$
$$p_{3,b}(T1) = 1.47 \cdot 10^{-6}, \tag{4.62}$$

where the first of them is the probability that an incoming photon with energy ω_a is transmitted to the second transmission line, $p_{2,b}(T1)$ is the probability that an incoming photon with energy ω_b is also transmitted to the second transmission line and $p_{3,a}(T1)$ and $p_{3,b}(T1)$ are the probabilities that an incoming photon with

energy ω_a or ω_b are transmitted to the third transmission line while the first, and not the third, transmon level is excited. In the absence of decoherence, the first two probabilities [Eq. (4.59) and (4.60)] are expected to go to 1 because the incoming photon has the right energy to excite the SQUID labeled with $2a$ and $2b$, respectively, and thus, be transmitted to the second transmission line. The other two probabilities [Eq. (4.61) and (4.62)], on the other hand, are expected to go to zero because in that case, the incoming photons do not have enough energy to excite the SQUIDs that are coupled to the third transmission line.

If the third level of the transmon is excited, the behavior should be the opposite. The probabilities found in this situation are

$$p_{2,a}(T3) = 7.12 \cdot 10^{-7} \tag{4.63}$$
$$p_{2,b}(T3) = 2.94 \cdot 10^{-7} \tag{4.64}$$
$$p_{3,a}(T3) = 0.952 \tag{4.65}$$
$$p_{3,b}(T3) = 0.964. \tag{4.66}$$

Chapter 5

Implementation of the Quantum Switch into a QRAM

5.1 Not all the requirements can be fulfilled

In the previous chapters I have introduced and analyzed a superconducting device capable of routing photons through different paths. The purpose of this quantum switch is to route an n-photon register from a root node to the memory cells in a quantum random access memory. In order to perform this function, the device must satisfy some requirements already discussed previously. These include:

1. A multilevel device coupled to three transmission lines. The proposed device must be coupled to an incoming transmission line, where the photons (address register in a QRAM) come from, and also to two outgoing transmission lines, thus creating the bifurcating path needed to build up a QRAM. This device must work independently, in the sense that an external interaction to control it (opening/closing the switch) is not needed. This device is the one proposed in FIG. 2.6, and is operated solely with the incoming photons it absorbs and emits. Moreover, this must have different energy levels (see the different energy spectra in the plots in Section 4.3.1) that interact differently with the photons and the transmission lines, as shown in FIG. 3.1.

2. Excitation of higher levels. In order to achieve the desired transmon-SQUID interactions that modify the energy spectrum of the device when two photons are absorbed, the higher levels of the transmon must be accessible by the absorption of a single photon. This is realized by introducing a nonlinear capacitor in the transmon (Sections 2.2 and 2.3).

3. Perfect absorption. The incoming photons have energy ω_{T1} or ω_{T3} to match the two accessible energy levels of the transmon (in case it is the first photon to be absorbed by the switch) or energy ω_a or ω_b if the photons are to be transmitted after the transmon has been excited. An incoming photon with the right energy is always absorbed by the device. This behavior is shown in Section 4.3.1 and it is due to an adequate energy spectrum of the device and the right value of the lifetimes of both the transmon and SQUIDs.

4. Reflection/transmission when necessary. After the incoming photon is absorbed it must be emitted back into one of the transmission lines, or the other, depending on the energy of the photons and the state of the excited transmon. The plots in Section 4.3.1 also show this behavior, which is described by the Hamiltonian in Eq. (3.47).

5. The transmon decides. After the first photon is absorbed (always by the transmon), the following photons are also absorbed by the device but they are only emitted into one of the outgoing transmission lines. It is the transmon which, according to the level that is excited, modifies the energy spectrum of the SQUIDs and forces the photons to be absorbed by only the SQUIDs that lead to one of the transmission lines, as is described in FIG. 3.1. This transmon-SQUID interaction is contained in the Hamiltonian in Eq. (3.43).

6. Scalability. In order to make the system scalable, which is necessary if we want to construct a QRAM based on a network of these quantum switches, there can only be two different energies: ω_a and ω_b. In a QRAM, when the second photon is transmitted it becomes the first of the new address register and, thus, will be absorbed by the transmon at the next quantum switch it will encounter in its way to the memory cells. It is necessary, therefore, that the second photon (and also all the rest) have the same possible energies as the first (ω_{T1} or ω_{T3}), but with the proposed device, the flux φ_1 (see FIG. 2.6) is influenced by the transmon and all the SQUIDs, whereas the other four fluxes are only influenced by the elements in their nearest SQUIDs. This is what makes the energy of the transmon (atom-like element described by the flux φ_1) larger than the energy of the SQUIDs for any choice of the capacitances and Josephson energies.

A possible solution to this problem may be to add another device between the nodes that enlarges the energy of only the first photon (without measuring it, otherwise the wave function will collapse) and leaves the others with the same energy. Simulated Raman Adiabatic Passage (STIRAP) processes may be a candidate for a device capable to transfer the population of a quantum state (with lower

Version of June 29, 2015– Created June 29, 2015 - 21:15

energy) into another (with higher energy). These processes have been studied in circuit-QED systems in [55, 56].

7. Lifetime relations. Since the transmon has to remain excited while all the photons go through the device, its lifetime must be larger than the lifetimes of the SQUIDs, but for the same reason described in the previous paragraph, the behavior is totally the opposite [see Eq. (3.24) to (3.33) and also Eq. (3.48) and (3.50)]. Thus, for a correct performance of the quantum switch, a way to extend the lifetime of the transmon must be found. One possibility may consist of making use of the Purcell effect, which can be used to extend the lifetime of the transmon [52] and also to reduce the lifetime of the SQUIDs [57]. Moreover, if the system is scalable then $\tau_{2a,1} \neq \tau_{2a,2}$. These two lifetimes must be equal or similar for a good performance of the device, as discussed in Chapter 4 (Section 4.3).

8. Absence of undesired interactions. The Lagrangian derived for the device in FIG. 2.6 led to a Hamiltonian with many interactions that should be canceled in order to obtain a quantum switch that routes the address registers without losing information by means of undesired processes such as e.g., a transmon excitation that decays into a SQUID excitation plus a photon. All these processes have been successfully canceled (or minimized) in Section 2.5 by introducing some extra inductors, by tuning the Josephson energies and by imposing some constraints to the capacitances (see also Section 3.1).

9. Low decoherence. Finally, any quantum device suffers from decoherence and this is not an exception. Nevertheless, with the values for the decoherence parameters used in Section 4.3.2, the quantum switch I propose can perform the work it is designed for with a small probability of failure.

Almost all of these requirements have been successfully satisfied, and those that cannot be realized may be amended by introducing extra elements into the system. Let us assume that these elements exist and can be easily implemented. Now that we know which are the basic elements needed to fabricate a QRAM, it is time to ask ourselves how can a register of photons arrive at the memory cells and come back with the information they contain.

5.2 How to get to the memory cells

In this section I consider two cases: (1) the lifetime of the transmon is very large ($\tau_{T1} >> \tau_{2a,1}$), and (2) it is smaller than that of the SQUIDs but large enough to

make the quantum switch work ($\tau_{T1} \lesssim \tau_{2a,1}$).

Consider, for simplicity, a QRAM formed by a root node, a quantum switch and a memory array with only two memory cells (c_1 and c_2), each containing a classical bit (either 1 or 0). For this device, the address register consists of two photons: the first of the photons is the one that excites the transmon, and the second (the bus photon) is the photon that interacts with the memory cell to extract its content. Each of the photons can be either in the state $|a\rangle$ or $|b\rangle$, with energies ω_a or ω_b, respectively*, but I will consider that the bus photon is always in the lowest energy state.

If we want to extract, from the QRAM, a wave function containing a superposition of the content of the cells c_1 and c_2, a superposition of address registers have to be sent to the QRAM. This will consist of a photon in the state $|a\rangle$ together with a bus photon –in the state $|a\rangle$ as well– in a quantum superposition with a photon in the state $|b\rangle$ together with another bus photon. The wave function of this address register is

$$|\psi\rangle = \frac{1}{\sqrt{2}}\left(|a\rangle|a\rangle + |b\rangle|a\rangle\right). \tag{5.1}$$

When the register arrives at the switch, the first photon is absorbed and the second is transmitted, as described in the previous chapters, but the wave function is not modified. Since the address register is in a superposition of states, the second photon will be in a superposition of states, also, between the transmission lines leading to c_1 and c_2. When the second photon arrives at the memory cells, they encounter an operator

$$U(x) = (1-x)\mathbb{1}\otimes\mathbb{1} + x\,\mathbb{1}\otimes\left(|a\rangle\langle b| + |b\rangle\langle a|\right), \tag{5.2}$$

where x is the content of the memory cell and can be either 0 or 1. The first identity acts on the space of the first photon and the second acts on the space of the second photon. Thus, if the content of the cell is 0, the state of the photon does not change and if the state is 1, it does. In a QRAM with $c_1 = 1$ and $c_1 = 0$, after reaching the memory cells, the wave function $|\psi\rangle$ becomes

$$|\psi'\rangle = \frac{1}{\sqrt{2}}\left(|a\rangle|b\rangle + |b\rangle|a\rangle\right). \tag{5.3}$$

If the QRAM contains n levels of nodes ($2^n - 1$ quantum switches, the root node is the first level), then $n+1$ photons are needed and the wave function $|\psi\rangle$ can

*Imagine that either the transmon and the SQUIDs have the same energies or that there is an element before the switch that enlarges the energy of the first incoming photon.

Version of June 29, 2015– Created June 29, 2015 - 21:15

contain the superposition of up to 2^n address registers.

Let us consider now the case (2) where $\tau_{T1} < \tau_{2a,1}$, but considering that these lifetimes are such that when the transmon is excited, the second photon has enough time to be absorbed before it decays. In this case, after the two photons have been absorbed, the transmon excitation decays emitting a photon with energy $\omega'_{T1} < \omega_{T1}$ (or $\omega'_{T3} < \omega_{T3}$), whereas the SQUID will emit a higher energy photon. This energy difference may not be a problem if there is a device before each node that rescales the energies of the incoming photons. The problem is that, in this case, no more than one photon can be transmitted. This can be amended by sending more photons: if we want to send two photons through one of the switches we will need to send one photon (this will excite the transmon and decay while the second photon is absorbed), then a second photon will be absorbed and transmitted; after this another photon equal to the first –it has to excite the transmon in exactly the same way as the first– will be absorbed, and finally a fourth photon will be absorbed and transmitted (second transmitted photon). For an n-level QRAM, since only half of the photons are transmitted (the other half are absorbed by the transmon and reflected), 2^n photons will be needed. For large QRAMs this is not optimal because it may not be possible to keep 2^n photons coherently coupled.

In any case, since the reflected photons are all identical, the wave function of the photon that has arrived at the memory cells is the same as before.

5.3 Retrieval of information

Now a photon (or a superposition) has reached the memory cells, but this is not enough. This photon has to come back. It cannot be reflected to the same path it came because the transmon have already decayed and emitted a photon (the switches are closed), so the bus photon must go through another path. Once the photon has interacted with the memory cell, it can be routed via superconducting hybrid ring couplers [27][†]. A schematic representation of this QRAM is shown in FIG. 5.1. The output will be a single photon whose state is a superposition of the content of the memory cells that have been evaluated, weighted by the amplitudes given by the states of the other incoming photons (that excited the transmon): just the wave function described in Eq. (5.3).

[†]These devices can route a photon through different paths according to their energy. They can be fabricated in a way that route all the photons (with any of the two possible frequencies) to the same path. For more information see [27].

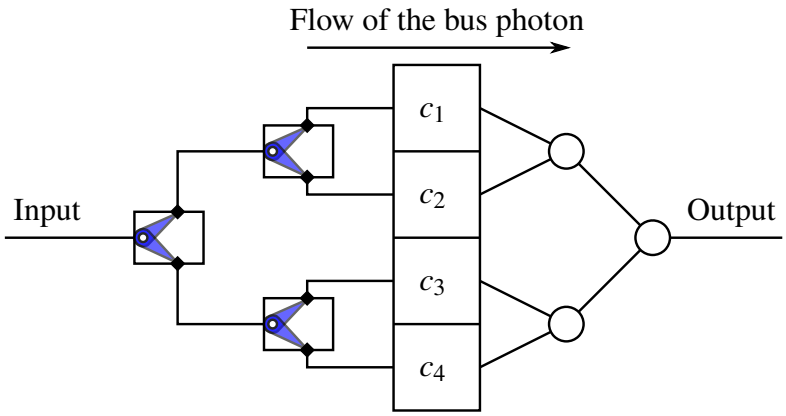

Figure 5.1: *This is a schematic representation of a 4-bit QRAM containing a mechanism to extract the bus photons once they have interacted with the memory cells. This is composed of an input bifurcation path with quantum switches at its nodes, an array of memory cells, each labeled with c_1 to c_4 and another bifurcation path. This last element contains a superconducting hybrid ring coupler at each node, and its function is to route the photons from the memory cells to the rightmost node. While the first (two) photons of the address register are absorbed and reflected, the bus photon goes all the way from the left to the right of the picture.*

This photon can be used to do calculations where a superposition of the input data is needed, but it could also be used to read the information of a single memory cell with complete privacy [16].

In the latter, a question is sent in (address register) and an answer is obtained (bus photon), but in order to read the answer, which can be in a superposition of states, the complete initial register (question) is needed. That is, the photons absorbed and reflected by the transmons are needed. These can be recovered by making use of the same superconducting hybrid ring couplers, but they can also be obtained if, at the beginning of the whole process, two identical instances of each photon are created. One of each pair is sent to the QRAM (and lost) whilst the other is kept to decode the output information. This may not be suitable if the address register is constructed using the output of a quantum computation (e.g., a wave function describing a mixed state) because the wave function that has to generate the address register cannot be copied[‡]. But in case we want to create a "hand made" quantum register, we can as well create two of them.

[‡]The No-cloning theorem does not allow to make copies of arbitrary unknown quantum states [11].

Whether the photons absorbed by the transmon are recovered or are lost, the process of reading the content of a memory cell without anyone knowing which cell has been evaluated consists in the following steps: imagine that Alice wants to evaluate the content of the cell c_j located in a QRAM in Bob's computer, but she does not want Bob to know which cell is evaluated.

- Alice prepares an $(n+1)$-photon register with a superposition of the addresses to m different memory cells and sends it to Bob. The first n photons contain the instructions to arrive to the memory array, and the last photon is the bus photon. The wave function is given by $|\psi_1\rangle = \frac{1}{\sqrt{m}}(|c_1\rangle|a\rangle + \cdots + |c_m\rangle|a\rangle)$, where $|c_i\rangle$ contains the instructions to arrive to the memory cell c_i and $|a\rangle$ is the bus photon (always initialized to $|a\rangle$).

- Bob sends the register into the memory array and obtains an output photon, given by $|\psi_1'\rangle = \frac{1}{\sqrt{m}}(|c_1\rangle|a\rangle + \cdots + |c_m\rangle|b\rangle)$. Now the bus photon contains the information previously stored in the memory cells (either a or b). He sends this photon back to Alice. In case the other photons can be recovered, he sends them to Alice as well.

- Alice constructs a new register $|\psi_2\rangle$ with the photons reflected by the transmon, in case they could be recovered, or the other copies of the same photons, in case the first register is lost. At the end of the register, instead of adding a bus photon, she adds the photon she received from Bob, which contains a superposition of the content of m memory cells. Since the address photons of this register are the same (or identical) to those in $|\psi_1\rangle$, this state is the same as $|\psi_1'\rangle$

- In order to read the content of c_j, she needs a QRAM with the same characteristics as Bob's. Alice sends the new register to her own QRAM, and the last photon arrives at the memory array.

- If Alice wants to read the content of the c_j memory cell in Bob's QRAM, she only has to evaluate the state of the photon in the cell c_j' on her own QRAM. This way she is collapsing the wave function in the c_j direction, leaving only one single ket with the content of the cell she wants to evaluate.

If Bob reads the register Alice sent him, the wave function will collapse and Alice can detect it by measuring other memory cells. Thus, Alice can detect if her privacy has been violated[§]. The full process is depicted in FIG. 5.2.

[§]More details on how to detect Bob's intrusion can be found in [16].

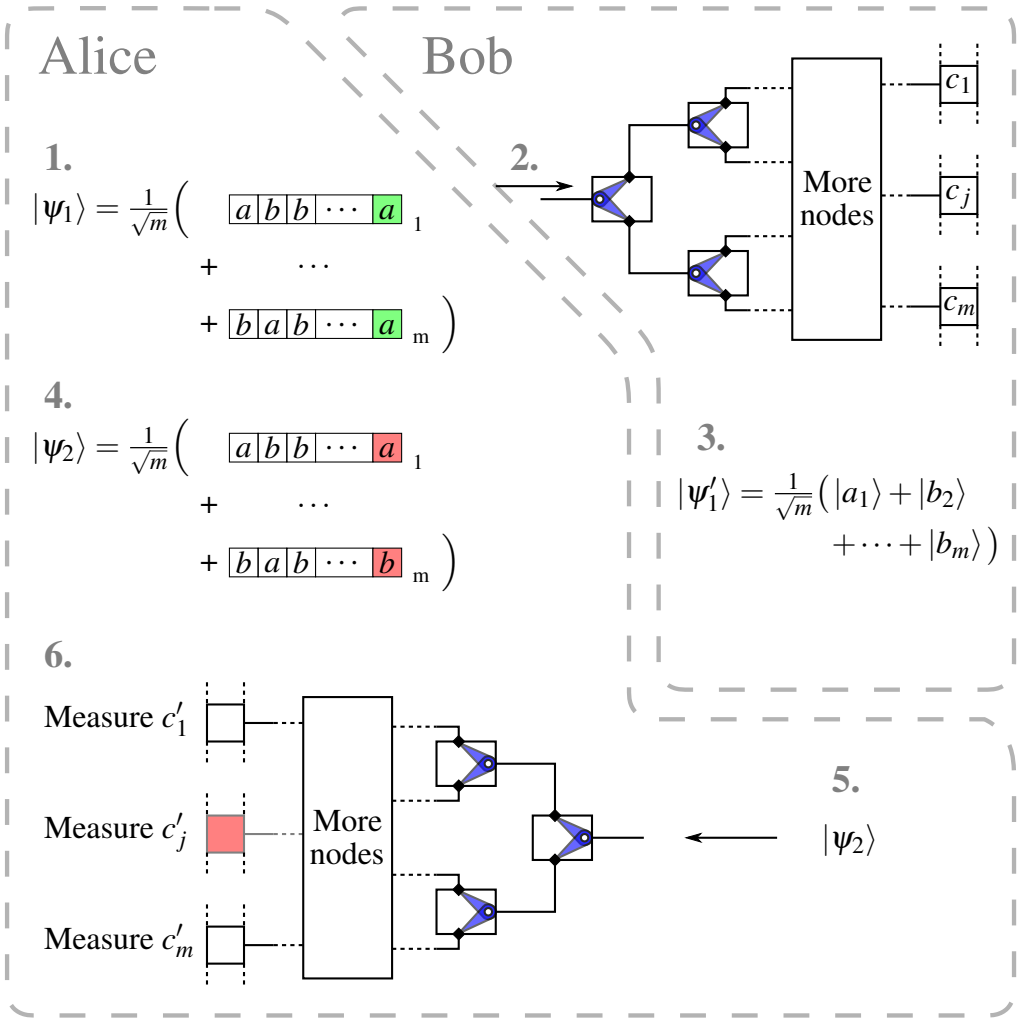

Figure 5.2: *This figure shows a schematic representation of the procedure Alice has to follow to read the content of one of the memory cells in Bob's QRAM. (1) Alice prepares a register of photons containing a superposition of the address of the memory cells that she wants to evaluate. (2) Alice sends the register to Bob and he introduces it into the QRAM. (3) Bob obtains a photon containing a superposition of the content of the memory cells. He sends this register to Alice. (4) Alice uses the register she received from Bob to create a new register. (5) This register is sent to a QRAM identical to that of Bob's but with measuring devices instead of memory cells. (6) By measuring the cell c_j', Alice is collapsing the wave function, revealing the content of Bob's c_j memory cell.*

Chapter 6

The Switch beyond the QRAM

Within a network, the quantum switch proposed and analyzed in the previous chapters has outstanding applications such as a QRAM, needed for the Grover search or the Deutsch-Jozsa algorithms [11] and also for quantum private queries (QPQ) [16], provided that mechanisms are found to enlarge the energy of the photons that have to be absorbed by the transmon and to extend the lifetime of the transmon far beyond the lifetime of the SQUIDs (both discussed in Chapter 5, Section 5.1). The QRAM can e.g., operate within the bucket brigade architecture proposed in [15].

Besides these significant applications, the quantum switch, by itself, has other remarkable uses. Some of them make this device different to any other similar quantum switch or router.

6.1 The switch as a single element

As discussed previously, this element can absorb two photons and transmit one of them (the second) in one outgoing transmission line or the other, according to the state of the first photon. This property has some relevant applications:

1. The switch can be used to create an entangled state out of two photons.

2. It can also be used to amplify an arbitrary one-photon signal describing a quantum state in a two-dimensional Hilbert space.

3. The quantum switch can be used to measure the frequency of a single photon, provided that only two different (and previously known) frequencies are possible.

In the next sections I discuss these three possible applications of the quantum switch.

6.1.1 Creation of entanglement

Quantum entanglement is a key element in quantum teleportation, quantum algorithms and quantum error-correction, thus is of great utility in quantum computation and quantum in formation [11]. Entanglement between two photons can be created using the device proposed in FIG. 2.6. Imagine that a state

$$|\psi\rangle = \frac{1}{\sqrt{2}}\left(|a\rangle|a\rangle + |b\rangle|b\rangle\right) \tag{6.1}$$

has to be created, where a and b label two possible states, one being a low energy state and the other a high energy state. To create this entangled state two photons are needed. The first should be in the superposition

$$|\phi_1\rangle = \frac{1}{\sqrt{2}}\left(|a\rangle + |b\rangle\right), \tag{6.2}$$

while the other can be in the state

$$|\phi_2\rangle = |a\rangle. \tag{6.3}$$

Consider an individual quantum switch with a device in one of the outgoing transmission lines that changes the energy of the transmitted photon (a NOT gate) but nothing in the other outgoing transmission line. After the first photon is absorbed, since it is in a superposition of states, the switch will forward the second photon into a superposition of the second and the third outgoing transmission lines. The output state will be given by

$$|\psi\rangle = \frac{1}{\sqrt{2}}\left(|a\rangle|a\rangle_2 + |b\rangle|a\rangle_3\right), \tag{6.4}$$

where the subscripts describe at which transmission line the second photon can be found. Since there is a NOT gate in one of the transmission lines that acts on, e.g., $|a\rangle_3$, at the very end of the process, the output state will be

$$|\psi\rangle = \frac{1}{\sqrt{2}}\left(|a\rangle|a\rangle + |b\rangle|b\rangle\right). \tag{6.5}$$

Thus a two-photon entangled state will be created.

6.1.2 Amplification of single-photon signals

When two people want to communicate through a noisy channel some mechanism has to be introduced to preserve the information to be transmitted. If a single photon is sent, there is a non-zero probability for the photon to be lost. It is convenient, for this reason, to amplify the signal. That is, to send, not one, but lots of photons carrying the same information. This can be achieved by creating an n-photon entangled state* using the same procedure as in the previous section but sending more than one photon while the transmon is excited.

Even in the case that some of the photons are lost, a group of them may arrive at the final destination and transmit the information contained in the first photon absorbed by the quantum switch (provided that the wave function has not been collapsed due to the noise in the channel). The performance of this process can be quantified by the number of photons that the quantum switch can transmit while the transmon is excited, that is, by the ratio $\tau_{T1}/\tau_{2a,1}$.

These cat states are also important for open-destination teleportation [59], quantum secret sharing [11] and fault-tolerant quantum computing [11], among others.

6.1.3 Measurement of the frequency of a single photon

Single-photon detectors are devices that can detect the presence of a photon and also measure its energy, but most of the current detectors have a finite probability of recording false counts [61].

The device I propose can detect single photons with a high probability of success provided that the photons can have only two previously known frequencies. In this scheme, if a photon with energy ω_{T_1} is sent to an individual quantum switch with detectors in the outgoing transmission lines, the switch will forward other photons (with any frequency) to the second (and not the third) outgoing transmission line, thus only one of the detectors will be triggered. Since many photons can be transmitted, the signal-to-noise ratio can be made small. Besides detecting the presence of a photon (absorbed by the transmon), given that only the detector in the second outgoing transmission line has been triggered, we also know the frequency of that photon.

*These states are called Schrödinger cat states or Greenberger–Horne–Zeilinger (GHZ) states and have been realized in multiple systems [58–60].

For any of these three applications only two SQUIDs are needed, each coupled to a different outgoing transmission line.

Chapter 7

Conclusions

This project was aimed at proposing and analyzing a quantum random access memory based on circuit QED, including possible relaxation and dephasing processes during the operation of the device.

In this thesis I have introduced the quantum switch, a central element in a QRAM. This circuit QED-based device, capable of routing an address register composed of photons in exactly the way required by the bucked brigade architecture [15], has been proposed and analyzed. It is composed of SQUIDs and a transmon (see FIG. 2.6), all of them capacitively coupled, with the peculiarity that the transmon contains a capacitor whose capacitance does not depend linearly on the applied potential. This capacitor –which is relatively easy to fabricate [42]– gives rise to a new set of interactions that I believe have never been studied before in cQED: with this capacitor, a single photon can be absorbed by the third energy level of a transmon that was, previously, in the ground state (see Chapters 2 and 3).

The excitation of the third level of the transmon by a single photon was just one of the challenges I had to face. Others were the difference between the energy levels of the SQUIDs and the transmon, the relation between τ_{T1} and $\tau_{2a,1}$ and the difficulties in analyzing, analytically, two-photon processes. These last obstacles have been partially solved (this is discussed in Chapter 4), but a more detailed analysis is needed and more imaginative solutions have to be found.

Beside these drawbacks, a quantum switch that fulfills (at least partially) all the requirements to be part of a QRAM has been studied, including relaxation and dephasing processes. This device has proved (in Chapter 4) to operate as expected, giving probabilities of success above 94% in all the possible processes.

Applications for this quantum switch have been discussed both in case the switch is connected to other similar devices to form a QRAM (in Chapter 5) and in case a single instance of this device is considered (in Chapter 6).

This work must not be regarded as a full study of a quantum switch, yielding an optimized device capable of routing photons. Much more work has to be done to improve the switch. A proper way to enlarge the lifetime of the transmon still has to be found, as well as a device capable of minimizing the consequences of having two different energy scales in the system (transmon levels and SQUID levels). The two-photon problem has to be solved in order to find the most optimal time delay between the emission, into the system, of two consecutive photons. If this is achieved, the number of photons that can be transmitted by the switch while the transmon is excited can be obtained. This will give a quantitative limit of how large the QRAM can be (in number of memory cells).

Other systems to extract the information of the memory cells should also be studied. It is important to recover all the photons that are reflected by each individual switch, but in this thesis I only give some ideas on how to do it (in Chapter 5).

And last but not least, the dynamics –and also the possibilities– of a single transmon containing a non-linear capacitor should be studied with much more detail. New interactions and capabilities may emerge, yielding devices such as –and now I am just speculating– a transmon whose first excited level is not coupled to the transmission lines. In this device, if an excitation in the second level decays into the first level, it will remain there for a long time (or infinite time, if the coupling to an external bath is neglected). This may be a good candidate for storing both classical and quantum information.

I have started this thesis claiming that the forthcoming development of a quantum computer is just a matter of time. Now, at the end of this research project, after reading and studying lots of papers about quantum processors, quantum memories, quantum information, etc., I have some more reasons to support my statement. I do not see any impediment for building a quantum processor or a QRAM (I just proposed one). It is true that state-of-the-art processors contain only few qubits but, in the last years, the numbers of qubits in these devices have been slowly increasing. Also, these qubits have been realized in multiple, different fields (see Chapter 1). I do not think that a quantum computer will be realized any time soon, but I am fully convinced that it will be realized some day.

Appendices

Appendix A

Lagrangians and Hamiltonians in cQED

Lagrangians are essential elements to study any system within the framework of circuit quantum electrodynamics. Circuit QED Lagrangians are derived in exactly the same way as in circuit theory. They are constructed by adding the energy of the capacitative elements and subtracting the energy of the inductive elements [30]. The only difference is that there is an element in cQED that is not present in classical circuitry: the Josephson junction. This element, inductive, has energy [29, 30]

$$E = -E_J \cos\left(\frac{\varphi}{\varphi_0}\right), \tag{A.1}$$

where φ_0 is the flux quantum divided by 2π and the variable φ is the flux across the two ends of the Josephson element (the difference between the flux at two nodes of the circuit diagram). The flux φ is defined as the time integral of the potential across the element considered [30],

$$\varphi(t) = \int_{-\infty}^{t} V(t')dt'. \tag{A.2}$$

Josephson junctions are usually integrated in circuits with the form of the device shown in FIG. A.1. This consists of a pair of Josephson junctions connected in parallel and with a potential difference between the two ends of the circuit.

The diagram in FIG. 2.1, containing four capacitors, two Josephson elements

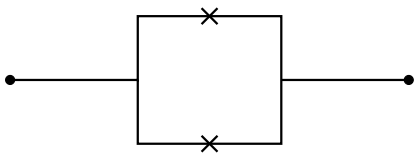

Figure A.1: *This is the circuit diagram of two Josephson junctions connected in parallel. Each of the Josephson junctions is represented by a cross.*

and two node variables φ_1 and φ_2, is completely described by the Lagrangian

$$L = \frac{C_1}{2}(\dot{\varphi}_1 - V_1)^2 + \frac{C_2}{2}(\dot{\varphi}_2 - V_2)^2 + \frac{C_s}{2}(\dot{\varphi}_1 - \dot{\varphi}_2)^2 + \frac{C_t}{2}\dot{\varphi}_1^2 + E_t \cos\left(\frac{\varphi_1}{\varphi_0}\right) + E_s \cos\left(\frac{\varphi_1 - \varphi_2}{\varphi_0}\right). \tag{A.3}$$

The first line describes the energy of each of the capacitances and the second line describes the energy of the Josephson elements. Recall that, from Eq. (A.2), the time derivative of φ_i is the potential at the i-th node of the circuit.

The dynamical variables in this Lagrangian are φ_1, φ_2 and their time derivatives. The Hamiltonian is obtained from this equation by means of a Legendre transformation

$$H = p_1\dot{\varphi}_1 + p_2\dot{\varphi}_2 - L, \tag{A.4}$$

with the conjugate momenta

$$p_1 = \frac{\partial L}{\partial \dot{\varphi}_1} = (C_1 + C_s + C_t)\,\dot{\varphi}_1 - C_s\dot{\varphi}_2 - C_1V_1 \tag{A.5}$$

$$p_2 = \frac{\partial L}{\partial \dot{\varphi}_2} = (C_2 + C_s)\,\dot{\varphi}_2 - C_s\dot{\varphi}_1 - C_2V_2. \tag{A.6}$$

In phase space, the Hamiltonian reads

$$H = \frac{1}{2\gamma}\left(p_1^2 + \frac{C_1 + C_s + C_t}{C_2 + C_s}p_2^2 + \frac{2C_s}{C_2 + C_s}p_1p_2 + 2C_1V_1p_1 + 2\frac{C_2C_s}{C_2 + C_s}V_2p_1 + 2C_2\frac{C_1 + C_s + C_t}{C_2 + C_s}V_2p_2 + 2\frac{C_1C_s}{C_2 + C_s}V_1p_2\right) - E_t\cos\left(\frac{\varphi_1}{\varphi_0}\right) - E_s\cos\left(\frac{\varphi_1 - \varphi_2}{\varphi_0}\right) + Const, \tag{A.7}$$

where $\gamma = C_1 + C_t + \frac{C_s C_2}{C_s+C_2}$. The expression *Const* contains all the terms with V_1^2, V_2^2 and $V_1 V_2$ (they are not dynamical variables). Although these potentials may depend on time –since an incoming pulse, a photon, can modify them– it is safe to consider them constant and take this Hamiltonian as a particular case, where a more general Hamiltonian contains the sum of the particular ones with different values of V_1 and V_2. In any case, all these expressions will be rearranged and added later.

A.1 Quantization of the Hamiltonian

Before proceeding to the quantization of the Hamiltonian, some transformations should be done. In order to simplify the notation, it is convenient to work with the flux $\phi_i = \varphi_i/\varphi_0$. With this transformation, the canonical commutation relation becomes $[\phi_i, p_i] = i\hbar/\varphi_0$.

The fluxes and their conjugate momenta, expressed as a function of some ladder operators, can be written as

$$p_1 = -\frac{i\hbar}{2\varphi_0}\left(\frac{\bar{E}_J}{2E_{c1}}\right)^{1/4}\left(a_1 - a_1^\dagger\right) \tag{A.8}$$

$$p_2 = -\frac{i\hbar}{2\varphi_0}\left(\frac{E_s}{2E_{c2}}\right)^{1/4}\left(a_2 - a_2^\dagger\right) \tag{A.9}$$

$$\phi_1 = \left(\frac{2E_{c1}}{\bar{E}_J}\right)^{1/4}\left(a_1 + a_1^\dagger\right) \tag{A.10}$$

$$\phi_2 = \left(\frac{2E_{c2}}{E_s}\right)^{1/4}\left(a_2 + a_2^\dagger\right), \tag{A.11}$$

with $\bar{E}_J = E_t + E_s$, $E_{c1} = \frac{\hbar^2}{8\gamma\varphi_0^2}$ and $E_{c2} = \frac{\hbar^2(C_1+C_2+C_t)}{8\gamma\varphi_0^2(C_2+C_s)}$. The interactions between the transmon and the SQUID levels show up after separating the cosines in local and non-local terms and expanding them in Taylor series of ϕ_1 and ϕ_2.

$$\begin{aligned} H_{cos} =& -\bar{E}_J\cos\phi_1 - E_s\cos\phi_2 \\ & - E_s\left(\left(\cos\phi_1 - 1\right)\left(\cos\phi_2 - 1\right) + \sin\phi_1\sin\phi_2\right) + Const. \\ \approx& \frac{\bar{E}_J}{2}\phi_1^2 + \frac{E_s}{2}\phi_2^2 - \frac{E_s}{2}\phi_1^2\phi_2^2 - E_s\phi_1\phi_2 + Const. \end{aligned} \tag{A.12}$$

After plugging the Eq. (A.8-A.11) into the Hamiltonian, its quantized form reads

$$\begin{aligned} H =& \sqrt{2E_{c1}\bar{E}_J}a_1^\dagger a_1 + \sqrt{2E_{c2}E_s}a_2^\dagger a_2 \\ &- \sum_{i,j\in\{1,2\}} D_{ij}\left(b_i - b_i^\dagger\right)\left(a_j - a_j^\dagger\right) \\ &- E_s\left(\frac{E_{c1}}{\bar{E}_J}\frac{E_{c2}}{E_s}\right)^{1/4}\left(a_1 + a_1^\dagger\right)^2\left(a_2 + a_2^\dagger\right)^2 \\ &- E_{c1}\frac{2C_s}{C_2 + C_s}\left(\frac{\bar{E}_J E_s}{4E_{c1}E_{c2}}\right)^{1/4}\left(a_1 - a_1^\dagger\right)\left(a_2 - a_2^\dagger\right) \\ &- E_s\left(\frac{4E_{c1}E_{c2}}{\bar{E}_J E_s}\right)^{1/4}\left(a_1 + a_1^\dagger\right)\left(a_2 + a_2^\dagger\right) + Const. \end{aligned} \tag{A.13}$$

The second line in this expression is obtained by imposing, on the operators V_1 and V_2, a similar quantization form as in the momenta operators. Thus, the operators $b_1^\dagger$ and $b_2^\dagger$ create photon modes in the different transmission lines. The form of the Coupling strength D_{ij} of each term is irrelevant, by now.

Let us focus on the last two lines. These expressions allow the exchange of an excitation between the transmon and the SQUID. Since the photon absorbed by the transmon has to be reflected, this interaction must be canceled. The main contribution to these processes com from the term containing $a_1^\dagger a_2$ and its hermitian conjugate, and it can be eliminated by imposing

$$\frac{C_s^2}{(C_1 + C_2 + C_t)(C_2 + C_s)} = \frac{E_s}{\bar{E}_J}. \tag{A.14}$$

The other terms coming from this expression vanish when the rotating wave approximation is assumed. Coming back to the Eq. (A.13) and making use of the rotating wave approximation again –in the third line, now–, the quantized Hamiltonian becomes

$$\begin{aligned} H =& \left(\sqrt{2E_{c1}\bar{E}_J} - 2E_s\left(\frac{E_{c1}E_{c2}}{\bar{E}_J E_s}\right)^{1/4}\right)a_1^\dagger a_1 \\ &+ \left(\sqrt{2E_{c2}E_s} - 2E_s\left(\frac{E_{c1}E_{c2}}{\bar{E}_J E_s}\right)^{1/4}\right)a_2^\dagger a_2 \\ &+ \sum_{i,j\in\{1,2\}} D_{ij}\left(b_i - b_i^\dagger\right)\left(a_j - a_j^\dagger\right) \\ &- 4E_s\left(\frac{E_{c1}E_{c2}}{\bar{E}_J E_s}\right)^{1/4} a_1^\dagger a_1 a_2^\dagger a_2 + Const. \end{aligned} \tag{A.15}$$

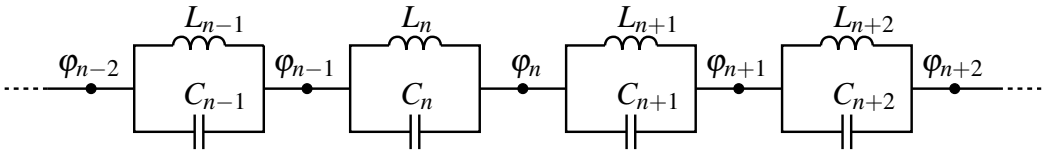

Figure A.2: *A broadly used model for a superconducting transmission line in cQED consists of an infinite chain of LC resonators [30].*

Now, the expression *Const* also includes small terms that hardly contribute to the Hamiltonian. In this new expression, the first and second lines describe the energy levels of the transmon and the SQUID, respectively. The third line contains the interaction between the two atom-like elements of the circuit and the incoming and outgoing transmission lines. The last expression gives the coupling between the transmon and the SQUID. Within this Hamiltonian, exchanges between the transmon and the SQUID excitations are forbidden.

A.2 Transmission lines

A Hamiltonian describing the transmission lines has also to be added to the previously derived equation to obtain a general Hamiltonian capable of describing the process of transmission and reflexion of photons through the quantum switch. The derivation of such Hamiltonian is not much different to the previous procedure. A transmission line [30] can be modeled as the continuum limit of an infinite chain of LC resonators. Once the transmission line is short-circuited (what is propagated are the quantum fluctuations of the flux defined at every node of the system), these resonators become independent and its Hamiltonian is just the sum of the independent Hamiltonians of each independent circuit. FIG. A.2 shows this broadly used model for the transmission lines. In the continuum limit, this Hamiltonian is expressed as [30, 48]

$$H_T = \int_{-\infty}^{\infty} d\omega\, \omega\, b_\omega^\dagger b_\omega, \tag{A.16}$$

for each semi-infinite transmission line. In case the transmission lines are infinite, with left-moving and right-moving modes, the transmission line Hamiltonian reads [48]

$$H_T = \int_{-\infty}^{\infty} d\omega\, \omega \left(r_\omega^\dagger r_\omega - l_\omega^\dagger l_\omega \right). \tag{A.17}$$

The terms that I have omitted in the Hamiltonian in Eq. (A.7) containing V_1 and V_2 are absorbed by the Hamiltonian of the transmission lines. Regarding

the terms containing V_1V_2, these can be omitted if the capacitance C_s, located at halfway between the two transmission lines, is small enough, given that the resulting term will be negligible compared to the other expressions in the Hamiltonian. This will prevent the transmission of a photon without interacting at all with the quantum switch. Finally, since an incoming photon –described by V_1 and V_2– can have multiple frequencies, not just those given by a fixed V_1 and V_2, an integral over all possible momenta has to be added to the final Hamiltonian, which reads

$$\begin{aligned} H = &\left(\sqrt{2E_{c1}\bar{E}_J} - 2E_s \left(\frac{E_{c1}E_{c2}}{\bar{E}_J E_s} \right)^{1/4} \right) a_1^\dagger a_1 \\ &+ \left(\sqrt{2E_{c2}E_s} - 2E_s \left(\frac{E_{c1}E_{c2}}{\bar{E}_J E_s} \right)^{1/4} \right) a_2^\dagger a_2 \\ &+ \int dp \sum_{i,j\in\{1,2\}} D_{ij}(p) \left(b_i(p) - b_i^\dagger(p) \right) \left(a_j - a_j^\dagger \right) \\ &- 4E_s \left(\frac{E_{c1}E_{c2}}{\bar{E}_J E_s} \right)^{1/4} a_1^\dagger a_1 a_2^\dagger a_2 \\ &+ \int dp\, p \left(b_1^\dagger(p) b_1(p) + b_2^\dagger(p) b_2(p) \right), \end{aligned} \tag{A.18}$$

plus an irrelevant constant.

Appendix B

Coefficients in the Hamiltonians

Within the main text large equations do not fit nicely. In order to keep the text clear and give all the necessary information I have decided show symbolic expressions within the main chapters and the full equations and coefficients in the Appendices.

B.1 Hamiltonian in Section 2.3

In Section 2.3 I have derived a Hamiltonian for a device containing a non-linear capacitor. This Hamiltonian have been split in different parts, each containing interactions of a different nature, to simplify the analysis. Some of these equations are too long to write them explicitly, so I have decided to write them more symbolically by introducing some coefficients in the Eq. (2.18). These coefficients are

$$A_{1211} = -\frac{\beta}{2\gamma^4}\left(\frac{C_{s2}}{C_{s2}+C_2}\right)^2$$
$$A_{1311} = -\frac{\beta}{2\gamma^4}\left(\frac{C_{s3}}{C_{s3}+C_3}\right)^2$$
$$A_{2311} = -\frac{\beta}{2\gamma^4}\left(\frac{C_{s2}C_{s3}}{(C_{s2}+C_2)(C_{s3}+C_3)}\right)^2$$

Version of June 29, 2015– Created June 29, 2015 - 21:15

$$A_{1222} = -\frac{35\beta^3}{9\gamma^{10}}\left(\frac{C_{s2}}{C_{s2}+C_2}\right)^4$$
$$A_{1322} = -\frac{35\beta^3}{9\gamma^{10}}\left(\frac{C_{s3}}{C_{s3}+C_3}\right)^4$$
$$A_{2322} = -\frac{35\beta^3}{9\gamma^{10}}\left(\frac{C_{s2}C_{s3}}{(C_{s2}+C_2)(C_{s3}+C_3)}\right)^4$$

$$A_{1233} = -\frac{7007\beta^5}{81\gamma^{16}}\left(\frac{C_{s2}}{C_{s2}+C_2}\right)^6$$
$$A_{1333} = -\frac{7007\beta^5}{81\gamma^{16}}\left(\frac{C_{s3}}{C_{s3}+C_3}\right)^6$$
$$A_{2333} = -\frac{7007\beta^5}{81\gamma^{16}}\left(\frac{C_{s2}C_{s3}}{(C_{s2}+C_2)(C_{s3}+C_3)}\right)^6$$

$$A_{1212} = \frac{5\beta^2}{6\gamma^7}\left(\frac{C_{s2}}{C_{s2}+C_2}\right)^4$$
$$A_{1221} = \frac{5\beta^2}{6\gamma^7}\left(\frac{C_{s2}}{C_{s2}+C_2}\right)^2$$
$$A_{1312} = \frac{5\beta^2}{6\gamma^7}\left(\frac{C_{s3}}{C_{s3}+C_3}\right)^4$$
$$A_{1321} = \frac{5\beta^2}{6\gamma^7}\left(\frac{C_{s3}}{C_{s3}+C_3}\right)^2$$
$$A_{2321} = \frac{5\beta^2}{6\gamma^7}\left(\frac{C_{s2}}{C_{s2}+C_2}\right)^4\left(\frac{C_{s3}}{C_{s3}+C_3}\right)^2$$
$$A_{2312} = \frac{5\beta^2}{6\gamma^7}\left(\frac{C_{s2}}{C_{s2}+C_2}\right)^2\left(\frac{C_{s3}}{C_{s3}+C_3}\right)^4$$

Version of June 29, 2015– Created June 29, 2015 - 21:15

$$
\begin{aligned}
A_{1212} &= -\frac{14\beta^3}{9\gamma^{10}}\left(\frac{C_{s2}}{C_{s2}+C_2}\right)^2\\
A_{1221} &= -\frac{14\beta^3}{9\gamma^{10}}\left(\frac{C_{s2}}{C_{s2}+C_2}\right)^6\\
A_{1312} &= -\frac{14\beta^3}{9\gamma^{10}}\left(\frac{C_{s3}}{C_{s3}+C_3}\right)^2\\
A_{1321} &= -\frac{14\beta^3}{9\gamma^{10}}\left(\frac{C_{s3}}{C_{s3}+C_3}\right)^6\\
A_{2321} &= -\frac{14\beta^3}{9\gamma^{10}}\left(\frac{C_{s2}}{C_{s2}+C_2}\right)^6\left(\frac{C_{s3}}{C_{s3}+C_3}\right)^2\\
A_{2312} &= -\frac{14\beta^3}{9\gamma^{10}}\left(\frac{C_{s2}}{C_{s2}+C_2}\right)^2\left(\frac{C_{s3}}{C_{s3}+C_3}\right)^6
\end{aligned}
$$

$$
\begin{aligned}
A_{1212} &= \frac{385\beta^4}{27\gamma^{13}}\left(\frac{C_{s2}}{C_{s2}+C_2}\right)^4\\
A_{1221} &= \frac{385\beta^4}{27\gamma^{13}}\left(\frac{C_{s2}}{C_{s2}+C_2}\right)^6\\
A_{1312} &= \frac{385\beta^4}{27\gamma^{13}}\left(\frac{C_{s3}}{C_{s3}+C_3}\right)^4\\
A_{1321} &= \frac{385\beta^4}{27\gamma^{13}}\left(\frac{C_{s3}}{C_{s3}+C_3}\right)^6\\
A_{2321} &= \frac{385\beta^4}{27\gamma^{13}}\left(\frac{C_{s2}}{C_{s2}+C_2}\right)^6\left(\frac{C_{s3}}{C_{s3}+C_3}\right)^4\\
A_{2312} &= \frac{385\beta^4}{27\gamma^{13}}\left(\frac{C_{s2}}{C_{s2}+C_2}\right)^4\left(\frac{C_{s3}}{C_{s3}+C_3}\right)^6.
\end{aligned}
$$

Version of June 29, 2015– Created June 29, 2015 - 21:15

The equation H_4 has also been simplified using the following coefficients

$$B_{211} = \frac{1}{\gamma}\left(\frac{C_{s2}}{C_{s2}+C_2}\right) \qquad B_{311} = \frac{1}{\gamma}\left(\frac{C_{s3}}{C_{s3}+C_3}\right)$$
$$B_{212} = -\frac{\beta}{3\gamma^4}\left(\frac{C_{s2}}{C_{s2}+C_2}\right)^3 \qquad B_{312} = -\frac{\beta}{3\gamma^4}\left(\frac{C_{s3}}{C_{s3}+C_3}\right)^3$$
$$B_{213} = \frac{\beta^2}{3\gamma^7}\left(\frac{C_{s2}}{C_{s2}+C_2}\right)^5 \qquad B_{313} = \frac{\beta^2}{3\gamma^7}\left(\frac{C_{s3}}{C_{s3}+C_3}\right)^5$$

$$B_{221} = -\frac{\beta}{3\gamma^4}\left(\frac{C_{s2}}{C_{s2}+C_2}\right) \qquad B_{321} = -\frac{\beta}{3\gamma^4}\left(\frac{C_{s3}}{C_{s3}+C_3}\right)$$
$$B_{222} = \frac{10\beta^2}{9\gamma^7}\left(\frac{C_{s2}}{C_{s2}+C_2}\right)^3 \qquad B_{322} = \frac{10\beta^2}{9\gamma^7}\left(\frac{C_{s3}}{C_{s3}+C_3}\right)^3$$
$$B_{223} = -\frac{28\beta^3}{9\gamma^{10}}\left(\frac{C_{s2}}{C_{s2}+C_2}\right)^5 \qquad B_{323} = -\frac{28\beta^3}{9\gamma^{10}}\left(\frac{C_{s3}}{C_{s3}+C_3}\right)^5$$

$$B_{231} = \frac{\beta^2}{3\gamma^7}\left(\frac{C_{s2}}{C_{s2}+C_2}\right) \qquad B_{331} = \frac{\beta^2}{3\gamma^7}\left(\frac{C_{s3}}{C_{s3}+C_3}\right)$$
$$B_{232} = -\frac{28\beta^3}{9\gamma^{10}}\left(\frac{C_{s2}}{C_{s2}+C_2}\right)^3 \qquad B_{332} = -\frac{28\beta^3}{9\gamma^{10}}\left(\frac{C_{s3}}{C_{s3}+C_3}\right)^3$$
$$B_{233} = \frac{154\beta^4}{9\gamma^{13}}\left(\frac{C_{s2}}{C_{s2}+C_2}\right)^5 \qquad B_{333} = \frac{154\beta^4}{9\gamma^{13}}\left(\frac{C_{s3}}{C_{s3}+C_3}\right)^5.$$

The following is the Hamiltonian H_5, containing processes that destroy the information (see Section 2.3).

$$\begin{aligned} H_5 = &-\frac{\beta}{\gamma^4}\left(C_1V_1 + \frac{C_{s2}}{C_{s2}+C_2}C_2V_2 + \frac{C_{s3}}{C_{s3}+C_3}C_3V_3\right)\times \\ &\left(2\frac{C_{s2}}{C_{s2}+C_2}\frac{C_{s3}}{C_{s3}+C_3}p_1p_2p_3 + \left(\frac{C_{s2}}{C_{s2}+C_2}\right)p_1^2p_2\right. \\ &+\left(\frac{C_{s2}}{C_{s2}+C_2}\right)^2 p_1p_2^2 + \left(\frac{C_{s3}}{C_{s3}+C_3}\right)p_1^2p_3 + \left(\frac{C_{s3}}{C_{s3}+C_3}\right)^2 p_1p_3^2 \\ &\left.+\left(\frac{C_{s2}}{C_{s2}+C_2}\right)^2\left(\frac{C_{s3}}{C_{s3}+C_3}\right)p_2^2p_3 + \left(\frac{C_{s2}}{C_{s2}+C_2}\right)\left(\frac{C_{s3}}{C_{s3}+C_3}\right)^2 p_2p_3^2\right). \end{aligned} \tag{B.1}$$

B.2 Hamiltonian in the Section 2.5

Section 2.5 contains the Hamiltonian (or a part of it) I have used to model a quantum switch. This Hamiltonian have been divided in few expressions to simplify the notation, and these expressions, in turn, have been simplified by adding some coefficients. The following is a list of the coefficients used in the Eq. (2.33), that is, in H_2

$$A'_{1\,2a} = -\frac{\beta}{12\gamma^4}\left(\frac{C_{2sa}}{C_{2a}+C_{2sa}}\right)^2 \qquad A'_{1\,2b} = -\frac{\beta}{12\gamma^4}\left(\frac{C_{2sb}}{C_{2b}+C_{2sb}}\right)^2$$
$$A'_{2\,2a} = \frac{5\beta^2}{6\gamma^7}\left(\frac{C_{2sa}}{C_{2a}+C_{2sa}}\right)^2 \qquad A'_{2\,2b} = \frac{5\beta^2}{6\gamma^7}\left(\frac{C_{2sb}}{C_{2b}+C_{2sb}}\right)^2$$
$$A'_{3\,2a} = -\frac{14\beta^3}{9\gamma^{10}}\left(\frac{C_{2sa}}{C_{2a}+C_{2sa}}\right)^2 \qquad A'_{3\,2b} = -\frac{14\beta^3}{9\gamma^{10}}\left(\frac{C_{2sb}}{C_{2b}+C_{2sb}}\right)^2$$

$$A'_{1\,3a} = -\frac{\beta}{12\gamma^4}\left(\frac{C_{3sa}}{C_{3a}+C_{3sa}}\right)^2 \qquad A'_{1\,3b} = -\frac{\beta}{12\gamma^4}\left(\frac{C_{3sb}}{C_{3b}+C_{3sb}}\right)^2$$
$$A'_{2\,3a} = \frac{5\beta^2}{6\gamma^7}\left(\frac{C_{3sa}}{C_{3a}+C_{3sa}}\right)^2 \qquad A'_{2\,3b} = \frac{5\beta^2}{6\gamma^7}\left(\frac{C_{3sb}}{C_{3b}+C_{3sb}}\right)^2$$
$$A'_{3\,3a} = -\frac{14\beta^3}{9\gamma^{10}}\left(\frac{C_{3sa}}{C_{3a}+C_{3sa}}\right)^2 \qquad A'_{3\,3b} = -\frac{14\beta^3}{9\gamma^{10}}\left(\frac{C_{3sb}}{C_{3b}+C_{3sb}}\right)^2.$$

The interaction with the transmission lines (H_3) is completely described by the coefficients

$$B'_{1\,1} = C_1\frac{1}{\gamma} \qquad B'_{1\,3} = -C_1\frac{\beta}{3\gamma^4}$$
$$B'_{2\,1} = \left(\frac{C_{2a}C_{2sa}}{C_{2a}+C_{2sa}}+\frac{C_{2b}C_{2sb}}{C_{2b}+C_{2sb}}\right)\frac{1}{\gamma} \qquad B'_{2\,3} = -\left(\frac{C_{2a}C_{2sa}}{C_{2a}+C_{2sa}}+\frac{C_{2b}C_{2sb}}{C_{2b}+C_{2sb}}\right)\frac{\beta}{3\gamma^4}$$
$$B'_{3\,1} = \left(\frac{C_{3a}C_{3sa}}{C_{3a}+C_{3sa}}+\frac{C_{3b}C_{3sb}}{C_{3b}+C_{3sb}}\right)\frac{1}{\gamma} \qquad B'_{3\,3} = -\left(\frac{C_{3a}C_{3sa}}{C_{3a}+C_{3sa}}+\frac{C_{3b}C_{3sb}}{C_{3b}+C_{3sb}}\right)\frac{\beta}{3\gamma^4}$$

$$B'_{1\,2a} = C_1\frac{C_{2sa}}{(C_{2a}+C_{2sa})\gamma}$$
$$B'_{2\,2a} = \left(\frac{C_{2a}C_{2sa}}{C_{2a}+C_{2sa}}+\frac{C_{2b}C_{2sb}}{C_{2b}+C_{2sb}}+\frac{C_{2a}\gamma}{C_{2sa}}\right)\frac{C_{2sa}}{(C_{2a}+C_{2sa})\gamma}$$
$$B'_{3\,2a} = \left(\frac{C_{3a}C_{3sa}}{C_{3a}+C_{3sa}}+\frac{C_{3b}C_{3sb}}{C_{3b}+C_{3sb}}\right)\frac{C_{2sa}}{(C_{2a}+C_{2sa})\gamma}$$

$$
\begin{aligned}
B'_{1\,2b} =& C_1 \frac{C_{2sb}}{(C_{2b}+C_{2sb})\gamma} \\
B'_{2\,2b} =& \left(\frac{C_{2a}C_{2sa}}{C_{2a}+C_{2sa}} + \frac{C_{2b}C_{2sb}}{C_{2b}+C_{2sb}} + \frac{C_{2b}\gamma}{C_{2sb}} \right) \frac{C_{2sb}}{(C_{2b}+C_{2sb})\gamma} \\
B'_{3\,2b} =& \left(\frac{C_{3a}C_{3sa}}{C_{3a}+C_{3sa}} + \frac{C_{3b}C_{3sb}}{C_{3b}+C_{3sb}} \right) \frac{C_{2sb}}{(C_{2b}+C_{2sb})\gamma}
\end{aligned}
$$

$$
\begin{aligned}
B'_{1\,3a} =& C_1 \frac{C_{3sa}}{(C_{3a}+C_{3sa})\gamma} \\
B'_{2\,3a} =& \left(\frac{C_{2a}C_{2sa}}{C_{2a}+C_{2sa}} + \frac{C_{2b}C_{2sb}}{C_{2b}+C_{2sb}} \right) \frac{C_{3sa}}{(C_{3a}+C_{3sa})\gamma} \\
B'_{3\,3a} =& \left(\frac{C_{3a}C_{3sa}}{C_{3a}+C_{3sa}} + \frac{C_{3b}C_{3sb}}{C_{3b}+C_{3sb}} + \frac{C_{3a}\gamma}{C_{3sa}} \right) \frac{C_{3sa}}{(C_{3a}+C_{3sa})\gamma}
\end{aligned}
$$

$$
\begin{aligned}
B'_{1\,3b} =& C_1 \frac{C_{3sb}}{(C_{3b}+C_{3sb})\gamma} \\
B'_{2\,3b} =& \left(\frac{C_{2a}C_{2sa}}{C_{2a}+C_{2sa}} + \frac{C_{2b}C_{2sb}}{C_{2b}+C_{2sb}} \right) \frac{C_{3sb}}{(C_{3b}+C_{3sb})\gamma} \\
B'_{3\,3b} =& \left(\frac{C_{3a}C_{3sa}}{C_{3a}+C_{3sa}} + \frac{C_{3b}C_{3sb}}{C_{3b}+C_{3sb}} + \frac{C_{3b}\gamma}{C_{3sb}} \right) \frac{C_{3sb}}{(C_{3b}+C_{3sb})\gamma}.
\end{aligned}
$$

Two more expressions conform the total Hamiltonian of the device in FIG. 2.5. These are H_5 and H_6, defined below. These two expression carry interactions that must be either canceled or neglected for a good performance of the quantum switch:

$$
\begin{aligned}
H_5 =& \left(-\frac{\beta}{6\gamma^4}p_1^2 + \frac{5\beta^2}{3\gamma^7}p_1^4 - \frac{28\beta^3}{9\gamma^{10}}p_1^6 \right) \frac{C_{2sa}}{C_{2a}+C_{2sa}} \frac{C_{2sb}}{C_{2b}+C_{2sb}} p_{2a}p_{2b} \\
&+ \left(-\frac{\beta}{6\gamma^4}p_1^2 + \frac{5\beta^2}{3\gamma^7}p_1^4 - \frac{28\beta^3}{9\gamma^{10}}p_1^6 \right) \frac{C_{3sa}}{C_{3a}+C_{3sa}} \frac{C_{3sb}}{C_{3b}+C_{3sb}} p_{3a}p_{3b} \\
&+ \left(-\frac{\beta}{6\gamma^4}p_1^2 + \frac{5\beta^2}{3\gamma^7}p_1^4 - \frac{28\beta^3}{9\gamma^{10}}p_1^6 \right) \frac{C_{2sa}}{C_{2a}+C_{2sa}} \frac{C_{3sa}}{C_{3a}+C_{3sa}} p_{2a}p_{3a} \\
&+ \left(-\frac{\beta}{6\gamma^4}p_1^2 + \frac{5\beta^2}{3\gamma^7}p_1^4 - \frac{28\beta^3}{9\gamma^{10}}p_1^6 \right) \frac{C_{2sb}}{C_{2b}+C_{2sb}} \frac{C_{3sb}}{C_{3b}+C_{3sb}} p_{2b}p_{3b} \\
&+ \left(-\frac{\beta}{6\gamma^4}p_1^2 + \frac{5\beta^2}{3\gamma^7}p_1^4 - \frac{28\beta^3}{9\gamma^{10}}p_1^6 \right) \frac{C_{2sa}}{C_{2a}+C_{2sa}} \frac{C_{3sb}}{C_{3b}+C_{3sb}} p_{2a}p_{3b} \\
&+ \left(-\frac{\beta}{6\gamma^4}p_1^2 + \frac{5\beta^2}{3\gamma^7}p_1^4 - \frac{28\beta^3}{9\gamma^{10}}p_1^6 \right) \frac{C_{2sb}}{C_{2b}+C_{2sb}} \frac{C_{3sa}}{C_{3a}+C_{3sa}} p_{2b}p_{3a}, \qquad \text{(B.2)}
\end{aligned}
$$

$$H_6 = -\left(\left(\frac{C_{2a}C_{2sa}}{C_{2a}+C_{2sa}}+\frac{C_{2b}C_{2sb}}{C_{2b}+C_{2sb}}\right)V_2+\left(\frac{C_{3a}C_{3sa}}{C_{3a}+C_{3sa}}+\frac{C_{3b}C_{3sb}}{C_{3b}+C_{3sb}}\right)V_3\right)\times$$
$$\frac{\beta p_1^2}{\gamma^4}\left(\frac{C_{2sa}p_{2a}}{C_{2a}+C_{2sa}}+\frac{C_{2sb}p_{2b}}{C_{2b}+C_{2sb}}+\frac{C_{3sa}p_{3a}}{C_{3a}+C_{3sa}}+\frac{C_{3sb}p_{3b}}{C_{3b}+C_{3sb}}\right)$$
$$-\frac{\beta C_1 V_1 p_1^2}{\gamma^4}\left(\frac{C_{2sa}p_{2a}}{C_{2a}+C_{2sa}}+\frac{C_{2sb}p_{2b}}{C_{2b}+C_{2sb}}+\frac{C_{3sa}p_{3a}}{C_{3a}+C_{3sa}}+\frac{C_{3sb}p_{3b}}{C_{3b}+C_{3sb}}\right). \quad \text{(B.3)}$$

Appendix C

Equations of motion within the *in/out* formalism

In this appendix, some equations of motion are derived using the *in/out* formalism of quantum optics [45, 47, 48]. The procedure followed is similar to [17, 45, 46, 48] Using the Hamiltonian in Eq. (3.34), and the Heisenberg equation, the equation of motion of the $b_1(\omega)$ operator is found

$$\begin{aligned}\dot{b}_1(\omega) &= i[H, b_1(\omega)] \\ &= -i\omega b_1(\omega) - i\left(\frac{a_{T1}}{\sqrt{\pi\tau_{T1}}} + \frac{a_{T3}}{\sqrt{\pi\tau_{T3}}} + \left(\sqrt{\frac{2}{\pi\tau_{T1}}} - \sqrt{\frac{3}{\pi\tau_{T3}}}\right) a_{T1}^{\dagger} a_{T2}\right. \\ &\quad \left. + \frac{a_{2a}}{\sqrt{\pi\tau_{2a,1}}} + \frac{a_{2b}}{\sqrt{\pi\tau_{2b,1}}} + \frac{a_{3a}}{\sqrt{\pi\tau_{3a,1}}} + \frac{a_{3b}}{\sqrt{\pi\tau_{3b,1}}}\right). \end{aligned} \tag{C.1}$$

The formal solution of this differential equation is

$$\begin{aligned} b_1(\omega,t) =& e^{-i\omega(t-t_0)} b_1(\omega,t_0) \\ & - i\int_{-\infty}^{t} dt'\, e^{i\omega(t'-t)} \left(\frac{a_{T1}}{\sqrt{\pi\tau_{T1}}} + \frac{a_{T3}}{\sqrt{\pi\tau_{T3}}} + \left(\sqrt{\frac{2}{\pi\tau_{T1}}} - \sqrt{\frac{3}{\pi\tau_{T3}}}\right) a_{T1}^{\dagger} a_{T2}\right. \\ & \left. + \frac{a_{2a}}{\sqrt{\pi\tau_{2a,1}}} + \frac{a_{2b}}{\sqrt{\pi\tau_{2b,1}}} + \frac{a_{3a}}{\sqrt{\pi\tau_{3a,1}}} + \frac{a_{3b}}{\sqrt{\pi\tau_{3b,1}}}\right), \end{aligned} \tag{C.2}$$

where the a_k operators are also time-dependent. $b_1(p,t_0)$ is an initial value of the Heisenberg operator defined at a time $t_0 \to -\infty$. Consider also the same equation

expressed with the opposite boundary condition

$$b_1(\omega,t) = e^{-i\omega(t-t_1)} b_1(\omega,t_1) - i\int_t^\infty dt'\, e^{i\omega(t'-t)} \left(\frac{a_{T1}}{\sqrt{\pi\tau_{T1}}} + \frac{a_{T3}}{\sqrt{\pi\tau_{T3}}} + \left(\sqrt{\frac{2}{\pi\tau_{T1}}} - \sqrt{\frac{3}{\pi\tau_{T3}}} \right) a_{T1}^\dagger a_{T2} + \frac{a_{2a}}{\sqrt{\pi\tau_{2a,1}}} + \frac{a_{2b}}{\sqrt{\pi\tau_{2b,1}}} + \frac{a_{3a}}{\sqrt{\pi\tau_{3a,1}}} + \frac{a_{3b}}{\sqrt{\pi\tau_{3b,1}}} \right). \tag{C.3}$$

Here $b_1(\omega,t_1)$ is a final value of the Heisenberg operator defined at a time $t_1 \to \infty$. Now take these equations and integrate them over ω together with a factor of $1/\sqrt{2\pi}$. The homogeneous part of the equation becomes, using Eq. (3.66)

$$\frac{1}{\sqrt{2\pi}} \int_{-\infty}^{\infty} d\omega\, e^{-i\omega(t-t_1)} b_1(\omega,t_1) = b_{1in}(t). \tag{C.4}$$

The particular part of the differential equation can also be integrated using the properties [45]

$$\int_{-\infty}^{\infty} d\omega\, e^{-i\omega(t-t_1)} = 2\pi\delta(t-t') \tag{C.5}$$

$$\int_{-\infty}^{t} dt'\, f(t')\delta(t-t') = \frac{1}{2} f(t). \tag{C.6}$$

The same procedure is applied to the Eq. (C.3) yielding

$$\frac{1}{\sqrt{2\pi}} \int_{-\infty}^{\infty} d\omega\, b_1(\omega,t) = b_{1in}(t) - i\frac{1}{\sqrt{2}} \left(\frac{a_{T1}}{\sqrt{\tau_{T1}}} + \frac{a_{T3}}{\sqrt{\tau_{T3}}} + \left(\sqrt{\frac{2}{\tau_{T1}}} - \sqrt{\frac{3}{\tau_{T3}}} \right) a_{T1}^\dagger a_{T2} + \frac{a_{2a}}{\sqrt{\tau_{2a,1}}} + \frac{a_{2b}}{\sqrt{\tau_{2b,1}}} + \frac{a_{3a}}{\sqrt{\tau_{3a,1}}} + \frac{a_{3b}}{\sqrt{\tau_{3b,1}}} \right), \tag{C.7}$$

and

$$\frac{1}{\sqrt{2\pi}} \int_{-\infty}^{\infty} d\omega\, b_1(\omega,t) = b_{1out}(t) + i\frac{1}{\sqrt{2}} \left(\frac{a_{T1}}{\sqrt{\tau_{T1}}} + \frac{a_{T3}}{\sqrt{\tau_{T3}}} + \left(\sqrt{\frac{2}{\tau_{T1}}} - \sqrt{\frac{3}{\tau_{T3}}} \right) a_{T1}^\dagger a_{T2} + \frac{a_{2a}}{\sqrt{\tau_{2a,1}}} + \frac{a_{2b}}{\sqrt{\tau_{2b,1}}} + \frac{a_{3a}}{\sqrt{\tau_{3a,1}}} + \frac{a_{3b}}{\sqrt{\tau_{3b,1}}} \right). \tag{C.8}$$

By combining the two equations one obtains

$$b_{1out}(t) = b_{1in}(t) - i\sqrt{2}\left(\frac{a_{T1}}{\sqrt{\tau_{T1}}} + \frac{a_{T3}}{\sqrt{\tau_{T3}}} + \left(\sqrt{\frac{2}{\tau_{T1}}} - \sqrt{\frac{3}{\tau_{T3}}}\right) a_{T1}^{\dagger} a_{T2} + \frac{a_{2a}}{\sqrt{\tau_{2a,1}}} + \frac{a_{2b}}{\sqrt{\tau_{2b,1}}} + \frac{a_{3a}}{\sqrt{\tau_{3a,1}}} + \frac{a_{3b}}{\sqrt{\tau_{3b,1}}}\right). \quad \text{(C.9)}$$

This equation relates the *input* and *output* operators. Similar expressions can be found for all the other operators describing moving particles:

$$b_{2out}(t) = b_{2in}(t) - i\sqrt{2}\left(\frac{a_{2a}}{\sqrt{\tau_{2a,2}}} + \frac{a_{2b}}{\sqrt{\tau_{2b,2}}}\right) \quad \text{(C.10)}$$

$$b_{3out}(t) = b_{3in}(t) - i\sqrt{2}\left(\frac{a_{3a}}{\sqrt{\tau_{3a,3}}} + \frac{a_{3b}}{\sqrt{\tau_{3b,3}}}\right). \quad \text{(C.11)}$$

And for the decoherence operators

$$r_{T1out}(t) = r_{T1in}(t) - i\sqrt{\gamma_{rT1}}a_{T1}(t) \quad \text{(C.12)}$$

$$r_{T3out}(t) = r_{T3in}(t) - i\sqrt{\gamma_{rT3}}a_{T3}(t) \quad \text{(C.13)}$$

$$r_{2aout}(t) = r_{2ain}(t) - i\sqrt{\gamma_{r2a}}a_{2a}(t) \quad \text{(C.14)}$$

$$r_{2bout}(t) = r_{2bin}(t) - i\sqrt{\gamma_{r2b}}a_{2b}(t) \quad \text{(C.15)}$$

$$r_{3aout}(t) = r_{3ain}(t) - i\sqrt{\gamma_{r3a}}a_{3a}(t) \quad \text{(C.16)}$$

$$r_{3bout}(t) = r_{3bin}(t) - i\sqrt{\gamma_{r3b}}a_{3b}(t) \quad \text{(C.17)}$$

$$d_{T1out}(t) = d_{T1in}(t) - i\sqrt{\frac{\gamma_{dT1}}{2}}a_{T1}^{\dagger}(t)a_{T1}(t) \quad \text{(C.18)}$$

$$d_{T3out}(t) = d_{T3in}(t) - i\sqrt{\frac{\gamma_{dT3}}{2}}a_{T3}^{\dagger}(t)a_{T3}(t) \quad \text{(C.19)}$$

$$d_{2aout}(t) = d_{2ain}(t) - i\sqrt{\frac{\gamma_{d2a}}{2}}a_{2a}^{\dagger}(t)a_{2a}(t) \quad \text{(C.20)}$$

$$d_{2bout}(t) = d_{2bin}(t) - i\sqrt{\frac{\gamma_{d2b}}{2}}a_{2b}^{\dagger}(t)a_{2b}(t) \quad \text{(C.21)}$$

$$d_{3aout}(t) = d_{3ain}(t) - i\sqrt{\frac{\gamma_{d3a}}{2}}a_{3a}^{\dagger}(t)a_{3a}(t) \quad \text{(C.22)}$$

$$d_{3bout}(t) = d_{3bin}(t) - i\sqrt{\frac{\gamma_{d3b}}{2}}a_{3b}^{\dagger}(t)a_{3b}(t). \quad \text{(C.23)}$$

Version of June 29, 2015– Created June 29, 2015 - 21:15

Appendix D

Derivation of single-photon scattering amplitudes

This appendix contains the derivation of some of the scattering amplitudes discussed in Chapter 4. To derive these quantities I have made use of the Langevin equations in Eq. (3.75) to (3.78). Recall that, using the *in/out* formalism, the probability amplitude for a photon being reflected is

$$S_1(p,k) = \langle 0| b_{1out}(p) b_{1in}^{\dagger}(k) |0\rangle . \tag{D.1}$$

This expression can only be evaluated by expressing the *out* operator as a function of the *in* and the other ladder operators that describe the transmon and SQUID excitations. In the previous appendix, the relation between these operators in time space is found, so they must be transformed to momentum space via a Fourier transform. Within this work, the convention I have used for the Fourier transform is the following:

$$\begin{aligned} \mathscr{F}\left[b(t)\right](p) &= \frac{1}{\sqrt{2\pi}} \int dt\, e^{ipt} b(t), \\ \mathscr{F}\left[b^{\dagger}(t)\right](p) &= \frac{1}{\sqrt{2\pi}} \int dt\, e^{-ipt} b^{\dagger}(t). \end{aligned} \tag{D.2}$$

By using the aforementioned relations and the Fourier transforms, the scattering amplitude of a photon being reflected is given by

$$\begin{aligned} S_1(p,k) = &\langle 0|\, b_{1in}(p) b_{1in}^\dagger(k)\,|0\rangle \\ &- i\left(\frac{2}{\sqrt{\tau_{T1}}} - \sqrt{\frac{6}{\tau_T}}\right)\frac{1}{\sqrt{2\pi}}\int dt\, \mathrm{e}^{ipt}\,\langle 0|\, a_{T1}^\dagger(t) a_{T2}(t) b_{1in}^\dagger(k)\,|0\rangle \\ &- i\sqrt{\frac{2}{\tau_{T1}}}\frac{1}{\sqrt{2\pi}}\int dt\, \mathrm{e}^{ipt}\,\langle 0|\, a_{T1}(t) b_{1in}^\dagger(k)\,|0\rangle \\ &- i\sqrt{\frac{2}{\tau_{T3}}}\frac{1}{\sqrt{2\pi}}\int dt\, \mathrm{e}^{ipt}\,\langle 0|\, a_{T3}(t) b_{1in}^\dagger(k)\,|0\rangle \\ &- i\sqrt{\frac{2}{\tau_{2a,1}}}\frac{1}{\sqrt{2\pi}}\int dt\, \mathrm{e}^{ipt}\,\langle 0|\, a_{2a}(t) b_{1in}^\dagger(k)\,|0\rangle \\ &+ (2a \to 2b,\ 3a,\ 3b)\,. \end{aligned} \tag{D.3}$$

The first element in this expression gives just a Dirac delta function $\delta(p-k)$. The second element vanishes because there is a creation operator acting on the vacuum by the left-hand side. Six more elements remain in the expression. These have to be evaluated one by one by making use of the Langevin equations.

The first element to be evaluated is $\langle 0|\, a_{T1}(t) b_{1in}^\dagger(k)\,|0\rangle$. The way to proceed consists of taking the time derivative of these expression and plug in the Langevin equations. The solution of the system of differential equations that has been generated gives the elements that conform the Eq. (D.3). After disregarding all the terms that vanish due to the presence of the vacuum bras and kets (such as $\langle 0|\, a_{T1}^\dagger = 0$ or $\langle 0|\, b_{2in}(k) b_{1in}^\dagger(k)\,|0\rangle = \delta(p-k)\delta_{1,2} = 0$) the considered element reads

$$\begin{aligned} &\frac{d}{dt}\langle 0|\, a_{T1}(t) b_{1in}^\dagger(k)\,|0\rangle = \\ &\quad -\left(i\omega_{T1} + \frac{1}{\tau_{T1}} + \frac{1}{2}\gamma_{rT1} + \frac{1}{4}\gamma_{dT1}\right)\langle 0|\, a_{T1}(t) b_{1in}^\dagger(k)\,|0\rangle \\ &\quad - \frac{1}{\sqrt{\tau_{T1}\tau_{T3}}}\langle 0|\, a_{T3}(t) b_{1in}^\dagger(k)\,|0\rangle \\ &\quad - \frac{1}{\sqrt{\tau_{T1}}}\langle 0|\, a_{T1}(t) a_{T1}^\dagger(t)\left(\frac{a_{2a}(t)}{\sqrt{\tau_{2a,1}}} + \frac{a_{2b}(t)}{\sqrt{\tau_{2b,1}}} + \frac{a_{3a}(t)}{\sqrt{\tau_{3a,1}}} + \frac{a_{3b}(t)}{\sqrt{\tau_{3b,1}}}\right) b_{1in}^\dagger(k)\,|0\rangle \\ &\quad - \frac{1}{\sqrt{\pi\tau_{T1}}}\langle 0|\, a_{T1}(t) a_{T1}^\dagger(t)\,|0\rangle\, e^{-ikt}. \end{aligned} \tag{D.4}$$

Similarly, five other expressions are found for the five last lines in Eq. (D.3).

$$\begin{aligned}
\frac{d}{dt}\langle 0|\, a_{T3}(t) b^{\dagger}_{1in}(k)\,|0\rangle = \\
&-\left(i\omega_{T3}+\frac{1}{\tau_{T3}}+\frac{1}{2}\gamma_{rT3}+\frac{1}{4}\gamma_{dT3}\right)\langle 0|\, a_{T3}(t) b^{\dagger}_{1in}(k)\,|0\rangle \\
&-\frac{1}{\sqrt{\tau_{T1}\tau_{T3}}}\langle 0|\, a_{T1}(t) b^{\dagger}_{1in}(k)\,|0\rangle \\
&-\frac{1}{\sqrt{\tau_{T3}}}\langle 0|\, a_{T3}(t) a^{\dagger}_{T3}(t)\left(\frac{a_{2a}(t)}{\sqrt{\tau_{2a,1}}}+\frac{a_{2b}(t)}{\sqrt{\tau_{2b,1}}}+\frac{a_{3a}(t)}{\sqrt{\tau_{3a,1}}}+\frac{a_{3b}(t)}{\sqrt{\tau_{3b,1}}}\right) b^{\dagger}_{1in}(k)\,|0\rangle \\
&-\frac{1}{\sqrt{\pi\tau_{T3}}}\langle 0|\, a_{T3}(t) a^{\dagger}_{T3}(t)\,|0\rangle\, e^{-ikt}, \qquad \text{(D.5)}
\end{aligned}$$

$$\begin{aligned}
\frac{d}{dt}\langle 0|\, a_{2a}(t) b^{\dagger}_{1in}(k)\,|0\rangle = \\
&-\left(i\omega_{2a}+\frac{1}{\tau_{2a,1}}+\frac{1}{\tau_{2a,2}}+\frac{1}{2}\gamma_{r2a}+\frac{1}{4}\gamma_{d2a}\right)\langle 0|\, a_{2a}(t) b^{\dagger}_{1in}(k)\,|0\rangle \\
&-\left(\frac{1}{\sqrt{\tau_{2a,1}\tau_{2b,1}}}+\frac{1}{\sqrt{\tau_{2a,2}\tau_{2b,2}}}\right)\langle 0|\, a_{2a}(t) b^{\dagger}_{1in}(k)\,|0\rangle \\
&-\frac{1}{\sqrt{\tau_{2a,1}\tau_{3a,1}}}\langle 0|\, a_{3a}(t) b^{\dagger}_{1in}(k)\,|0\rangle \\
&-\frac{1}{\sqrt{\tau_{2a,1}\tau_{3b,1}}}\langle 0|\, a_{3b}(t) b^{\dagger}_{1in}(k)\,|0\rangle \\
&-\frac{1}{\sqrt{\tau_{2a,1}\tau_{T1}}}\langle 0|\, a_{T1}(t) b^{\dagger}_{1in}(k)\,|0\rangle \\
&-\frac{1}{\sqrt{\tau_{2a,1}\tau_{T3}}}\langle 0|\, a_{T3}(t) b^{\dagger}_{1in}(k)\,|0\rangle \\
&-\frac{1}{\sqrt{\pi\tau_{2a,1}}}e^{-ikt}, \qquad \text{(D.6)}
\end{aligned}$$

and three more expressions that are found by replacing $2a \to 2b,\ 3a,\ 3b$. This last equation contains a set of terms that also appear in all the other five equations, hence this can be solved, in principle, as a linear system of differential equation. However, the Eq. (D.4) and (D.5) contain other terms that have to be explicitly evaluated. These are in the two last lines of both equations. Let me start with $\langle 0|\, a_{T1}(t) a^{\dagger}_{T1}(t)\,|0\rangle$. This can be written as

$$\langle 0|\, a_{T1}(t) a^{\dagger}_{T1}(t)\,|0\rangle = \langle 0|\, e^{iHt} a_{T1} a^{\dagger}_{T1} e^{-iHt}\,|0\rangle\,, \qquad \text{(D.7)}$$

where a_{T1} and $a_{T1}^{\dagger}$ are the Schrödinger picture operators defined in Eq. (3.36)-(3.38). Since the vacuum is an eigenstate of the Hamiltonian with eigenvalue 0 ($H|0\rangle = 0$), this expression becomes

$$\langle 0| a_{T1}(t) a_{T1}^{\dagger}(t) |0\rangle = \langle 0| a_{T1} a_{T1}^{\dagger} |0\rangle = 1. \tag{D.8}$$

The same applies to $\langle 0| a_{T3}(t) a_{T3}^{\dagger}(t) |0\rangle$ and also to the remaining two expressions which, in this case yield

$$\begin{aligned}\langle 0| a_{T1}(t) a_{T1}^{\dagger}(t) \left(\frac{a_{2a}}{\tau_{2a,1}} + \frac{a_{2b}}{\tau_{2b,1}} + \frac{a_{3a}}{\tau_{3a,1}} + \frac{a_{3b}}{\tau_{3b,1}} \right) b_{1in}^{\dagger}(k) |0\rangle = \\ \langle 0| \left(\frac{a_{2a}}{\tau_{2a,1}} + \frac{a_{2b}}{\tau_{2b,1}} + \frac{a_{3a}}{\tau_{3a,1}} + \frac{a_{3b}}{\tau_{3b,1}} \right) b_{1in}^{\dagger}(k) |0\rangle ,\end{aligned} \tag{D.9}$$

$$\begin{aligned}\langle 0| a_{T3}(t) a_{T3}^{\dagger}(t) \left(\frac{a_{2a}}{\tau_{2a,1}} + \frac{a_{2b}}{\tau_{2b,1}} + \frac{a_{3a}}{\tau_{3a,1}} + \frac{a_{3b}}{\tau_{3b,1}} \right) b_{1in}^{\dagger}(k) |0\rangle = \\ \langle 0| \left(\frac{a_{2a}}{\tau_{2a,1}} + \frac{a_{2b}}{\tau_{2b,1}} + \frac{a_{3a}}{\tau_{3a,1}} + \frac{a_{3b}}{\tau_{3b,1}} \right) b_{1in}^{\dagger}(k) |0\rangle .\end{aligned} \tag{D.10}$$

Now the system can be solved. Given that only the Fourier transform of the solution is needed, the calculations can be much simplified by taking the Fourier transform of the differential equations. This gives the following linear system of equations.

$$\begin{aligned}\left(i(\omega_{T1} - p) + \frac{1}{\tau_{T1}} + \frac{1}{2}\gamma_{rT1} + \frac{1}{4}\gamma_{dT1} \right) x_1(p,k) = \\ - \frac{1}{\sqrt{\tau_{T1}}} \left(\frac{x_2(p,k)}{\sqrt{\tau_{T3}}} + \frac{x_3(p,k)}{\sqrt{\tau_{2a,1}}} + \frac{x_4(p,k)}{\sqrt{\tau_{2b,1}}} + \frac{x_5(p,k)}{\sqrt{\tau_{3a,1}}} + \frac{x_6(p,k)}{\sqrt{\tau_{3b,1}}} \right) \\ - i\sqrt{\frac{2}{\tau_{T1}}}\delta(p-k)\end{aligned} \tag{D.11}$$

$$\begin{aligned}\left(i(\omega_{T3} - p) + \frac{1}{\tau_{T3}} + \frac{1}{2}\gamma_{rT3} + \frac{1}{4}\gamma_{dT3} \right) x_2(p,k) = \\ - \frac{1}{\sqrt{\tau_{T3}}} \left(\frac{x_1(p,k)}{\sqrt{\tau_{T1}}} + \frac{x_3(p,k)}{\sqrt{\tau_{2a,1}}} + \frac{x_4(p,k)}{\sqrt{\tau_{2b,1}}} + \frac{x_5(p,k)}{\sqrt{\tau_{3a,1}}} + \frac{x_6(p,k)}{\sqrt{\tau_{3b,1}}} \right) \\ - i\sqrt{\frac{2}{\tau_{T3}}}\delta(p-k)\end{aligned} \tag{D.12}$$

$$\left(i(\omega_{2a}-p)+\frac{1}{\tau_{2a,1}}+\frac{1}{\tau_{2a,2}}+\frac{1}{2}\gamma_{r2a}+\frac{1}{4}\gamma_{d2a}\right)x_3(p,k)=$$
$$-\frac{1}{\sqrt{\tau_{2a}}}\left(\frac{x_1(p,k)}{\sqrt{\tau_{T1}}}+\frac{x_2(p,k)}{\sqrt{\tau_{T3}}}+\frac{x_5(p,k)}{\sqrt{\tau_{3a,1}}}+\frac{x_6(p,k)}{\sqrt{\tau_{3b,1}}}\right)$$
$$-\left(\frac{1}{\sqrt{\tau_{2a,1}\tau_{2b,1}}}+\frac{1}{\sqrt{\tau_{2a,2}\tau_{2b,2}}}\right)x_4(p,k)-i\sqrt{\frac{2}{\tau_{2a,1}}}\delta(p-k) \qquad \text{(D.13)}$$

$$\left(i(\omega_{2b}-p)+\frac{1}{\tau_{2b,1}}+\frac{1}{\tau_{2b,2}}+\frac{1}{2}\gamma_{r2b}+\frac{1}{4}\gamma_{d2b}\right)x_4(p,k)=$$
$$-\frac{1}{\sqrt{\tau_{2b}}}\left(\frac{x_1(p,k)}{\sqrt{\tau_{T1}}}+\frac{x_2(p,k)}{\sqrt{\tau_{T3}}}+\frac{x_5(p,k)}{\sqrt{\tau_{3a,1}}}+\frac{x_6(p,k)}{\sqrt{\tau_{3b,1}}}\right)$$
$$-\left(\frac{1}{\sqrt{\tau_{2a,1}\tau_{2b,1}}}+\frac{1}{\sqrt{\tau_{2a,2}\tau_{2b,2}}}\right)x_3(p,k)-i\sqrt{\frac{2}{\tau_{2b,1}}}\delta(p-k) \qquad \text{(D.14)}$$

$$\left(i(\omega_{3a}-p)+\frac{1}{\tau_{3a,1}}+\frac{1}{\tau_{3a,3}}+\frac{1}{2}\gamma_{r3a}+\frac{1}{4}\gamma_{d3a}\right)x_5(p,k)=$$
$$-\frac{1}{\sqrt{\tau_{3a}}}\left(\frac{x_1(p,k)}{\sqrt{\tau_{T1}}}+\frac{x_2(p,k)}{\sqrt{\tau_{T3}}}+\frac{x_3(p,k)}{\sqrt{\tau_{2a,1}}}+\frac{x_4(p,k)}{\sqrt{\tau_{2b,1}}}\right)$$
$$-\left(\frac{1}{\sqrt{\tau_{3a,1}\tau_{3b,1}}}+\frac{1}{\sqrt{\tau_{3a,3}\tau_{3b,3}}}\right)x_6(p,k)-i\sqrt{\frac{2}{\tau_{3a,1}}}\delta(p-k) \qquad \text{(D.15)}$$

$$\left(i(\omega_{3b}-p)+\frac{1}{\tau_{3b,1}}+\frac{1}{\tau_{3b,3}}+\frac{1}{2}\gamma_{r3b}+\frac{1}{4}\gamma_{d3b}\right)x_6(p,k)=$$
$$-\frac{1}{\sqrt{\tau_{3b}}}\left(\frac{x_1(p,k)}{\sqrt{\tau_{T1}}}+\frac{x_2(p,k)}{\sqrt{\tau_{T3}}}+\frac{x_3(p,k)}{\sqrt{\tau_{2a,1}}}+\frac{x_4(p,k)}{\sqrt{\tau_{2b,1}}}\right)$$
$$-\left(\frac{1}{\sqrt{\tau_{3a,1}\tau_{3b,1}}}+\frac{1}{\sqrt{\tau_{3a,3}\tau_{3b,3}}}\right)x_5(p,k)-i\sqrt{\frac{2}{\tau_{3b,1}}}\delta(p-k), \qquad \text{(D.16)}$$

where the functions $x_i(p,k)$ are defined as

$$x_1(p,k) = \mathscr{F}\left[\langle 0|\, a_{T1}(t) b^\dagger_{1in}(k)\,|0\rangle\right](p,k) \tag{D.17}$$

$$x_2(p,k) = \mathscr{F}\left[\langle 0|\, a_{T3}(t) b^\dagger_{1in}(k)\,|0\rangle\right](p,k) \tag{D.18}$$

$$x_3(p,k) = \mathscr{F}\left[\langle 0|\, a_{2a}(t) b^\dagger_{1in}(k)\,|0\rangle\right](p,k) \tag{D.19}$$

$$x_4(p,k) = \mathscr{F}\left[\langle 0|\, a_{2b}(t) b^\dagger_{1in}(k)\,|0\rangle\right](p,k) \tag{D.20}$$

$$x_5(p,k) = \mathscr{F}\left[\langle 0|\, a_{3a}(t) b^\dagger_{1in}(k)\,|0\rangle\right](p,k) \tag{D.21}$$

$$x_6(p,k) = \mathscr{F}\left[\langle 0|\, a_{3b}(t) b^\dagger_{1in}(k)\,|0\rangle\right](p,k). \tag{D.22}$$

This system of six coupled equations can be reduced to a system of three linearly independent (coupled) equations, because three of the variables are not independent. Let me discard e.g., x_2, x_4 and x_6 using the functions introduced in the main text [in Eq. (4.9), (4.10) and (4.11)].

$$x_2(p,k) = \sqrt{\frac{\tau_{T1}}{\tau_{T3}}}\alpha_1(p) x_1(p,k) \tag{D.23}$$

$$x_4(p,k) = \sqrt{\frac{\tau_{2a,1}}{\tau_{2b,1}}}\alpha_2(p) x_3(p,k) \tag{D.24}$$

$$x_6(p,k) = \sqrt{\frac{\tau_{3a,1}}{\tau_{3b,1}}}\alpha_3(p) x_5(p,k). \tag{D.25}$$

Now the system can be easily solved by using linear algebra, but the solution is a set of long equations. The solution of x_2, x_4 and x_6 is

$$x_1(p,k) = -\frac{i\sqrt{\frac{2}{\tau_{T1}}}\delta(p-k)}{T_1(p) + \frac{1}{\tau_{T1}} + \frac{\alpha_1(p)}{\tau_{T3}} + \left(\frac{1}{\tau_{2a,1}} + \frac{\alpha_2(p)}{\tau_{2b,1}}\right)\frac{T_1(p)}{T_2(p)} + \left(\frac{1}{\tau_{3a,1}} + \frac{\alpha_3(p)}{\tau_{3b,1}}\right)\frac{T_1(p)}{T_3(p)}} \tag{D.26}$$

$$x_2(p,k) = -\frac{i\sqrt{\frac{2}{\tau_{2a,1}}}\delta(p-k)}{T_2(p) + \frac{1}{\tau_{2a,1}} + \frac{\alpha_2(p)}{\tau_{2b,1}} + \left(\frac{1}{\tau_{T1}} + \frac{\alpha_1(p)}{\tau_{T3}}\right)\frac{T_2(p)}{T_1(p)} + \left(\frac{1}{\tau_{3a,1}} + \frac{\alpha_3(p)}{\tau_{3b,1}}\right)\frac{T_2(p)}{T_3(p)}} \tag{D.27}$$

$$x_3(p,k) = -\frac{i\sqrt{\frac{2}{\tau_{3a,1}}}\delta(p-k)}{T_3(p) + \frac{1}{\tau_{3a,1}} + \frac{\alpha_3(p)}{\tau_{3b,1}} + \left(\frac{1}{\tau_{T1}} + \frac{\alpha_1(p)}{\tau_{T3}}\right)\frac{T_3(p)}{T_1(p)} + \left(\frac{1}{\tau_{2a,1}} + \frac{\alpha_2(p)}{\tau_{2b,1}}\right)\frac{T_3(p)}{T_2(p)}}. \tag{D.28}$$

In this expressions, the functions in Eq. (4.6), (4.7) and (4.8) have been used to simplify the notation. The scattering amplitudes are recovered by using the solution to the Fourier-transformed system of equations, yielding

$$\begin{aligned} S_1(p,k) =& \delta(p-k) - i\sqrt{\frac{2}{\tau_{T1}}}x_1(p,k) - i\sqrt{\frac{2}{\tau_{T3}}}x_2(p,k) - i\sqrt{\frac{2}{\tau_{2a,1}}}x_3(p,k) \\ & - i\sqrt{\frac{2}{\tau_{2b,1}}}x_4(p,k) - i\sqrt{\frac{2}{\tau_{3a,1}}}x_5(p,k) - i\sqrt{\frac{2}{\tau_{3b,1}}}x_6(p,k), \end{aligned} \tag{D.29}$$

for the reflection of a photon, and

$$S_2(p,k) = -i\sqrt{\frac{2}{\tau_{2a,2}}}x_3(p,k) - i\sqrt{\frac{2}{\tau_{2b,2}}}x_4(p,k), \tag{D.30}$$

$$S_3(p,k) = -i\sqrt{\frac{2}{\tau_{3a,3}}}x_5(p,k) - i\sqrt{\frac{2}{\tau_{3b,3}}}x_6(p,k), \tag{D.31}$$

for the transmission of a photon through the second and third transmission line, respectively.

Appendix E

Failed attempts (1): numerical integration

The equations of motion found in Chapter 4 together with the Hamiltonian of the system [Eq. (3.34) together with Eq. (3.35), (3.43), (3.47) and (3.52)] are the necessary tools to study the dynamics of operation of the quantum switch. To check that the device works as expected, the probabilities of transmission and reflection of photons under different conditions have to be found. This can be done, in principle, analytically, but the complexity of the system of differential equations that has to be solved makes it impossible in the case where two photons are sent to the quantum switch. After dismissing this option, a numerical approach has been considered. Numerical calculations are performed to obtain the desired scattering amplitudes and probabilities. In this Appendix I give a short description of the steps I have followed to derive the expressions for the scattering amplitudes numerically.

In order to find the scattering probabilities numerically we should reconsider whether we want to work within the Schrödinger picture or the Heisenberg picture. In any case, the Hilbert space has to be bounded. Both on the Hamiltonian and in the equations of motion there is a large number of different operators, and some of them are under an integral sign. The elements under the integrals are supposed to belong to different Hilbert spaces for each of the value the integration variable takes, thus making the Hilbert space infinitely large. Since it is not possible to work, numerically, with an infinite Hilbert space, we have to consider just one or some representative elements inside the integral. Afterwards, the simulations can be repeated with other values for the integration variables.

E.1 Schrödinger picture

The equations of motion in Chapter 4 have been derived in the Heisenberg picture because of the impossibility to diagonalize the Hamiltonian. This difficulties only arise when working analytically, but numerically, one can find fast algorithms to exponentiate –that is, diagonalize– any matrix. Let's see how the *in/out* formalism looks like in this picture. Consider the probability amplitude of an incoming photon being absorbed by the system and reflected back.

$$S = \langle 0 | \, b_{out}(p) \, b_{in}^{\dagger}(k) \, | 0 \rangle \, . \tag{E.1}$$

The $b_{in}^{\dagger}(k)$ operator acting on the initial state $|0\rangle$ represents a photon that has been created far away from the influence of the system we are considering –it is, thus, a free moving photon– but acting on the present time. The vacuum $|0\rangle$ is a wave function defined at the present time. The action of the free moving photon on the vacuum is given by

$$\lim_{t_0 \to \infty} b_k^{\dagger} \mathrm{e}^{-iH_T t_0} \mathrm{e}^{iHt_0} \, |0\rangle \, , \tag{E.2}$$

where H is the total Hamiltonian and H_T is the Hamiltonian of the transmission lines, a Hamiltonian that describes the dynamics of a free moving photon. In this expression I have brought the vacuum to $-\infty$ with the full Hamiltonian, then I have driven it back to the present time with the free Hamiltonian and finally a photon has been created. After this, the system has to be brought back to $-\infty$ with the free Hamiltonian and again to the present with the full Hamiltonian. This way we will have a ket describing the a free photon at time $t = 0$.

$$|\psi_{in}\rangle = \lim_{t_0 \to \infty} \mathrm{e}^{-iHt_0} \mathrm{e}^{iH_T t_0} b_k^{\dagger} \mathrm{e}^{-iH_T t_0} \mathrm{e}^{iHt_0} \, |0\rangle \, . \tag{E.3}$$

Similarly, an *out* operator acting on the vacuum gives*

$$|\psi_{out}\rangle = \lim_{t_0 \to \infty} \mathrm{e}^{iHt_0} \mathrm{e}^{-iH_T t_0} b_k^{\dagger} \mathrm{e}^{iH_T t_0} \mathrm{e}^{-iHt_0} \, |0\rangle \, . \tag{E.4}$$

With this notation, the probability amplitude reads

$$\begin{aligned} S &= \langle \psi_{out} | \psi_{in} \rangle \\ &= \lim_{t_0 \to \infty} \langle 0 | \, \mathrm{e}^{iHt_0} \mathrm{e}^{-iH_T t_0} b_p \, \mathrm{e}^{iH_T t_0} \mathrm{e}^{-iHt_0} \mathrm{e}^{-iHt_0} \mathrm{e}^{iH_T t_0} b_k^{\dagger} \mathrm{e}^{-iH_T t_0} \mathrm{e}^{iHt_0} \, |0\rangle \, . \end{aligned} \tag{E.5}$$

Given that in these equations there are lots of oscillating functions that have to be evaluated at large t, the numerical algorithm will not be stable. Moreover, the largest values of t that a computer can handle are far from infinity, given that the exponential function is a function that grows very fast.

*Compare these two expressions with Eq. (3.64).

Version of June 29, 2015– Created June 29, 2015 - 21:15

E.2 Heisenberg picture

Given that the numerical simulations within the Schrödinger picture do not seem to give a reliable answer we can try it within the Heisenberg picture. In this picture the operators evolve with time so, in order to find the probability amplitude, the Langevin equations of motion have to be solved.

Before doing any calculation with our system it is convenient to try it first with a simpler Hamiltonian. If it works then the algorithm can be generalized to our more complicated device. Consider the Hamiltonian describing a single-photon transistor composed of two transmon qubits and a SQUID [17].

$$\begin{aligned} H =& \frac{\omega_1}{2}\sigma_1^z + \frac{\omega_2}{2}\sigma_2^z - J\sigma_1^z\sigma_2^z \\ &+ \int dp \left(\frac{\sigma_1^+ (r_p + l_p)}{\sqrt{2\pi\tau_1}} + \frac{\sigma_2^+ b_p}{\sqrt{2\pi\tau_2}} + h.c. \right) \\ &+ \int dp\, p \left(r_p^\dagger r_p - l_p^\dagger l_p + b_p^\dagger b_p \right). \end{aligned} \tag{E.6}$$

This Hamiltonian has some similarities with the Hamiltonian described in E. (3.34). I will work with 9 operators: σ_1^-, σ_1^+, σ_2^-, σ_2^+, σ_1^z, σ_2^z, r, l and b. In order to keep the Hilbert space small, I have imposed that the incoming pulse has frequency ω_t (not a distribution in the momentum space).

The problem with the Langevin equations is that most of the algorithms used to solve them are numerically unstable because the exponential function grows very fast [†]. So far I have not been able to find a solution for these equations for large t. Nevertheless, the solution I have found shows the behavior of the system within a time range large enough (at least for a one-photon interaction).

Before plotting the results let me compute, analytically, what is expected to be found numerically, so we can have enough information to tell whether the numerical calculations are right (and useful) or not.

Since the Langevin equations give us a set of functions that depend on time and we are working at a small time scale, the Fourier transform cannot be performed on the results. Moreover, since the incoming photons have one definite frequency, it makes no sense to find a result that depends on the frequency. For the process involving an incoming photon moving to the right and an outgoing photon moving

[†] Equations of this kind are called stiff equations.

to the right (transmission), this element of the scattering matrix reads

$$S = \langle 0 | \, r_{out}(t) \, r_{in}^{\dagger}(t') \, | 0 \rangle \tag{E.7}$$

$$= \langle 0 | \left(r_{in}(t) - \frac{i}{\sqrt{\tau_1}} \sigma_1^{-}(t) \right) r_{in}^{\dagger}(t') \, | 0 \rangle \tag{E.8}$$

$$= 1 - \frac{e^{ikt'}}{\tau_1} \frac{e^{-ikt} - e^{-(i\omega_1 + 2iJ + \frac{1}{\tau_1})t}}{i(\omega_1 + 2J - k) + \frac{1}{\tau_1}} \tag{E.9}$$

Let me separate this equation in two parts, the first part being

$$S_1 = 1 - \frac{1}{\tau_1} \frac{e^{-ik(t-t')}}{i(\omega_1 + 2J - k) + \frac{1}{\tau_1}}, \tag{E.10}$$

and the second part

$$S_2 = \frac{e^{ikt'}}{\tau_1} \frac{e^{-(i\omega_1 + 2iJ + \frac{1}{\tau_1})t}}{i(\omega_1 + 2J - k) + \frac{1}{\tau_1}}, \tag{E.11}$$

with $S_1 + S_2 = S$. By imposing the same parameters as in the numerical calculations ($t = t'$, $k = \omega_t = \omega_1 + 2J$) these two equations become $S_1 = 0$ and $S_2 = e^{-t/\tau_1}$. Now we can compare the curve describing the numerical result with the expression we have just found. These curves are plotted in FIG. E.1.

The numerical integration may seem right because the results agree with the analytic calculations, but if the analytic expression are computed again without imposing any condition to the pulse shape and frequency, we will see that S_2 do not contribute to the final expression and is S_1 the term that contains the information of the scattering process. So, these plots should actually be completely flat (after taking the Fourier transform).

It can not be solved in the Schrödinger picture because it may give large numerical errors. In the Heisenberg picture we have to face the numerical errors (for large times) and also some extra contributions coming from expressions that within the analytical derivation do not exist. For these reasons I believe that the numerical integrations are not a good approach, at least at this stage.

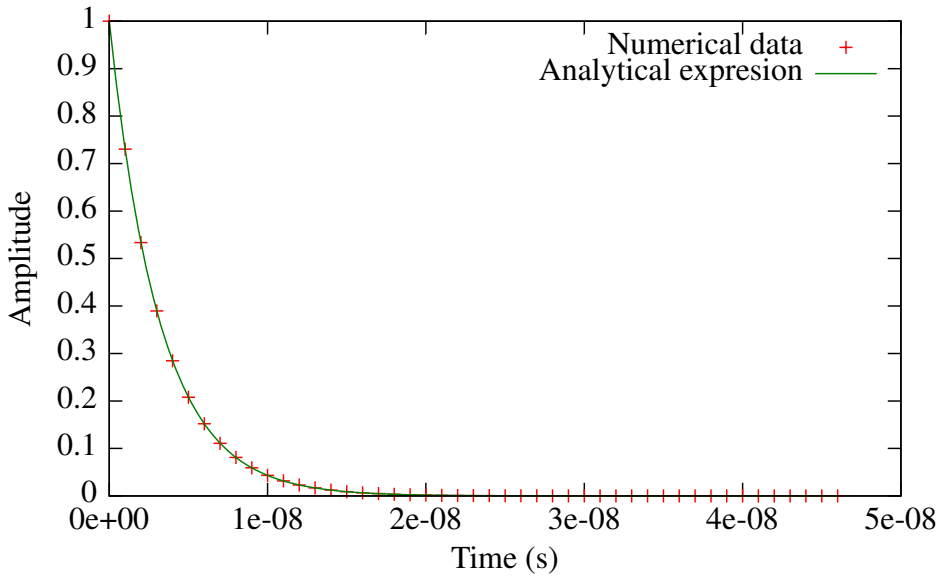

Figure E.1: *This figure contains the probability amplitude computed using numerical methods (red points) and also analytical methods (green curve) for a photon being transmitted. For these curves I have used* $\omega_1 = \omega_2 = \pi \cdot 10^{-10}$ *Hz,* $J = 0.01\omega_1$ *and* $\tau_1 = \tau_2 = 100/\omega_1$.

Appendix F

Failed attempts (2): propagators and Green's functions

In Chapter 4 I have explained that the amplitude probabilities for a photon being reflected and transmitted are, respectively

$$S_1(p,k) = \langle 0| b_{1out}(p) b^\dagger_{1in}(k) |0\rangle , \tag{F.1}$$

$$S_2(p,k) = \langle 0| b_{2out}(p) b^\dagger_{1in}(k) |0\rangle , \tag{F.2}$$

$$S_3(p,k) = \langle 0| b_{3out}(p) b^\dagger_{1in}(k) |0\rangle . \tag{F.3}$$

Eq. (F.1) to (F.3) have been derived by quantizing the Hamiltonian in Eq. (2.31), but another approach can be considered. The scattering amplitude in Eq. (F.1) can also be expressed, up to a constant factor, using some variable $\psi_1(t)$, whose quantized form is given by

$$\psi_1(t) = A_1^{-1/4}(b_1(t) + b_1^\dagger(t)). \tag{F.4}$$

This yields the expression for S_1:

$$S_1 \sim \lim_{\substack{t\to\infty \\ t'\to-\infty}} \langle 0| \psi_1(t)\psi_1(t') |0\rangle , \tag{F.5}$$

in the Heisenberg picture, as well. The scattering amplitudes can now be solved by using Green's functions. The advantage of working with the flux ψ_1 instead of the ladder operators is that, in this case, the equations of motion do not contain as much products of operators as before.

This Appendix contains a glimpse of this attempt to derive an expression for the scattering amplitudes discussed in Chapter 4 by making use of Green's functions in the Lagrangian formalism.

Version of June 29, 2015– Created June 29, 2015 - 21:15

The Lagrangian in Eq. (2.24) only described the system containing the transmon and SQUIDs, but not the transmission lines or the extra inductors. Given that the transmission lines behave like an infinite chain of oscillators, we can guess the extra terms that need to be added into the Lagrangian. The full Lagrangian now reads

$$\begin{aligned}
L = &+\frac{1}{2}\left(A_1'\dot{\psi}_1^2 - A_1\psi_1^2\right) + \frac{1}{2}\left(A_2'\dot{\psi}_2^2 - A_2\psi_2^2\right) + \frac{1}{2}\left(A_3'\dot{\psi}_3^2 - A_3\psi_3^2\right) \\
&+\frac{C_{2a}}{2}(\dot{\varphi}_{2a}-\dot{\psi}_2)^2 + \frac{C_{2b}}{2}(\dot{\varphi}_{2b}-\dot{\psi}_2)^2 + \frac{C_{3a}}{2}(\dot{\varphi}_{3a}-\dot{\psi}_3)^2 + \frac{C_{3b}}{2}(\dot{\varphi}_{3b}-\dot{\psi}_3)^2 \\
&+\frac{C_{2sa}}{2}(\dot{\varphi}_1-\dot{\varphi}_{2a})^2 + \frac{C_{2sb}}{2}(\dot{\varphi}_1-\dot{\varphi}_{2b})^2 + \frac{C_{3sa}}{2}(\dot{\varphi}_1-\dot{\varphi}_{3a})^2 + \frac{C_{3sb}}{2}(\dot{\varphi}_1-\dot{\varphi}_{3b})^2 \\
&\frac{C_1}{2}(\dot{\varphi}_1-\dot{\psi}_1)^2 + \frac{C_t}{2}\left(\dot{\varphi}_1^2 + \alpha_t\dot{\varphi}_1^4\right) + E_{Jt}\cos\left(\frac{\varphi_1}{\varphi_0}\right) \\
&+E_{J2a}\cos\left(\frac{\varphi_1-\varphi_{2a}}{\varphi_0}\right) + E_{J2b}\cos\left(\frac{\varphi_1-\varphi_{2b}}{\varphi_0}\right) \\
&+E_{J3a}\cos\left(\frac{\varphi_1-\varphi_{3a}}{\varphi_0}\right) + E_{J3b}\cos\left(\frac{\varphi_1-\varphi_{3b}}{\varphi_0}\right) \\
&-\frac{1}{2}\varphi_{3a}^2\left(\frac{1}{L_1}+\frac{1}{L_2}+\frac{1}{L_3}\right) - \frac{1}{2}\varphi_{3b}^2\left(\frac{1}{L_1}+\frac{1}{L_5}+\frac{1}{L_6}\right) \\
&-\frac{1}{2}\varphi_{2a}^2\left(\frac{1}{L_3}+\frac{1}{L_4}+\frac{1}{L_6}\right) - \frac{1}{2}\varphi_{2b}^2\left(\frac{1}{L_2}+\frac{1}{L_4}+\frac{1}{L_5}\right) \\
&+\frac{\varphi_{3a}\varphi_{3b}}{L_1} + \frac{\varphi_{3a}\varphi_{2b}}{L_2} + \frac{\varphi_{3a}\varphi_{2a}}{L_3} + \frac{\varphi_{2a}\varphi_{2b}}{L_4} + \frac{\varphi_{3b}\varphi_{2b}}{L_5} + \frac{\varphi_{3b}\varphi_{2a}}{L_6}.
\end{aligned} \tag{F.6}$$

In this expression, the potentials V_1, V_2 and V_3 that appeared in Eq. (2.24) now are substituted by $\dot{\psi}_1 = V_1$, $\dot{\psi}_2 = V_2$ and $\dot{\psi}_3 = V_3$. In this Lagrangian, A_i and A_i' are just constants. Although some expressions have been added and the V_i's are treated as variables instead of constants, this Lagrangian is assumed to lead to the Hamiltonian found in Eq. (2.31), plus the expressions that describe the transmission lines.

With this Lagrangian, the equations of motion of the time-dependent fluxes are found using the Euler-Lagrange equation:

$$\begin{aligned}
&(C_1 + C_{2sa} + C_{2sb} + C_{3sa} + C_{3sb} + C_t)\,\ddot{\varphi}_1 + 6\alpha_t C_t\dot{\varphi}_1^2\ddot{\varphi}_1 \\
&-C_{2sa}\ddot{\varphi}_{2a} - C_{2sb}\ddot{\varphi}_{2b} - C_{3sa}\ddot{\varphi}_{3a} - C_{3sb}\ddot{\varphi}_{3b} - C_1\ddot{\psi}_1 \\
&+E_{Jt}\sin\left(\frac{\varphi_1}{\varphi_0}\right) + E_{J2a}\sin\left(\frac{\varphi_1-\varphi_{2a}}{\varphi_0}\right) + E_{J2b}\sin\left(\frac{\varphi_1-\varphi_{2b}}{\varphi_0}\right) \\
&+E_{J3a}\sin\left(\frac{\varphi_1-\varphi_{3a}}{\varphi_0}\right) + E_{J3b}\sin\left(\frac{\varphi_1-\varphi_{3b}}{\varphi_0}\right) = 0
\end{aligned} \tag{F.7}$$

$$(C_{2a}+C_{2sa})\,\ddot{\varphi}_{2a}-C_{2sa}\ddot{\varphi}_1-C_{2a}\ddot{\psi}_2 + E_{J2a}\sin\left(\frac{\varphi_1-\varphi_{2a}}{\varphi_0}\right)+\varphi_{2a}\left(\frac{1}{L_3}+\frac{1}{L_4}+\frac{1}{L_6}\right)-\frac{\varphi_{3a}}{L_3}-\frac{\varphi_{2b}}{L_4}-\frac{\varphi_{3b}}{L_6}=0 \quad \text{(F.8)}$$

$$(C_{2b}+C_{2sb})\,\ddot{\varphi}_{2b}-C_{2sb}\ddot{\varphi}_1-C_{2b}\ddot{\psi}_2 + E_{J2b}\sin\left(\frac{\varphi_1-\varphi_{2b}}{\varphi_0}\right)+\varphi_{2b}\left(\frac{1}{L_2}+\frac{1}{L_4}+\frac{1}{L_4}\right)-\frac{\varphi_{3a}}{L_2}-\frac{\varphi_{2a}}{L_4}-\frac{\varphi_{3b}}{L_5}=0 \quad \text{(F.9)}$$

$$(C_{3a}+C_{3sa})\,\ddot{\varphi}_{3a}-C_{3sa}\ddot{\varphi}_1-C_{3a}\ddot{\psi}_3 + E_{J3a}\sin\left(\frac{\varphi_1-\varphi_{3a}}{\varphi_0}\right)+\varphi_{3a}\left(\frac{1}{L_1}+\frac{1}{L_2}+\frac{1}{L_3}\right)-\frac{\varphi_{3b}}{L_1}-\frac{\varphi_{2b}}{L_2}-\frac{\varphi_{2a}}{L_3}=0 \quad \text{(F.10)}$$

$$(C_{3b}+C_{3sb})\,\ddot{\varphi}_{3b}-C_{3sb}\ddot{\varphi}_1-C_{3b}\ddot{\psi}_3 + E_{J3b}\sin\left(\frac{\varphi_1-\varphi_{3b}}{\varphi_0}\right)+\varphi_{3b}\left(\frac{1}{L_1}+\frac{1}{L_5}+\frac{1}{L_6}\right)-\frac{\varphi_{3a}}{L_1}-\frac{\varphi_{2b}}{L_5}-\frac{\varphi_{2a}}{L_6}=0, \quad \text{(F.11)}$$

and also

$$\tilde{A_1}\,\ddot{\psi}_1+A_1\psi_1=C_1\ddot{\varphi}_1 \quad \text{(F.12)}$$

$$\tilde{A_2}\,\ddot{\psi}_2+A_2\psi_2=C_{2a}\ddot{\varphi}_{2a}+C_{2b}\ddot{\varphi}_{2b} \quad \text{(F.13)}$$

$$\tilde{A_3}\,\ddot{\psi}_3+A_3\psi_3=C_{3a}\ddot{\varphi}_{3a}+C_{3b}\ddot{\varphi}_{3b}. \quad \text{(F.14)}$$

In these last three equations I have introduced the variables $\tilde{A}_1=C_1+A_1'$, $\tilde{A}_2=C_{2a}+C_{2b}+A_2'$ and $\tilde{A}_3=C_{3a}+C_{3b}+A_3'$.

Now, the way to proceed consists in solving this system of coupled equations and plug the solution into Eq. (F.5) to obtain the scattering amplitude for the reflection of a single photon. If the system can be solved, two-photon processes could be easily found, but this system of coupled, second-order differential equation is not easy to solve, although the equations are much simpler than those in Chapter 3 (Section 3.5).

Let me try now a different approach. Consider the time-ordered propagator:

$$\langle 0|\,G(t,t')\,|0\rangle=\langle 0|\,T\{\psi_1(t)\psi_1(t')\}\,|0\rangle\,, \quad \text{(F.15)}$$

where T is the time-ordering operator and $G(t,t')$ is defined as

$$G(t,t')=\Theta(t-t')\psi_1(t)\psi_1(t')+\Theta(t'-t)\psi_1(t')\psi_1(t). \quad \text{(F.16)}$$

In this expression the function $\Theta(t-t')$ is the Heaviside step function. I want to find (and solve) the equation of motion of this propagator. Its solution will give the scattering amplitude we are looking for. The time derivative of this operator is:

$$\begin{aligned}\frac{d}{dt}G(t-t') =&\delta(t-t')\psi_1(t)\psi_1(t') + \Theta(t-t')\frac{d\psi_1(t)}{dt}\psi_1(t') \\ &- \delta(t-t')\psi_1(t')\psi_1(t) + \Theta(t'-t)\psi_1(t')\frac{d\psi_1(t)}{dt} \\ =&\Theta(t-t')\frac{d\psi_1(t)}{dt}\psi_1(t') + \Theta(t'-t)\psi_1(t')\frac{d\psi_1(t)}{dt},\end{aligned} \tag{F.17}$$

and the second derivative

$$\begin{aligned}\frac{d^2}{dt^2}G(t-t') =&\delta(t-t')\left[\frac{d\psi_1(t)}{dt},\psi_1(t')\right]_{t=t'} \\ &+\Theta(t-t')\frac{d^2\psi_1(t)}{dt^2}\psi_1(t') + \Theta(t'-t)\psi_1(t')\frac{d^2\psi_1(t)}{dt^2}.\end{aligned} \tag{F.18}$$

If we neglect C_1 [in the Eq. (F.12)] and impose the quantization of the fluxes and momenta, the commutator in the previous expression becomes

$$\left[\dot{\psi}_1(t),\psi_1(t')\right]_{t=t'} \approx -i\hbar. \tag{F.19}$$

With this, the equation of motion of the propagator reads

$$\left(\frac{d^2}{dt^2}+\frac{A_1}{\tilde{A}_1}\right)\langle 0|\,G(t-t')\,|0\rangle \approx -i\hbar\delta(t-t') + \frac{C_1}{\tilde{A}_1}\langle 0|\,T\left\{\ddot{\varphi}_1(t)\psi_1(t')\right\}|0\rangle\,. \tag{F.20}$$

Now, the value of $\langle 0|\,T\left\{\ddot{\varphi}_1(t)\psi_1(t')\right\}|0\rangle$ has to be found, but this will not give a simple and short differential equation. With this procedure a highly coupled system of differential equations is obtained, so we have the same problem as before. Thus, another mechanism to find the scattering amplitudes has to be found.

Appendix G

Failed attempts (3): Feynman diagrams

The last fruitless attempt I have made to find an expression for the scattering amplitudes of the single- and two-photons processes discussed in Chapter 4 is described in this Appendix. Here I make use of quantum field theory techniques to obtain an expression for the propagator in Eq. (F.15) by using Feynman diagrams. The notation in this Appendix is the same as in Appendix F.

The derivation of all the necessary tools to construct the Feynman rules is a long procedure and, since this section is just illustrative and will not bring anything new to this research project, I will skip some steps and give only the relevant results. The first of these results is the Hamiltonian I will work with. In the Interaction picture, the total Hamiltonian of the system has to be split into an interacting part H_I and a part that describes the free, non-interacting system H_0. The non-interacting part of the Hamiltonian, derived from the Lagrangian in Eq. (F.6), is

$$\begin{aligned} H_0 =& 4E_T q_1^2 + \frac{1}{2}\bar{E}_J \phi_1^2 \\ &+ \left(\frac{1}{2\varphi_0^2 \left(C_{2a} + C_{2sa}\right)} + 4E_T \frac{C_{2sa}^2}{\left(C_{2a} + C_{2sa}\right)^2} \right) q_{2a}^2 + \frac{1}{2} E_{J2a} \phi_{2a}^2 \\ &+ \{2a \to 2b, 3a, 3b\} \\ x &+ \frac{1}{2}\frac{\chi_1^2}{\tilde{A}_1} + \frac{1}{2}\frac{\chi_2^2}{\tilde{A}_2} + \frac{1}{2}\frac{\chi_3^2}{\tilde{A}_3} + \frac{1}{2}A_1 \psi_1^2 + \frac{1}{2}A_2 \psi_2^2 + \frac{1}{2}A_3 \psi_3^2, \end{aligned} \tag{G.1}$$

where, in this expression, the variables χ_1, χ_2 and χ_3 are the conjugate momenta of the fluxes ψ_1, ψ_2 and ψ_3 (the cosines have been expanded in a power series).

The interaction part of the Hamiltonian, H_I, contains all the other expressions, each of them with a coupling constant different for every term. This expression contains the couplings between the transmon and SQUIDs with the transmission lines and also between themselves. Each of these coupling constants will be referred as λ_i and will be considered small.

Following [62], the propagator in Eq. (F.15), in the interaction picture, reads

$$\langle\Omega|\,T\left\{\psi_1(t_1)\psi_1(t_2)\right\}|\Omega\rangle = \lim_{T\to\infty(1-i\varepsilon)} \frac{\langle 0|\,T\left\{\psi_{I1}(t_1)\psi_{I1}(t_2)\exp\left[-i\int_{-T}^{T}dtH_I(t)\right]\right\}|0\rangle}{\langle 0|\,T\left\{\exp\left[-i\int_{-T}^{T}dtH_I(t)\right]\right\}|0\rangle}, \tag{G.2}$$

where the subscript I stands for Interaction picture and $|\Omega\rangle$ is the ground state of the interaction theory, which is generally different from $|0\rangle$. Moreover, the Hamiltonian $H_I(t)$ is

$$H_I(t) = e^{iH_0t}H_Ie^{-iH_0t} = \lambda e^{iH_0t}H_I'e^{-iH_0t}. \tag{G.3}$$

By expanding the propagator in Eq. (G.2) as a Taylor series in small λ we obtain

$$\langle\Omega|\,T\left\{\psi_1(t_1)\psi_1(t_2)\right\}|\Omega\rangle \approx \lim_{T\to\infty(1-i\varepsilon)} \frac{\langle 0|\,T\left\{\psi_{I1}(t_1)\psi_{I1}(t_2)+\psi_{I1}(t_1)\psi_{I1}(t_2)\left[-i\int_{-T}^{T}dtH_I(t)\right]+\ldots\right\}|0\rangle}{\langle 0|\,T\left\{\exp\left[-i\int_{-T}^{T}dtH_I(t)\right]\right\}|0\rangle}, \tag{G.4}$$

which can be evaluated by using free-field propagators such as $D_F(t_1-t_2) = \langle 0|\,T\left\{\psi_{I1}(t_1)\psi_{I1}(t_2)\right\}|0\rangle$ together with Wick's theorem [62].

G.1 Propagators within the free field theory

In this section only the Hamiltonian H_0 [Eq. (G.1)] will be considered. I am interested in computing two-point propagators within this theory. Let me start with

$$D_{F1}(t_1-t_2) = \langle 0|\,T\left\{\psi_1(t_1)\psi_1(t_2)\right\}|0\rangle. \tag{G.5}$$

In order to find this propagator, its equation of motion has to be solved, but first, the equations of motion of the flux and momentum involved in this expression

have to be found. These are

$$\begin{aligned}\dot{\psi}_1 =& \frac{\partial H_0}{\partial \chi_1}\\ \dot{\chi}_1 =& -\frac{\partial H_0}{\partial \psi_1},\end{aligned} \tag{G.6}$$

which gives

$$\ddot{\psi}_1 = -\omega_1^2 \psi_1, \tag{G.7}$$

where $\omega_1^2 = A_1/\tilde{A}_1$. The quantization condition $[\psi_1, \chi_1] = i\hbar$ must be imposed, as well. Consider also the operator

$$\begin{aligned}\mathscr{O}_1(t_1 - t_2) &= T\{\psi_1(t_1)\psi_1(t_2)\}\\ &= \Theta(t_1 - t_2)\psi_1(t_1)\psi_1(t_2) + \Theta(t_2 - t_1)\psi_1(t_2)\psi_1(t_1),\end{aligned} \tag{G.8}$$

whose second derivative gives

$$\begin{aligned}\frac{d^2}{dt_1^2}\mathscr{O}_1(t_1 - t_2) =& \delta(t_1 - t_2)\left[\frac{d\psi_1(t_1)}{dt_1}, \psi_1(t_2)\right]_{t_1 = t_2}\\ &+ \Theta(t_1 - t_2)\frac{d^2\psi_1(t_1)}{dt_1^2}\psi_1(t_2) + \Theta(t_2 - t_1)\psi_1(t_2)\frac{d^2\psi_1(t_1)}{dt_1^2}.\end{aligned} \tag{G.9}$$

Recall that, within the free theory, the conjugate momentum of the field $\psi_1(t)$ is $\chi_1(t) = \tilde{A}_1\dot{\psi}_1(t)$. With this, the equation of motion of the operator $\mathscr{O}_1$ becomes

$$\left(-\frac{d^2}{dt_1^2} - \omega_1^2\right)\mathscr{O}_1(t_1 - t_2) = \frac{i\hbar}{\tilde{A}_1}\delta(t_1 - t_2). \tag{G.10}$$

Since the vacuum ket $|0\rangle$ does not depend on time, the propagator $D_{F1}(t_1 - t_2)$ follows the same equation of motion. Its solution in Fourier space it is

$$D_{F1}(k_1) = \frac{i\hbar}{\tilde{A}_1\sqrt{2\pi}}\frac{1}{k_1^2 - \omega_1^2 + i\varepsilon}. \tag{G.11}$$

Similarly, for the propagators

$$G_{F1}(t_1 - t_2) = \langle 0|\, T\{\chi_1(t_1)\psi_1(t_2)\}\,|0\rangle, \tag{G.12}$$

$$H_{F1}(t_1 - t_2) = \langle 0|\, T\{\chi_1(t_1)\chi_1(t_2)\}\,|0\rangle, \tag{G.13}$$

similar expressions are found:

$$G_{F1}(k_1) = \frac{\hbar}{\sqrt{2\pi}} \frac{k_1}{k_1^2 - \omega_1^2 + i\varepsilon}, \tag{G.14}$$

$$H_{F1}(k_1) = \frac{i\hbar A_1}{\sqrt{2\pi}} \frac{1}{k_1^2 - \omega_1^2 + i\varepsilon}. \tag{G.15}$$

For any other combination of fields and momenta –like $\psi_1 \phi_{2a}$ or $q_1 \psi_{3a}$, etc.– the propagators vanish, in Fourier space.

G.2 From n-point correlation functions to the S-matrix

In this Appendix I make use of a theory where, by making use of the two-point propagators, any n-point correlation function can be found. In this theory, a free particle propagating from t_2 to t_1, represented by the diagram

is given by

$$D_{F1}(t_1 - t_2) = \frac{i\hbar}{\tilde{A}_1 \sqrt{2\pi}} \int_{-\infty}^{\infty} dk \frac{e^{-ik(t_1 - t_2)}}{k^2 - \omega^2 + i\varepsilon}. \tag{G.16}$$

I am interested in a scenario where $t_1 \to \infty$ and $t_2 \to -\infty$. I also want to make this particle that goes from t_1 to t_2 a real particle, and not a virtual one. This means that it has to be on-shell. Particles on-shell satisfy the relation $k^2 - \omega^2 = 0$, as can be seen by solving the equations of motion of the fields [in Eq. (G.7)] in Fourier space. To transform this equation –and the diagram– into something physical, I will make use of the LSZ reduction formula [62–64], which states that the scattering amplitude $\langle p_1 \dots p_n | S | k_1 \dots k_m \rangle$ containing m incoming particles and n outgoing particles is related to the $(n+m)$-point correlation function (in Fourier space) as

$$\begin{aligned} \langle p_1 \dots p_n | S | k_1 \dots k_m \rangle = \lim_{on-shell} & \prod_{i=1}^{n} \frac{p_i^2 - \omega^2 + i\varepsilon}{i\sqrt{Z}} \prod_{j=1}^{m} \frac{k_j^2 - \omega^2 + i\varepsilon}{i\sqrt{Z}} \\ & \times \prod_{i=1}^{n} \int \frac{dt_i}{\sqrt{2\pi}} e^{-ip_i t_i} \prod_{j=1}^{m} \int \frac{dt'_j}{\sqrt{2\pi}} e^{+ik_j t'_j} \\ & \times \langle \Omega | T \left\{ \phi(t_1) \dots \phi(t_n) \phi(t'_1) \dots \phi(t'_m) \right\} | \Omega \rangle , \end{aligned} \tag{G.17}$$

where Z is the field renormalization strength. It is defined as the residue of the single-particle pole in the two-point function of fields. As can be seen in [62, 63], Eq. (G.17) is a function of the interaction strengts λ_i whose value as $\lambda_i \to 0$ goes to 1. Hence we can safely assume $Z = 1$ if we restrict ourselves to low orders of λ_i in the computation of the scattering amplitudes. Actually this is the result for $\langle p_1 \dots p_n | S - 1 | k_1 \dots k_m \rangle$, but since the initial state and the final stare are different (and orthogonal), the 1 can be omitted.

Notice also that the exponent in the Fourier transform of the incoming fields has a plus sign whereas the Fourier transform of the outgoing fields has a minus sign.

Given that the factors introduced in Eq. (G.17) go to zero when the on-shell condition is imposed, the only diagrams that contribute to any scattering processes are the fully connected diagrams, since the n factors of zero only cancel when the diagram generates n factors of zero in a denominator, and this only happens when there are n external points in the same diagram.

G.3 Feynman rules

At this point we have enough elements to write down the Feynman rules, which are indispensable to extract physical information from the Feynman diagrams. Given a scattering diagram

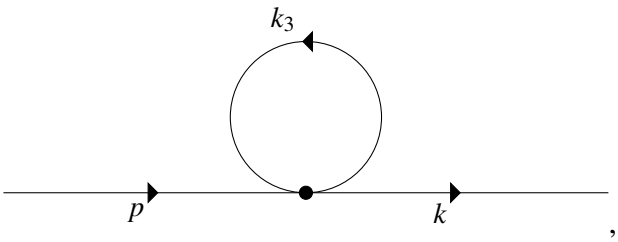

,

where the arrows indicate the propagation of a photon, the symbols p, k and k_3 are the momentum of each particle (either real or virtual) and the black dot is a vertex, the rules to construct the S-matrix elements for any scattering processes are, in momentum space,

1. For each internal propagator, add $D_F(k)$;
2. For n vertices, add $\dfrac{(-2\pi i)^n}{n!}\lambda_1\lambda_2\dots\lambda_n$;
3. For each external line, $-iD_0$;

4. Impose momentum conservation at each vertex: $\delta\left(\sum k_i\right)$;

5. Integrate over each undetermined momentum: $\int \frac{dk}{\sqrt{2\pi}}$;

6. Multiply by the number of equivalent contractions.

G.4 Scattering processes

Now that we know how to express a scattering amplitude in Feynman diagrams and find its expression using the Feynman rules, processes involving one and two incoming photons can be computed. Let me start with an incoming photon that is reflected.

By looking at the interaction Hamiltonian we can see that scatterings of order $O(\lambda)$ are not possible. The lowest order at which something happens is $O(\lambda^2)$. At this order, the following are the only possible diagrams with two vertices:

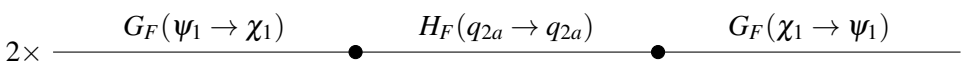

(G.18.a)

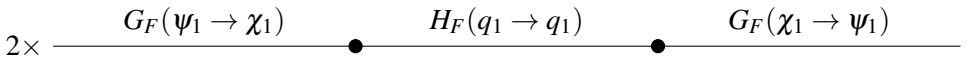

(G.18.b)

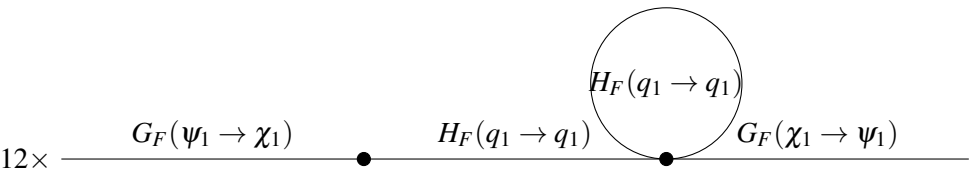

(G.18.c)

Version of June 29, 2015– Created June 29, 2015 - 21:15

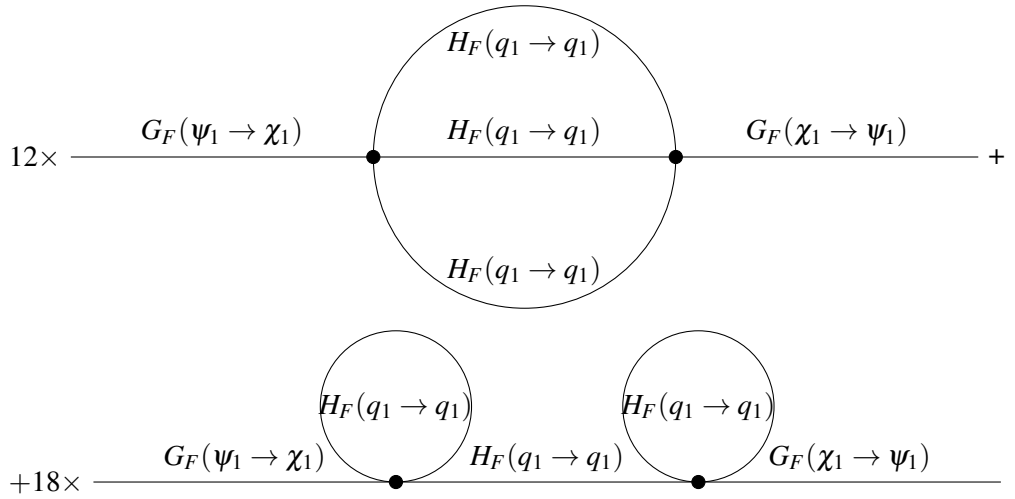

(G.18.d)

For the transmission of a photon from transmission line 1 to transmission line 2 there is only one diagram at $O(\lambda^2)$.

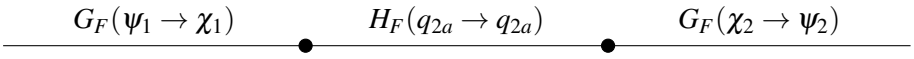

(G.19)

The factor in front of each diagram is the number of contractions of the fields that give the same diagram, and the relation between the diagrams and the fields is the following: consider the external fields to be at the points t_1 and t_2, and the intermediate vertices at t_3 and t_4.

- The diagram in (G.19) is generated by contracting $\psi_1(t_1)\psi_2(t_2)\chi_1(t_3)q_{2a}(t_3)\chi_2(t_4)q_{2a}(t_4)$.
- The diagram in (G.18.b) is generated by contracting $\psi_1(t_1)\psi_1(t_2)\chi_1(t_3)q_1(t_3)\chi_1(t_4)q_1(t_4)$.
- The diagram in (G.18.c) is generated by contracting $\psi_1(t_1)\psi_1(t_2)\chi_1(t_3)q_1(t_3)\chi_1(t_4)q_1^3(t_4)$.
- The diagrams in (G.18.d) are generated by contracting $\psi_1(t_1)\psi_1(t_2)\chi_1(t_3)q_1^3(t_3)\chi_1(t_4)q_1(t_4)$.
- The diagram in (G.18.a) is generated by contracting $\psi_1(t_1)\psi_1(t_2)\chi_1(t_3)q_{2a}(t_3)\chi_1(t_4)q_{2a}(t_4)$. Three more diagrams can be generated by substituting $q_{2a} \to q_{2b}$, q_{3a}, q_{3b}.

After a careful examination it can be seen that the diagrams with loops such as G.18.c or the second part of G.18.d represent a small contribution to the scattering

amplitude, so they can be omitted. Nevertheless, the scattering amplitude at such low orders give something different to what we obtained previously in Chapter 4 [scattering amplitude of single-photon processes, Eq. (4.5), (4.12) and (4.13)]. Moreover, the expressions obtained from these diagrams do not converge after integrating them for all the incoming and outgoing momenta.

The diagram in G.18.b gives an expression that goes as $\frac{p^2}{p^2-\omega^2+i\varepsilon}$, and the first diagram in G.18.d gives an expression that goes as $\frac{p^2}{p^2-(3\omega)^2+i\varepsilon}$. After squaring it and integrating over p, the final expression diverges. Also, it does not contain the energy of the transmon excitation nor its lifetime. ω is the frequency of the incoming pulse.

If we go to higher orders of the coupling constant (more vertices), then the assumption we made stating that $Z \approx 1$ does not hold anymore.

For these reasons I believe that this in not a good approach to derive the expressions for the scattering amplitudes for the two-photon processes.

Acknowledgements

I want to thank, in first place, my supervisor Miriam Blaauboer for giving me the opportunity to work in her group in Delft, for introducing me to the field of circuit quantum electrodynamics and superconducting qubits, for her guidance and good advices and also for all the time she dedicated to me. I also want to acknowledge my supervisor in Leiden, C. W. J. Beenakker. Without his approval I would not have been allowed to do the research project in an external institution.

During the two years I have been in the Netherlands I have learned a lot, and not only abut physics. Studying abroad has been a good experience, mostly because of all the colleagues and friends I have met, both in Leiden and in Delft. I especially want to thank all the numerous people I have sheared the office with for the nice environment they provided.

This thesis would not have been possible without my family. I want to thank them for their emotional and also financial support, for giving me the opportunity to study abroad and for visiting me in the Netherlands from time to time.

Het enige wat ik betreur, is dat ik kan geen Nederlands spreken.

References

[1] L. DiCarlo, J. M. Chow, J. M. Gambetta, L. S. Bishop, B. R. Johnson, D. I. Schuster, J. Majer, A. Blais, L. Frunzio, S. M. Girvin, and R. J. Schoelkopf, *Demonstration of two-qubit algorithms with a superconducting quantum processor*, Nature **460**, 240 (2009).

[2] E. Lucero, R. Barends, Y. Chen, J. Kelly, M. Mariantoni, A. Megrant, P. O'Malley, D. Sank, A. Vainsencher, J. Wenner, T. White, Y. Yin, A. N. Cleland, and J. M. Martinis, *Computing prime factors with a Josephson phase qubit quantum processor*, Nat. Phys. **8**, 719 (2012).

[3] H. Häffner, C. Roos, and R. Blatt, *Quantum computing with trapped ions*, Physics Reports **469**, 155 (2008).

[4] C. Monroe and J. Kim, *Scaling the Ion Trap Quantum Processor*, Science **339**, 1164 (2013).

[5] A. Politi, J. C. F. Matthews, and J. L. O'Brien, *Shor's Quantum Factoring Algorithm on a Photonic Chip*, Science **325**, 1221 (2009).

[6] S. Barz, I. Kassal, M. Ringbauer, Y. O. Lipp, B. Dakić, A. Aspuru-Guzik, and P. Walther, *A two-qubit photonic quantum processor and its application to solving systems of linear equations*, Sci. Rep. **4** (2014).

[7] L. Childress and R. Hanson, *Diamond NV centers for quantum computing and quantum networks*, MRS Bulletin **38**, 134 (2013).

[8] T. H. Taminiau, J. Cramer, T. van der Sar, V. V. Dobrovitski, and R. Hanson, *Universal control and error correction in multi-qubit spin registers in diamond*, Nat. Nano. **9**, 171 (2014).

[9] T. van der Sar, Z. H. Wang, M. S. Blok, H. Bernien, T. H. Taminiau, D. M. Toyli, D. A. Lidar, D. D. Awschalom, R. Hanson, and V. V. Dobrovitski, *Decoherence-protected quantum gates for a hybrid solid-state spin register*, Nature **484**, 82 (2012).

Version of June 29, 2015– Created June 29, 2015 - 21:15

[10] V. Ranjan, G. de Lange, R. Schutjens, T. Debelhoir, J. P. Groen, D. Szombati, D. J. Thoen, T. M. Klapwijk, R. Hanson, and L. DiCarlo, *Probing Dynamics of an Electron-Spin Ensemble via a Superconducting Resonator*, Phys. Rev. Lett. **110**, 067004 (2013).

[11] M. Nielsen and I. Chuang, *Quantum Computation and Quantum Information*, Cambridge Series on Information and the Natural Sciences, Cambridge University Press, 2000.

[12] P. Kok, W. J. Munro, K. Nemoto, T. C. Ralph, J. P. Dowling, and G. J. Milburn, *Linear optical quantum computing with photonic qubits*, Rev. Mod. Phys. **79**, 135 (2007).

[13] M. H. Devoret and R. J. Schoelkopf, *Superconducting Circuits for Quantum Information: An Outlook*, Science **339**, 1169 (2013).

[14] R. Jaeger and T. Blalock, *Microelectronic Circuit Design*, McGraw-Hill Series in Electrical and Computer Engineering, McGraw-Hill, 2010.

[15] V. Giovannetti, S. Lloyd, and L. Maccone, *Quantum Random Access Memory*, Phys. Rev. Lett. **100**, 160501 (2008).

[16] V. Giovannetti, S. Lloyd, and L. Maccone, *Quantum Private Queries*, Phys. Rev. Lett. **100**, 230502 (2008).

[17] L. Neumeier, M. Leib, and M. J. Hartmann, *Single-Photon Transistor in Circuit Quantum Electrodynamics*, Phys. Rev. Lett. **111**, 063601 (2013).

[18] M. T. Manzoni, F. Reiter, J. M. Taylor, and A. S. Sørensen, *Single-photon transistor based on superconducting systems*, Phys. Rev. B **89**, 180502 (2014).

[19] D. E. Chang, A. S. Sørensen, E. A. Demler, and M. D. Lukin, *A single-photon transistor using nanoscale surface plasmons*, Nat Phys **3**, 807 (2007).

[20] V. Giovannetti, S. Lloyd, and L. Maccone, *Architectures for a quantum random access memory*, Phys. Rev. A **78**, 052310 (2008).

[21] T. Kyaw, S. Felicetti, G. Romero, E. Solano, and L.-C. Kwek, *Scalable quantum memory in the ultrastrong coupling regime*, Scientific Reports **5**, 8621 (2015).

[22] F. Hong, Y. Xiang, Z. Zhu, L. Jiang, and L. Wu, *Robust quantum random access memory*, Phys. Rev. A **86**, 010306 (2012).

[23] M. Mariantoni, F. Deppe, A. Marx, R. Gross, F. K. Wilhelm, and E. Solano, *Two-resonator circuit quantum electrodynamics: A superconducting quantum switch*, Phys. Rev. B **78**, 104508 (2008).

[24] M. Haeberlein et al., *Fast microwave beam splitters from superconducting resonators*, arXiv preprint arXiv:1302.0729 (2013).

[25] C. M. Quintana, K. D. Petersson, L. W. McFaul, S. J. Srinivasan, A. A. Houck, and J. R. Petta, *Cavity-Mediated Entanglement Generation Via Landau-Zener Interferometry*, Phys. Rev. Lett. **110**, 173603 (2013).

[26] L. Chirolli, G. Burkard, S. Kumar, and D. P. DiVincenzo, *Superconducting Resonators as Beam Splitters for Linear-Optics Quantum Computation*, Phys. Rev. Lett. **104**, 230502 (2010).

[27] E. Hoffmann, F. Deppe, T. Niemczyk, T. Wirth, E. P. Menzel, G. Wild, H. Huebl, M. Mariantoni, T. Weißl, A. Lukashenko, A. P. Zhuravel, A. V. Ustinov, A. Marx, and R. Gross, *A superconducting 180 ° hybrid ring coupler for circuit quantum electrodynamics*, Applied Physics Letters **97**, (2010).

[28] J. Koch, T. M. Yu, J. Gambetta, A. A. Houck, D. I. Schuster, J. Majer, A. Blais, M. H. Devoret, S. M. Girvin, and R. J. Schoelkopf, *Charge-insensitive qubit design derived from the Cooper pair box*, Phys. Rev. A **76**, 042319 (2007).

[29] L. S. Bishop, *Circuit Quantum Electrodynamics*, PhD thesis, Yale University, 2010.

[30] M. H. Devoret, *Course 10 Quantum fluctuations in electrical circuits*, in *Quantum Fluctuations École d'été de Physique des Houches Session LXIII*, edited by S. Raimond, E. Giacobino, and J. Zinn-Justin, Les Houches, pages 351 – 386, Elsevier, 1995.

[31] C. A.-P. de Araujo, J. D. Cuchiaro, L. D. McMillan, M. C. Scott, and J. F. Scott, *Fatigue-free ferroelectric capacitors with platinum electrodes*, Nature **374**, 627 (1995).

[32] E. Gluskin, *The use of non-linear capacitors*, International Journal of Electronics **58**, 63 (1985).

[33] E. Gluskin, *A nonlinear resistor and nonlinear inductor using a nonlinear capacitor*, Journal of the Franklin Institute **336**, 1035 (1999).

[34] H. Li, V. Khilkevich, T. Li, D. Pommerenke, S. Kwon, and W. Hackenberger, *Nonlinear capacitors for ESD protection*, Electromagnetic Compatibility Magazine, IEEE **1**, 38 (2012).

[35] J. Macdonald and M. Brachman, *The Charging and Discharging of Nonlinear Capacitors*, Proceedings of the IRE **43**, 71 (1955).

[36] J. Colinge and C. Colinge, *Physics of Semiconductor Devices*, Springer, 2002.

[37] J. Khan, M. Lingalugari, F. Al-Amoody, and F. Jain, *Voltage-Dependent Charge Storage in Cladded Zn0.56Cd0.44Se Quantum Dot MOS Capacitors for Multibit Memory Applications*, Journal of Electronic Materials **42**, 3267 (2013).

[38] C. Hu, *Modern Semiconductor Devices for Integrated Circuits*, Prentice Hall, 2010.

[39] V. Duez, M. Henini, O. Vanbesien, J. M. Chamberlain, and D. Lippens, *Highly nonlinear capacitance in quantum well/barrier heterostructures: application to harmonic multiplication at terahertz frequency*, Proc. SPIE **3828**, 108 (1999).

[40] B. Wang, X. Zhao, J. Wang, and H. Guo, *Nonlinear quantum capacitance*, Applied Physics Letters **74**, 2887 (1999).

[41] S. Ilani, L. A. K. Donev, M. Kindermann, and P. L. McEuen, *Measurement of the quantum capacitance of interacting electrons in carbon nanotubes*, Nat. Phys. **2**, 687 (2006).

[42] D. Akinwande, Y. Nishi, and H.-S. Wong, *Analytical Model of Carbon Nanotube Electrostatics: Density of States, Effective Mass, Carrier Density, and Quantum Capacitance*, in *Electron Devices Meeting, 2007. IEDM 2007. IEEE International*, pages 753–756, 2007.

[43] J. Hagen, *Radio-Frequency Electronics: Circuits and Applications*, Cambridge University Press, 2009.

[44] G. Ithier, E. Collin, P. Joyez, P. J. Meeson, D. Vion, D. Esteve, F. Chiarello, A. Shnirman, Y. Makhlin, J. Schriefl, and G. Schön, *Decoherence in a superconducting quantum bit circuit*, Phys. Rev. B **72**, 134519 (2005).

[45] C. W. Gardiner and M. J. Collett, *Input and output in damped quantum systems: Quantum stochastic differential equations and the master equation*, Phys. Rev. A **31**, 3761 (1985).

[46] M. P. Blencowe and A. D. Armour, *Probing the quantum coherence of a nanomechanical resonator using a superconducting qubit: II. Implementation*, New Journal of Physics **10**, 095005 (2008).

[47] J. Taylor, *Scattering Theory: The Quantum Theory of Nonrelativistic Collisions*, Dover Books on Engineering, Dover Publications, 2012.

[48] S. Fan, Ş. E. Kocabaş, and J.-T. Shen, *Input-output formalism for few-photon transport in one-dimensional nanophotonic waveguides coupled to a qubit*, Phys. Rev. A **82**, 063821 (2010).

[49] C. Rigetti, J. M. Gambetta, S. Poletto, B. L. T. Plourde, J. M. Chow, A. D. Córcoles, J. A. Smolin, S. T. Merkel, J. R. Rozen, G. A. Keefe, M. B. Roth-

well, M. B. Ketchen, and M. Steffen, *Superconducting qubit in a waveguide cavity with a coherence time approaching 0.1 ms*, Phys. Rev. B **86**, 100506 (2012).

[50] M. J. Peterer, S. J. Bader, X. Jin, F. Yan, A. Kamal, T. J. Gudmundsen, P. J. Leek, T. P. Orlando, W. D. Oliver, and S. Gustavsson, *Coherence and Decay of Higher Energy Levels of a Superconducting Transmon Qubit*, Phys. Rev. Lett. **114**, 010501 (2015).

[51] M. D. Reed, L. DiCarlo, S. E. Nigg, L. Sun, L. Frunzio, S. M. Girvin, and R. J. Schoelkopf, *Realization of three-qubit quantum error correction with superconducting circuits*, Nature **482**, 382 (2012).

[52] M. D. Reed, B. R. Johnson, A. A. Houck, L. DiCarlo, J. M. Chow, D. I. Schuster, L. Frunzio, and R. J. Schoelkopf, *Fast reset and suppressing spontaneous emission of a superconducting qubit*, Applied Physics Letters **96**, (2010).

[53] E. Rephaeli, J.-T. Shen, and S. Fan, *Full inversion of a two-level atom with a single-photon pulse in one-dimensional geometries*, Phys. Rev. A **82**, 033804 (2010).

[54] M. Sandberg, M. R. Vissers, T. A. Ohki, J. Gao, J. Aumentado, M. Weides, and D. P. Pappas, *Radiation-suppressed superconducting quantum bit in a planar geometry*, Applied Physics Letters **102**, (2013).

[55] J. Siewert, T. Brandes, and G. Falci, *Adiabatic passage with superconducting nanocircuits*, Optics Communications **264**, 435 (2006), Quantum Control of Light and Matter In honor of the 70th birthday of Bruce Shore.

[56] Z.-B. Feng, Z.-L. Cai, C. Zhang, L. Fan, and T. Feng, *Quantum information transfer with Cooper-pair box qubits in circuit QED*, Optics Communications **283**, 1975 (2010).

[57] P. Goy, J. M. Raimond, M. Gross, and S. Haroche, *Observation of Cavity-Enhanced Single-Atom Spontaneous Emission*, Phys. Rev. Lett. **50**, 1903 (1983).

[58] W.-B. Gao, C.-Y. Lu, X.-C. Yao, P. Xu, O. Guhne, A. Goebel, Y.-A. Chen, C.-Z. Peng, Z.-B. Chen, and J.-W. Pan, *Experimental demonstration of a hyper-entangled ten-qubit Schrodinger cat state*, Nat Phys **6**, 331 (2010).

[59] D. Leibfried, E. Knill, S. Seidelin, J. Britton, R. B. Blakestad, J. Chiaverini, D. B. Hume, W. M. Itano, J. D. Jost, C. Langer, R. Ozeri, R. Reichle, and D. J. Wineland, *Creation of a six-atom 'Schrodinger cat' state*, Nature **438**, 639 (2005).

[60] X.-C. Yao, T.-X. Wang, P. Xu, H. Lu, G.-S. Pan, X.-H. Bao, C.-Z. Peng, C.-Y. Lu, Y.-A. Chen, and J.-W. Pan, *Observation of eight-photon entanglement*, Nat Photon **6**, 225 (2012).

[61] R. H. Hadfield, *Single-photon detectors for optical quantum information applications*, Nat Photon **3**, 696 (2009).

[62] M. Peskin and D. Schroeder, *An Introduction to Quantum Field Theory*, Advanced book classics, Addison-Wesley Publishing Company, 1995.

[63] M. Srednicki, *Quantum Field Theory*, Cambridge University Press, 2007.

[64] D. Tong, *Quantum Field Theory*, Lecture notes on QFT for a Master's level course at the University of Cambridge, 2012.

Version of June 29, 2015– Created June 29, 2015 - 21:15